5-1996

Discharge Coefficient Scale Effects Analysis for Weirs

Michael Clyde Johnson
Utah State University

DISCHARGE COEFFICIENT SCALE EFFECTS ANALYSIS FOR WEIRS

by

Michael Clyde Johnson

A dissertation submitted in partial fulfillment
of the requirements for the degree

of

DOCTOR OF PHILOSOPHY

in

Civil and Environmental Engineering

Approved:

UTAH STATE UNIVERSITY
Logan, Utah

1996

ABSTRACT

Discharge Coefficient Scale Effects Analysis for Weirs

by

Michael Clyde Johnson, Doctor of Philosophy

Utah State University, 1996

Major Professor: Dr. J. Paul Tullis
Department: Civil and Environmental Engineering

Much work has been published regarding discharge coefficients for various weir structures. What has not been published to the same extent are the effects of model scale associated with the weirs being studied. If laboratory weirs are too small, scale effects can affect the magnitude of the discharge coefficient. These errors may be significant if the weir serves as a control structure for an emergency spillway. It is imperative that discharge be accurately predicted to enable safe design and operation.

Numerical and physical means were employed to analyze the effects of scale associated with Froude Modeling of weirs with sharp and flat crests. An inverse formulation for the ideal flow of water over a weir was developed. The formulation appeared to be sound; however, the numerical method failed because the boundary condition on the free surface had multiple roots, which were almost equal in magnitude and sign.

Laboratory data were collected and analyzed to determine the existence of scale effects and the flow conditions under which they were manifested. Results indicate that scale effects are present even with relatively large model sizes (12 inches high with a crest thickness of 24 inches). The scale effects appear to be associated with the size of the weir-wall and the viscosity. Although the viscosity was not altered, the results show a characteristic Reynolds Number for a given crest thickness-to-height ratio where scale effects cease to exist for increasing total head.

Several graphs defining the conditions where scale effects exist for a given weir size were developed. Use of the graphs allows one to determine the minimum total head (piezometric plus velocity head) that one may operate a given size of weir or size a weir given the minimum total head to be tested to avoid scale effects.

A design curve for discharge coefficients was developed to be used for determining the capacity of prototype weirs. The curve can be used to determine the discharge coefficient for new or existing hydraulic control structures.

(121 Pages)

ACKNOWLEDGMENTS

I would like to express my gratitude to my advisor and friend, Dr. J. Paul Tullis, for his enduring patience and encouragement while this research was being conducted. Dr. Tullis spent many hours directing the research and reviewing this manuscript to ensure its completion in a timely manner. Special thanks is also given to Dr. Roland W. Jeppson for his guidance through the inverse solution for weir flow. Gratitude is also given to the other members of my committee, Dr. Gary P. Merkley, Dr. William J. Rahmeyer, and Dr. Gilberto Urroz, for their careful reading of the manuscript and helpful suggestions. Gratitude is also due to the Utah Water Research Laboratory and Dr. J. Paul Tullis for the financial support rendered to complete this research.

Much thanks is due to my loving wife, Shawna, who provided a special kind of encouragement and support to me as the research progressed. I would also like to thank my parents, Clyde W. and Susan W. Johnson, for their support and encouragement throughout my educational pursuits. Finally, gratitude must be expressed to Almighty God for providing me with the abilities necessary to pursue and complete this work.

Michael Clyde Johnson

CONTENTS

LIST OF TABLES

LIST OF FIGURES

LIST OF SYMBOLS

The following symbols were used in this dissertation:

a = acceleration of fluid element or coefficient of weir geometry where specified

A = area of fluid element

b = coefficient of weir geometry

c = coefficient of fluid properties

C = discharge coefficient (dimensional)

C_e = effective discharge coefficient

C_d = discharge coefficient

C_1 = constant multiplier

C_2 = constant multiplier

dA = differential area

dC = differential coefficient of discharge

dh = differential piezometric head

dv = differential velocity

dy = differential depth or height

$\Delta\psi$ = differential amount of the stream function

$\Delta\Phi$ = differential amount of the potential function

$E_\forall$ = bulk modulus of elasticity

F_E = elastic force

F_g = gravity force

F_I = inertial force

F_p = pressure force

Fr = Froude Number (subscripted m or p indicates model or prototype respectively)

F_σ = surface tension force

F_V = viscous force

g = acceleration of gravity (subscripted r, m or p subscript indicates ratio, model or prototype respectively)

γ = specific weight of fluid

h = piezometric head

h_e = effective piezometric head

H_t = total head over weir (piezometric head plus velocity head)

h_v = velocity head

K_l = correction for surface tension and viscous effects

k_h = piezometric head correction

k_L = length correction

l = characteristic length (subscripted with r, m or p indicates ratio, model or prototype respectively) or length of one face of a cubic fluid element

L = length of weir

L_e = effective weir length

lbs = pounds

m = meters

μ = dynamic viscosity of fluid

N = Newtons

O() = order of error with magnitude ()

p	=	pressure on a fluid element (subscripted with 1 or 2 indicates location)
P	=	height of weir
q	=	unit flow rate
Q	=	flow rate (subscripted with r indicates ratio)
r	=	radius of crest curvature
Re	=	Reynolds Number
ρ	=	density of fluid
s	=	seconds
Φ	=	potential function
ψ	=	stream function
σ	=	surface tension of fluid
t	=	time (subscripted with r indicates ratio)
u	=	component of velocity in x direction
v	=	component of velocity in y direction
V	=	velocity (subscripted with r, m, p, 1 or 2 indicates ratio, model, prototype, location 1 or location 2, respectively)
$\forall$	=	volume of fluid element
w	=	thickness of weir crest parallel to the flow
We	=	Weber Number
ω	=	uncertainty of measurement
x	=	ordinate of 2-dimensional Cartesian coordinate system
y	=	depth (subscripted 1 or 2 indicates location) and abscissa of 2-dimensional Cartesian coordinate system

y_o = known input depth

z = elevation (subscripted 1 or 2 indicates location)

INTRODUCTION

With advances in hydrologic forecasting and the availability of storm records, improved estimates of the probable maximum flood are available. With improved estimates, engineers are better able to assess the safety of existing dams. For the assessment, the engineer must know the stage-discharge relationships of the service and emergency spillways as well as the stage-discharge relationship for the entire dam if it should overtop (overtopping is a more difficult problem because of irregular boundaries, vegetation, and overland flow phenomena). Significant loss of property and potential loss of life can occur if a dam fails, so it is necessary that service and emergency spillway capacities be known as accurately as possible.

If the discharge capacity of the control structure is unknown, it must be estimated because it is virtually impossible to calibrate a full-scale spillway. Numerical models and/or physical models of the spillway can be used to estimate its discharge characteristics; however, both numerical and physical models have limitations.

Even with the most sophisticated supercomputers, the complete solution of simple turbulent flows, particularly those with a free surface, are extremely difficult. Because an infinitesimally small grid or mesh spacing would be required for the numerical solution of the full Navier-Stokes governing equations, a very large amount of computer memory would be required for even a small region of interest. However, exact solutions are possible for many hydrostatic and laminar-flow problems (Roberson and Crowe, 1993).

Surface water flowing in nature is rarely laminar, and, if it were, it would still require a tremendous computational effort to solve the governing equations.

Because it is so difficult to solve engineering problems involving fluid flow numerically or analytically, many solutions to these problems are obtained through experimental means. Physical modeling is the process by which the engineer is able to obtain information about the prototype through a scale model reproduction of the prototype. Models of hydraulic structures are almost always built smaller than the prototype for practical and economic reasons. Even with an exact geometric reproduction of the structure of interest, the engineer must be aware that information obtained from the model may not represent what is actually occurring for the prototype structure because of scale effects.

Scale effects are discrepancies between the model and the prototype caused by a combination of dynamic and kinematic effects introduced in the scaling process. Discrepancies of discharge, pressure, flow regime, and energy dissipation can occur. If these discrepancies are not properly accounted for, errors in predicting prototype performance will result. Errors in discharge prediction can result in underestimating or overestimating the spillway's capacity. Underestimating the spillway's capacity in the design phase can lead to costly construction expenditures, while overestimating a spillway's capacity may lead to dam failure if it cannot pass the probable maximum flood.

If a model is built too small, viscous and surface tension forces may dominate inertial forces. In prototype structures, viscous and surface tension forces are very small when compared to inertial forces. This phenomenon was observed in some of the writer's

experiments with small models and small flow rates. Other problems that can cause scale effects include relative roughness, inability to maintain aeration of the nappe, and maintaining experimental accuracy with regard to observed measurements.

Because much information and insight is obtainable through the use of hydraulic models, a study that investigates the effects of scale is justified. The writer chose to study scale effects for various configurations of weir-walls (flat-topped weirs which have a rectangular profile). Weir-walls were chosen because essentially every hydraulic control structure is, in some sense, a variation of a weir-wall. Much information has been published on the study of flow over weirs, but the literature does not contain a specific study on scale effects for weir flows.

The main objectives for this dissertation were:

1) Evaluate the capabilities and limits of use for a potential fluid flow numerical model to determine the discharge coefficients for various weir wall configurations. The inverse solution was utilized for the model development

2) Perform extensive laboratory experiments on weir-walls with similar geometries built to different scales to determine if scale effects exist and the flow conditions under which scale effects are present for each size.

3) Provide guidelines to avoid scale effects for modeling weir-walls or similar structures.

4) Provide discharge coefficients for weir-walls with crest thickness to height ratios of 0.0, 0.25, 0.50, 1.0, and 2.0.

This dissertation begins with an overview of the present knowledge of scale effects related to free surface flows. Then the governing equations of weir flow and similarity are developed. A potential model to predict the discharge coefficient is developed and evaluated. Next, the experiments are described and the results are analyzed. A procedure is developed for selecting the required model size or minimum model test conditions for a specified size that will avoid discharge coefficient scale effects. Finally, the results of the study are summarized and guidelines are given for hydraulic modeling of weirs and similar structures.

REVIEW OF LITERATURE

It is surprising that with the seemingly endless supply of weir information in the literature, limited information is available regarding the issue of scale effects. Some of the available information is cleverly disguised and intermingled with equations of discharge coefficients for numerous weir configurations.

Horton (1907, p. 999) stated, "Prior to 1850 the practice of weir measurement was in a somewhat chaotic condition. Experiments were made on so small a scale that the influences affecting the measurements and the lack of proper standards made the results untrustworthy." Horton (1907, p. 999) also added, "Greater advancement had been made in France, and that some of the work of the early French experimenters has proved to be of considerable value."

Rehbock (1929) conducted studies at Karlsruhe, Germany, on models of weirs of different scales. The models used were made of brass or wood, and in some cases were coated with sand to determine the influence of roughness. His studies included semi-circular crests, round-topped, and sharp-crested weirs. For weirs with semi-circular crests, the scales varied from 1:100 to 1:5 (crest radius of 1.25 cm to 25 cm). For the round-topped weir the range was smaller, while the sharp-crested weirs varied nine fold. His results showed that no deviations from the Froude law of similarity could be traced for weirs with rounded crests. His results also showed that roughness, length of weir, or temperature of water had little effect on the discharge coefficient. However, for the sharp-crested weir he noted considerable deviations from the law of similitude at low

flows and low heads. Shimoryama (1935) also found that viscosity has a completely negligible effect but that surface tension is important at low heads for sharp-crested weirs.

Johnson (1943) described the results of work completed on models of the Upper Narrows Dam on the Yuba River. Three models of this dam were used, with scales of 1:25, 1:40, 1:100. Each model was 6 inches wide, and about 24 inches high. The prototype structure is 225 feet high so only the top portion of the dam was modeled for the 1:25 and 1:40 model scales. The spillway has a steep upstream face with a quarter-round top sloping to a lip, which allows the water to spring from the downstream vertical face. The top is approximately 25 feet wide and the spillway is 225 feet high. One obvious scale effect noted was that for heads below 0.03 feet, the nappe would cling to the downstream face of the smallest model scale. All tests were made with the downstream nappe aerated by means of a 1-inch vent pipe. Each model was constructed of smooth varnished wood, but tests were also performed on the 1:25 and 1:40 scale models with a roughened surface. Significant findings for this study show that the influence of roughening was negligible, and that the discharge coefficient for the 1:100 scale model was consistently smaller than the others by 3 to 5 percent.

Kindsvater and Carter (1957) studied both suppressed and contracted thin-plate weirs. They noted that both viscosity and surface tension effect the discharge coefficient for low weirs with low heads. They proposed effective values of head and length of weir to be used in the following equation (to avoid confusion some symbols have been standardized and are not those given in the citations; however, the equations are the same as cited):

$$Q = C_e L_e h_e^{\frac{3}{2}} \quad (1)$$

where Q is the discharge in ft^3/s, C_e is the effective discharge coefficient, L_e is the effective weir length in feet, h_e is the effective head in feet. Equations for the effective length, L_e, and effective piezometric head, h_e, were given by:

$$L_e = L + k_L \quad (2)$$

$$h_e = h + k_h \quad (3)$$

where L is the weir width in feet and h is the piezometric head over the weir in feet. The terms k_L and k_h are quantities that represent the combined effects of the phenomena attributed to viscosity and surface tension. In their work, Kindsvater and Carter desired that the corrections k_L and k_h be constants or functions of not more than one variable. Both of these quantities were evaluated experimentally. In their work, Kindsvater and Carter proposed that the value of k_h is a constant value of 0.003 feet. The term k_L was given graphically by the authors and ranges from -0.003 feet to 0.013 feet depending on the flow conditions.

From work performed by the writer, adding 0.013 feet to the width or 0.003 feet to the piezometric head over the weir, when a small heads over the weir existed, significantly changed the value of the discharge coefficient. For large flow rates and heads, the addition of 0.003 feet is of no significance since it is possible for the surface wave fluctuations to be of that magnitude. When one is dealing with prototype structures, these corrections will not have a significant impact on the discharge. However, to make

these corrections to a 2-inch high weir in a 3-foot wide channel would give results deviating dramatically from those expected.

Singer (1964) attempted to assess the effects of crest roughness for broad-crested weirs. However, his attempts were unsuccessful. He did state that a smooth weir will have a slightly higher coefficient. He further added that in the case of extreme crest roughness, the reduction in the coefficient is quite marked and continuous.

Sreetharan (1988) studied the discharge characteristics of rectangular profiled weirs and investigated whether geometrically similar weirs yielded hydraulically similar flows. His results showed that for weirs with the same w/P ratio, w being the weir crest thickness and P being the weir height, that the same discharge coefficient resulted. However, for weirs of small height, less than 75 millimeters, the discharge coefficient was higher than for the larger scale models that were geometrically similar. The higher discharge coefficient could be due to an error in establishing the datum.

Kirkpatrick (1955) performed model studies on spillways at Tennessee Valley Authority dams. Model scales of 1:50, 1:100, and 1:200 were constructed of the Pickwick Landing Spillway. The prototype structure is approximately 46 feet high and has a vertical face. The downstream face of the spillway was designed with three compound circular curves. The crest radius is 12.5 feet, which is then joined by radii of 45.5 feet and 75.65 feet, respectively. The results of this study showed that maximum spread of the discharge coefficient curves for the three models did not exceed 2 percent and that no consistent relationship existed. Kirkpatrick concluded that because there was no consistent relationship, the variations were the result of experimental error and that

model scale did not affect the discharge coefficient. The lowest total head he tested was 0.0163 feet on the 1:200 model.

Hall, Maxwell, and Weggel (1969) conducted experiments to evaluate the effect of surface tension in Froude models. They studied both uniform and curvilinear flows, such as would be expected over a spillway. In their work with curvilinear flows with weirs and spillways, they hoped to develop a lower scale limit involving surface tension which would be independent of geometry. To do this, they used a surface tension additive (ZONYL A), which reduced the surface tension by a factor of 2.7 while only increasing the viscosity by 4 percent. They found considerable difficulty in obtaining a true value of surface tension since the effectiveness of the additive on the fluid varied with time. In their measurements, they showed surface tension varying from 0.0002 pounds per foot for the "older" free surface and 0.0005 pounds per foot for the "younger" free surface. Because of this effect, they used an "indicated surface tension." Their results showed that the influence of surface tension is masked by the inherent scatter of the data. They concluded that the smallest scale to which a Froude model may be built is not, in general, determined by surface tension. They further added that the smallest scale that a model may be built is determined by the accuracy with which the datum is established, the accuracy with which the data are obtained, and the accuracy with which the model represents the prototype.

Sarginson (1972) studied the effects of surface tension for flows over sharp-crested and circular crested weirs. He found that the discharge coefficient over a sharp-crested weir is a simple function of the Weber Number. He proposed a theoretically

obtained equation which compared well with the Rehbock formula, differing by no more than 1.5 percent. Sarginson's formula is given by:

$$Q = \left(1.81 + \frac{4.22}{We} + 0.22\frac{h}{P}\right) L h^{\frac{3}{2}} \tag{4}$$

where Q is the discharge in m^3/s, We is the Weber Number ($\gamma h^2/\sigma$), γ is the specific weight of water in N/m^3, σ is the surface tension of the water in N/m, P is the weir height in meters, and L is the width of the weir in meters. Equation 4 is only valid when the nappe springs free from the crest and is well aerated. For comparison, the empirical Rehbock formula is given by:

$$Q = \left(1.78 + 0.24\frac{h}{P}\right) L\left(h + 0.0011\right)^{\frac{3}{2}} \tag{5}$$

where Q is the discharge in m^3/s and all other variables are as previously defined. The terms 0.24h/P and 0.0011 are allowances for the approach velocity and surface tension respectively. The term 4.22/We has negligible effects for heads over 50 millimeters but becomes increasingly important with decreasing heads less than 50 millimeters. No equations will be given for circular crests, but they showed similar results. When the diameter of the circular crest exceeds 50 millimeters and the head exceeds 30 millimeters, the effect of surface tension is negligible. However, it becomes increasingly important at lower heads and smaller crest diameters.

Matthew (1963) studied curvature, surface tension, and viscosity of flows over round-crested weirs. His intent was to explain some of the scale effects encountered in hydraulic modeling. He suggested that for crests with a smaller radius of curvature, the

discharge coefficient would be larger than for crests with a larger radius of curvature. He also stated that for a given radius of curvature for a weir, the discharge coefficient increased with head. His studies on surface tension showed that at low heads the discharge coefficient was significantly reduced. His studies on the effects of viscosity were confined to a laminar boundary layer, which was small in comparison to the main body of flow. He proposed a general equation for the discharge coefficient, which can be applied to parabolic and circular crested weirs and is given by:

$$C_d = 0.385\left(1 + a\left(\frac{H_t}{r}\right) - b\left(\frac{H_t}{r}\right)^2 - c\left(\frac{r}{H_t}\right)\right) \tag{6}$$

where C_d is the dimensionless discharge coefficient, H_t is the total head in feet (piezometric head plus velocity head), r is the radius of curvature of the weir crest in feet, and the coefficients a and b are depend on weir geometry while the coefficient c incorporates the influences of surface tension and viscosity.

Raju and Asawa (1977) were concerned with flows over rectangular and 90° V-notch weirs associated with low heads. They argued that their equations for discharge were accurate at high heads but that the accuracy is questionable at low heads. To identify the effects of surface tension and viscosity, they used a mixture of kerosene and oil. They suggested the following equations for rectangular and 90° V-notch weirs, respectively:

$$Q = \left(\left(0.611 + 0.075\frac{h}{P}\right)\frac{2}{3}L\sqrt{2g}h^{\frac{3}{2}}\right)K_1 \tag{7}$$

$$Q = \left(\frac{8}{15} C_d \sqrt{2g} h^{\frac{5}{2}} \right) K_1 \qquad (8)$$

where h is the piezometric head, P is the height of the weir crest above the channel bed, L is the width of the weir, g is the acceleration of gravity, C_d the discharge coefficient, and K_1 is the correction factor for surface tension and viscosity effects. The correction factor is a function of the Reynolds Number (Re) with an exponent of 0.2 and the product of the Weber Number (We) with an exponent of 0.6. The corrrection factor is obtained graphically given $Re^{0.2}We^{0.6}$. For $Re^{0.2}We^{0.6} > 900$ the correction factor has no effect on the discharge for either the rectangular or the 90° V-notch weir.

Some of the more important findings in the literature are summarized below to set the stage for the present work. They are as follows:

1) There is disagreement in the literature as to whether or not scale effects exist or are significant for circular-crested weirs.

2) Roughness, length of weir, and temperature of water have little effect on the discharge coefficient.

3) Deviations from the law of similarity exist for sharp-crested weirs when they are operated with low flows and low heads.

4) There is some disagreement as to whether or not viscosity and surface tension affect weir flow. Accurately quantifying surface tension effects is nearly impossible.

5) From the research of Hall, Maxwell, and Weggel (1969), the smallest scale to which a model may be built is not related to fluid properties.

6) The results of scale effects on spillway crests are mixed. Kirkpatrick (1955) found no deviations exceeding 2 percent while Johnson (1943) found a 3 to 5 percent deviation.

7) No scale effects studies have been documented in the literature for flat-topped weirs.

With these points in mind, a study of dishcarge coefficient scale effects for weirs follows.

DEVELOPMENT OF EQUATIONS

Derivation of Weir Equation

The primary objective of this research is to examine scale effects over various weir-wall configurations, so it is necessary to develop the general equation which is used to predict discharge over weirs. This derivation is adapted from Flammer, Jeppson, and Keedy (1986).

To begin, the following are assumed: 1) the fluid is ideal and one-dimensional, 2) the pressure above the weir and throughout the nappe is atmospheric, 3) the streamlines above the weir and at some location upstream from the weir are straight and horizontal, and 4) the effects of viscosity and surface tension are negligible. Figure 1 shows the flow over a weir based on these assumptions.

The energy and continuity equations form the building blocks for the derivation to be presented. The continuity and energy equations are:

$$Q = v_1 y_1 = \int_A v_2 dA = \int_0^H v_2 L dh \tag{9}$$

$$\frac{p_1}{\gamma} + z_1 + \frac{v_1^2}{2g} = \frac{p_2}{\gamma} + z_2 + \frac{v_2^2}{2g} \tag{10}$$

where v is velocity, y is depth, A is area of flow, L is weir length, h is the length measured downward from the elevation of the water surface, H is the piezometric head over the weir, p is the gage pressure, z is the elevation above the datum, γ is the unit weight of water, and g is the acceleration of gravity. The subscripts indicate the location of the

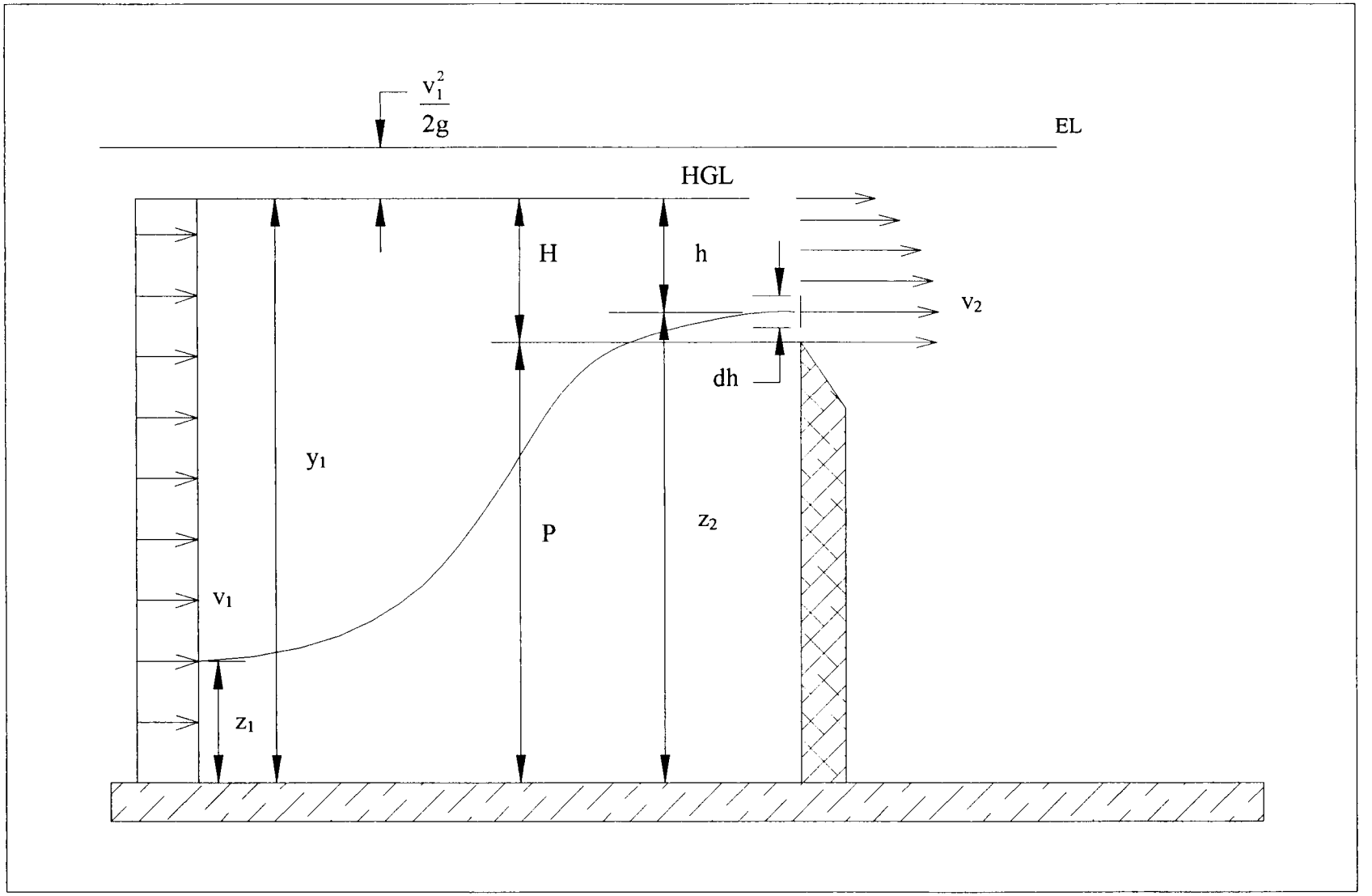

Figure 1. Ideal flow of water over a sharp-crested weir.

velocity, depth, elevation, and pressure for the quantity subscripted on a selected streamline.

The first step in the derivation is to determine the velocity v_2. To do this, the energy equation is written along a streamline from point 1 to point 2 in Figure 1 (points 1 and 2 exist in vertical planes some distance upstream and at the leading edge of the weir, respectively). The following equation results:

$$y_1 + \frac{v_1^2}{2g} = 0 + z_2 + \frac{v_2^2}{2g} \tag{11}$$

If the datum is at the channel bottom, then y_1 is the elevation of the hydraulic grade line (HGL) or $p_1/\gamma + z_1$. To further simplify the derivation, y_1 may be written as H + P and z_2 may be written as H + P - h, where H is the distance from the crest of the weir to the HGL. Making these substitutions and simplifying yields the following relationship for v_2:

$$v_2 = \sqrt{2g\left(h + \frac{v_1^2}{2g}\right)} \tag{12}$$

To finalize the derivation, the velocity v_2 is substituted into Equation 9 as follows:

$$Q = \int_0^H \sqrt{2g\left(h + \frac{v_1^2}{2g}\right)}\, L\, dh \tag{13}$$

Integration of Equation 13 yields the following discharge equation:

$$Q = \frac{2}{3} L\sqrt{2g}\left[\left(H + \frac{v_1^2}{2g}\right)^{\frac{3}{2}} - \left(\frac{v_1^2}{2g}\right)^{\frac{3}{2}}\right] \tag{14}$$

Equation 14 was derived based on several assumptions that apply only to an ideal fluid. Unfortunately, ideal fluid flow does not occur in nature; therefore, a correction coefficient or discharge coefficient must be applied to Equation 14 to account for the assumptions made in the derivation. Equation 14 takes the following form:

$$Q = C_d \frac{2}{3} L\sqrt{2g}\left(\left(H + \frac{v_1^2}{2g}\right)^{\frac{3}{2}} - \left(\frac{v_1^2}{2g}\right)^{\frac{3}{2}}\right) \tag{15}$$

where C_d is the discharge coefficient and H is the piezometric head over the weir.

Equation 15 is implicit because it involves an unknown flow rate Q, and associated with the unknown flow rate is the unknown velocity head at the location where the piezometric head over the weir is measured. It is often convenient to simplify the discharge equation by ignoring the velocity of approach. This yields a simple equation that allows a direct solution for the flow rate. However, for shallow approach channels, the approaching fluid may have a significant velocity component. It is important to account for the velocity of approach because it can significantly increase the discharge over the weir. Except where noted, the writer has adopted the commonly accepted, simplified form of the discharge equation for weirs:

$$Q = C_d \frac{2}{3} L\sqrt{2g}\left(H + \frac{v_1^2}{2g}\right)^{\frac{3}{2}} \tag{16}$$

Equation 16 is a simplified version of Equation 15 and maintains the effects of the velocity of approach.

Similarity Relationships

In order to perform hydraulic model studies of prototype structures, one must be sure the model represents the prototype structure. To accomplish similarity, relationships have been developed so that modelers can scale model data to the prototype and make sound judgments of model results. These relationships will be derived and discussed.

There are six forces that act on a fluid particle, and in order for similarity to exist, the force ratios from the prototype to the model must be equal. These forces are:

Inertia: $$F_I = \rho \forall a \quad (17)$$

Pressure: $$F_P = pA \quad (18)$$

Viscous: $$F_V = \mu \frac{du}{dy} A \quad (19)$$

Gravity: $$F_g = \gamma \forall \quad (20)$$

Elastic: $$F_E = E_\forall A \quad (21)$$

Surface Tension: $$F_\sigma = \sigma l \quad (22)$$

where ρ is the fluid density, $\forall$ is the volume of the fluid element, a is the acceleration of the fluid element, p is the pressure on the fluid element, A is the area of one face of the fluid element, μ is the dynamic viscosity of the fluid, u is the velocity of the fluid element normal to y, y is the direction normal to and into the flow, γ is the unit weight of the fluid, $E_\forall$ is the bulk modulus of elasticity of the fluid, σ is the surface tension of the fluid, and l is the length of one face of the fluid element or characteristic length. The most important of these forces for flow over a weir are the inertial, gravity, viscous, and surface tension

forces. It is the ratios of these forces that will be developed into dimensionless parameters used in correlating the model to the prototype and vice versa.

Because the inertial force is always present, ratios of this force to the other forces will provide dimensionless numbers that can then be used to develop model prototype relationships. The square root of ratio of inertial force to the gravity force is called the Froude Number (Fr) and is given by:

$$Fr = \sqrt{\frac{F_I}{F_g}} = \frac{V}{\sqrt{lg}} \tag{23}$$

where V is the total velocity and the other symbols are as previously defined. For these derivations the geometric and kinematic properties are written in terms of their fundamental dimensions, i.e., $\forall = l^3$ and $a = l/t^2$. The square root of the ratio of the inertial force to the viscous force is called the Reynolds Number (Re) and is given by:

$$Re = \sqrt{\frac{F_I}{F_V}} = \frac{\rho V l}{\mu} \tag{24}$$

The square root of the ratio of the inertial force to the surface tension force is called the Weber Number (We) and is given by:

$$We = \sqrt{\frac{F_I}{F_\sigma}} = \sqrt{\frac{\rho V^2 l}{\sigma}} \tag{25}$$

All of these numbers, Froude, Reynolds, and Weber, are dimensionless and provide the basis for similarity in hydraulic modeling with free surfaces.

Because weir flows are not effected by the elastic properties of water, i.e., it its incompressible the ratio of the inertial force to the elastic force is insignificant. The ratio

of the inertial force to the pressure force closes the force polygon meaning it is automatically satisfied by default when all other force ratios are equal.

Spillway flows are driven by gravity, as are many other flows involving a free surface. Therefore, it is customary to model these flows using Froude similitude. It is difficult to maintain complete similarity because the other dimensionless numbers may not have the same value for the prototype and the model. This is the primary reason that scale effects exist in hydraulic modeling.

Froude Modeling

To correlate the model to the prototype, the Froude Number for the model and the prototype must be equal ($Fr_m = Fr_p$, the subscripts indicate model and prototype, respectively). To derive the ratios of velocity, flow, and time, set the Froude Number for the prototype equal to the Froude Number for the model as follows:

$$Fr_p = Fr_m = \frac{V_p}{\sqrt{g_p l_p}} = \frac{V_m}{\sqrt{g_m l_m}} \tag{26}$$

The ratio of V_p to V_m is the velocity ratio V_r. It is given by:

$$V_r = \frac{V_p}{V_m} = \frac{\sqrt{g_p l_p}}{\sqrt{g_m l_m}} = \sqrt{g_r l_r} = \sqrt{l_r} \tag{27}$$

The gravity ratio (g_r) is unity and is omitted in the final form of the ratio indicated. To get the flow ratio, one can multiply the velocity ratio by the area ratio as follows:

$$Q_r = V_r A_r = \sqrt{g_r l_r} l_r^2 = \sqrt{g_r l_r^5} = \sqrt{l_r^5} \tag{28}$$

Manipulation of the velocity ratio yields the time ratio:

$$t_r = \frac{l_r}{V_r} = \frac{l_r}{\sqrt{L_r}} = \sqrt{l_r} \tag{29}$$

With these relationships in hand, it is useful to show that scale effects are caused by not maintaining complete similarity. Suppose Froude modeling is used with the prototype weir structure being 10 feet high and 10 feet wide with a sharp crest. To simplify the example, suppose that the model to be built is 1 foot high and 1 foot wide. Now suppose that a 1-foot deep flow with a velocity of 5 ft/s is going over the prototype and correspondingly a 0.1-foot deep flow with a velocity of 1.58 ft/s is flowing over the model. The Froude Number, based on flow depth, for both the prototype and model is 0.88. Now assume that the water in both the model and prototype is at 40 degrees Fahrenheit and has a viscosity, surface tension, and density of 3.23E-5 lb·s/ft^2, 0.51E-2 lb/ft, and 1.94 slugs/ft^3, respectively. The Reynolds Numbers for the prototype and model, based on flow depth, are 300310 and 9500, respectively. Likewise, the Weber Numbers, based on flow depth, for the model and prototype are 97.5 and 9.75, respectively. This shows that both Reynolds and Weber similarity are violated from the prototype to the model. Thus, scale effects might be present.

To have Froude, Reynolds, and Weber similarity, one would be required to use a fluid for the model which has a density to viscosity ratio which is 31.6 times greater than that of the prototype and a density to surface tension ratio which is 100 times greater than that of the prototype. These numbers indicate that the surface tension and viscosity would need to be significantly reduced. It would be extremely difficult to find a fluid with the

properties necessary to maintain Froude, Reynolds, and Weber similarity. Modelers usually use water and assume that the effects associated with not having complete dynamic similarity are minor when the model results are extrapolated to the prototype. Fortunately, experienced hydraulic modelers normally use models that are large enough to avoid serious scale effects.

For hydraulic modeling, there is a critical model size, or a critical model flow condition for the given size of the model. Operation below this size or flow condition will introduce scale effects. This research will lend insight into this problem and provide modeling guidelines to avoid and correct for scale effects.

POTENTIAL THEORY FOR FREE SURFACE FLOWS

Background

Because the full solution of the Navier-Stokes equations is difficult, if not impossible to obtain for a free surface discharge problem, potential theory has been used to determine discharge coefficients for spillways. This is because the boundary layer affects only a small portion of the flow near the crest of the spillway where the streamlines abruptly contract. Such flows are approximately irrotational in nature (Rouse, 1946).

Furthermore, to investigate the effects of viscosity, it would be useful to solve the flow of an ideal fluid flowing over a weir. Some work has already been accomplished in this area, but no review of literature shall be given. Numerical solutions to free surface flows are provided by Cassidy (1965), Markland (1965), or Vanden-Broeck and Keller (1987). The writer was unable to find any inverse solutions for weir flow in the literature.

Ideal Flow over a Weir

Figure 2 shows the ideal flow of water over a weir in the physical or x-y plane with the governing flow equations. The difficulty in solving this problem is that the location of the free surface, y, is unknown at the outset. The equations of continuity and irrotationality govern the problem and are given by:

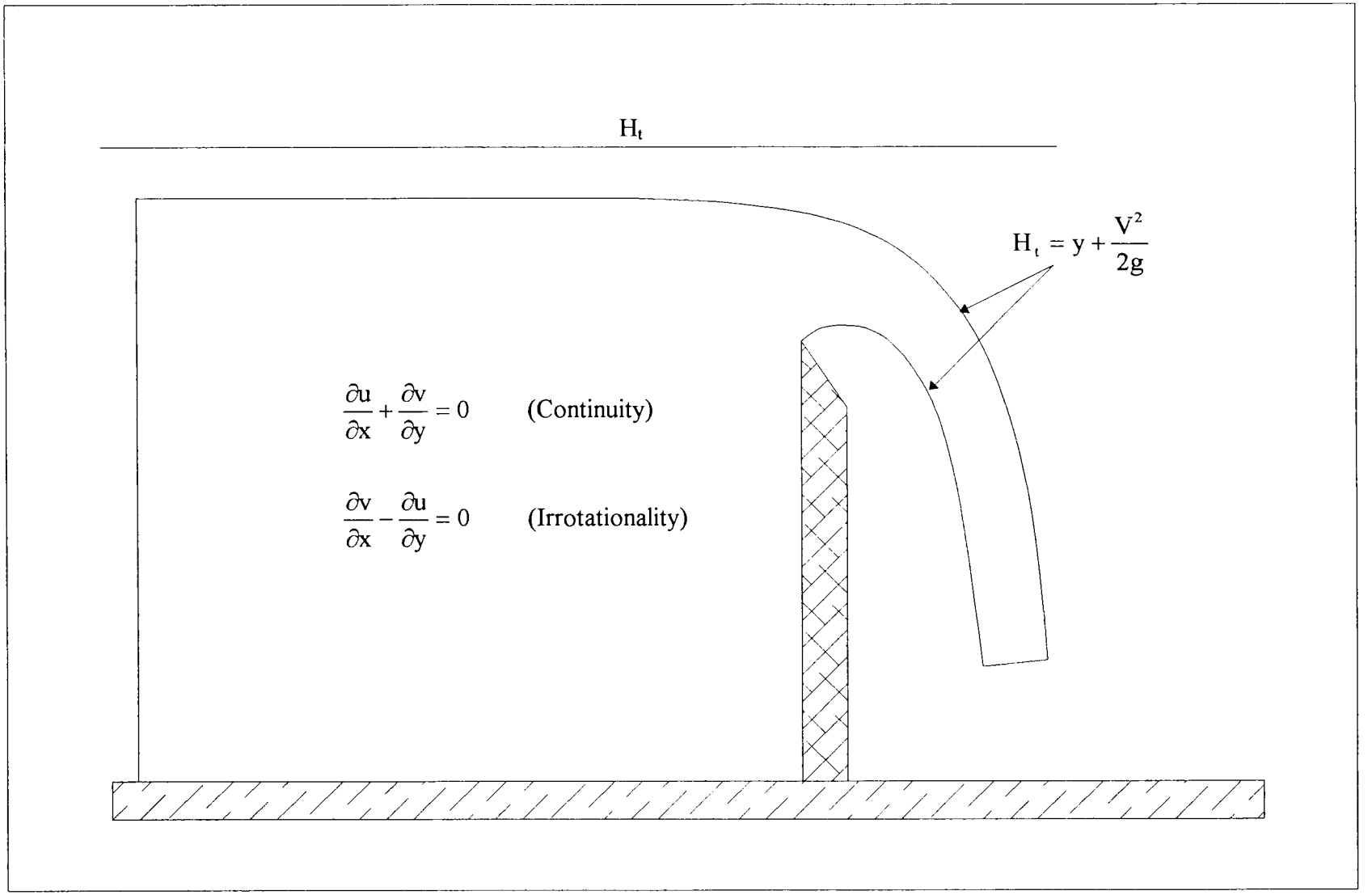

Figure 2. Ideal flow of water over a sharp-crested weir with governing equation and boundary conditions.

$$\frac{\partial u}{\partial x}+\frac{\partial v}{\partial y}=0 \tag{30}$$

$$\frac{\partial v}{\partial x}-\frac{\partial u}{\partial y}=0 \tag{31}$$

where u and v are components of velocity in the x and y direction, respectively.

A special boundary condition exists for the free surfaces of the flow, including the nappe. This boundary condition was adapted from one-dimensional hydraulics and is given by:

$$H_t = y+\frac{V^2}{2g} \tag{32}$$

where V is the absolute magnitude of the velocity ($V^2=u^2+v^2$), H_t is the total head, y is the depth, and g is the acceleration of gravity.

The x component of velocity, u, and the y component of velocity, v, equal the partial derivatives of the stream and potential functions as follows:

$$u=\frac{\partial \Phi}{\partial x}=\frac{\partial \Psi}{\partial y} \tag{33}$$

$$v=\frac{\partial \Phi}{\partial y}=-\frac{\partial \Psi}{\partial x} \tag{34}$$

where Φ is the potential function and Ψ is the stream function.

Substitution of Equations 33 and 34 into Equations 30 and 31, the continuity and irrotationalty equations, produce LaPlace's equation for Φ and Ψ, respectively. To make the problem more manageable, an inverse solution to the problem will be described.

Inverse Solution for Weir Flow

Inverse solutions are such that the dependent and independent variables swap roles. The utility of inverse solutions for flow through the core of a dam has been documented and proven an effective means for obtaining a solution to the location of the free surface or streamline (Jeppson, 1968). Because weir flow involves a free streamline with an unknown elevation, the inverse formulation defines the problem nicely. The flow rate must be specified and an initial depth of flow at some upstream location. The inverse solution makes the elevation of the free surface and the elevations of the stream and potential line intersections in the domain of the problem the unknown variables. When the elevations at each calculation point, or intersection of stream and potential lines, are solved, the corresponding values of the horizontal distance or x values can be calculated using the fact that x and y are conjugate functions. This technique provides the elevation of the free streamline and the elevation of the crest of the weir. With the initial flow rate specified, and the elevation of the free streamline known, the discharge coefficient can be calculated using Equation 16.

The inverse solution for weir flow will now be developed. To begin, substituting partial derivatives of the stream and potential functions for the u and v velocities gives:

$$V^2 = u^2 + v^2 = \left(\frac{\partial \Psi}{\partial y}\right)^2 + \left(\frac{\partial \Phi}{\partial y}\right)^2 \tag{35}$$

which are then substituted into the energy equation as follows:

$$H_t = y + \frac{\left(\frac{\partial \Psi}{\partial y}\right)^2 + \left(\frac{\partial \Phi}{\partial y}\right)^2}{2g} \tag{36}$$

where all variables are as previously defined. Because Φ and Ψ are described by the LaPlace equation, the equation that considers y the dependent variable in the Φ-Ψ plane is:

$$\frac{\partial^2 y}{\partial \Phi^2} + \frac{\partial^2 y}{\partial \Psi^2} = 0 \tag{37}$$

and the free streamline boundary condition becomes (Lamb, 1945):

$$\left(\frac{\partial y}{\partial \Phi}\right)^2 + \left(\frac{\partial y}{\partial \Psi}\right)^2 = \frac{1}{2g(H_t - y)} \tag{38}$$

The dependent variable is y in equations 37 and 38 with all other variables specified.

The solution for Equation 37 in the domain of the problem and Equation 38 on the free streamlines will enable prediction of the discharge coefficient given initial depth y_o and the corresponding total head H_t,. Figure 3 shows the ideal flow of water over a weir with the needed equations and boundary conditions to obtain a solution for the y elevations. Figure 4 shows the mapping from the physical plane to in the Φ-Ψ plane. The utility of using the Φ-Ψ plane is that H_t and y_o are specified, which, in turn, sets the total unit flow rate, q, which is equal to Ψ, the value of the free streamline in the computational plane.

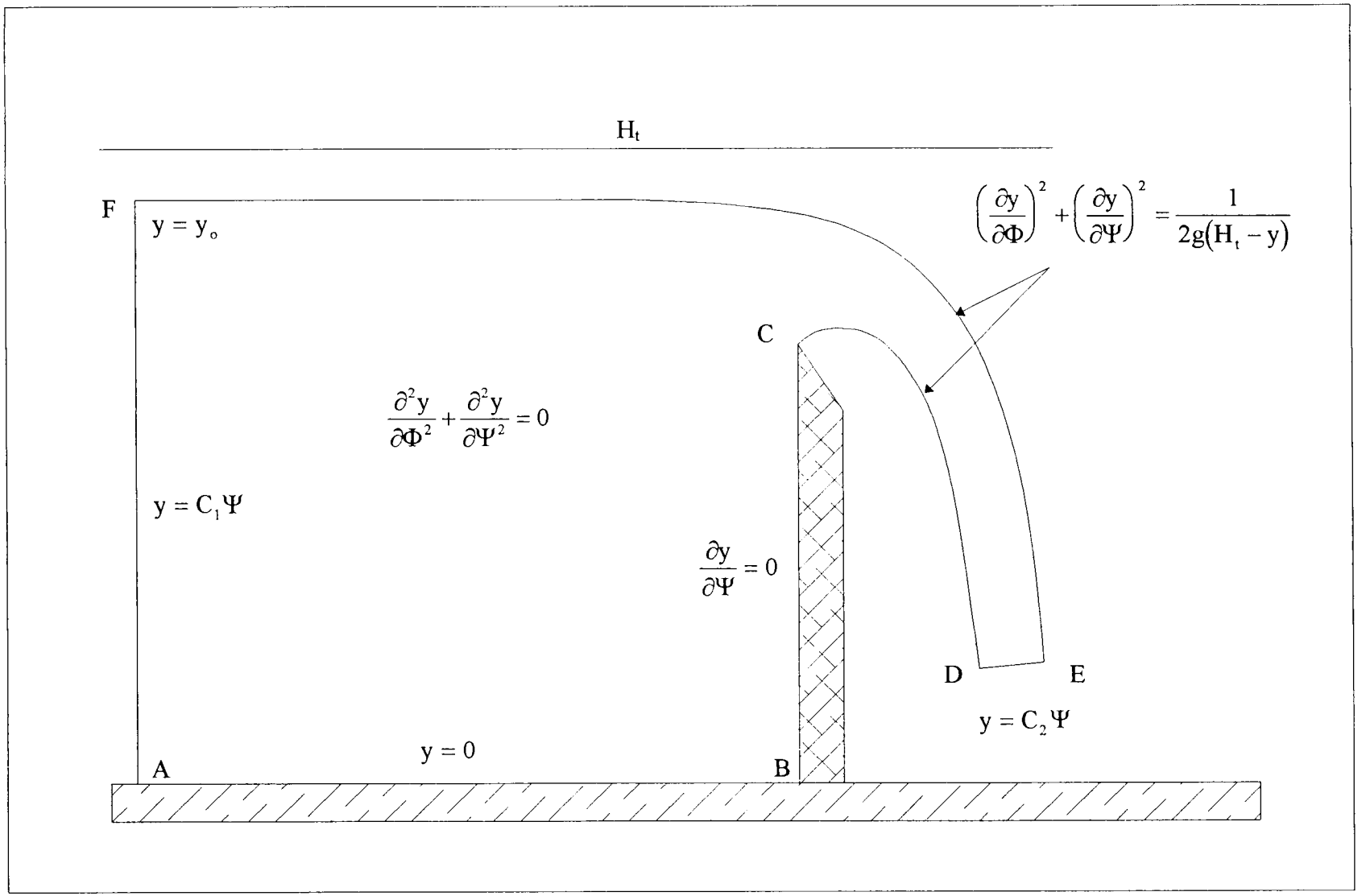

Figure 3. Ideal flow of water over a sharp-crested weir with governing equation and boundary conditions for inverse formulation.

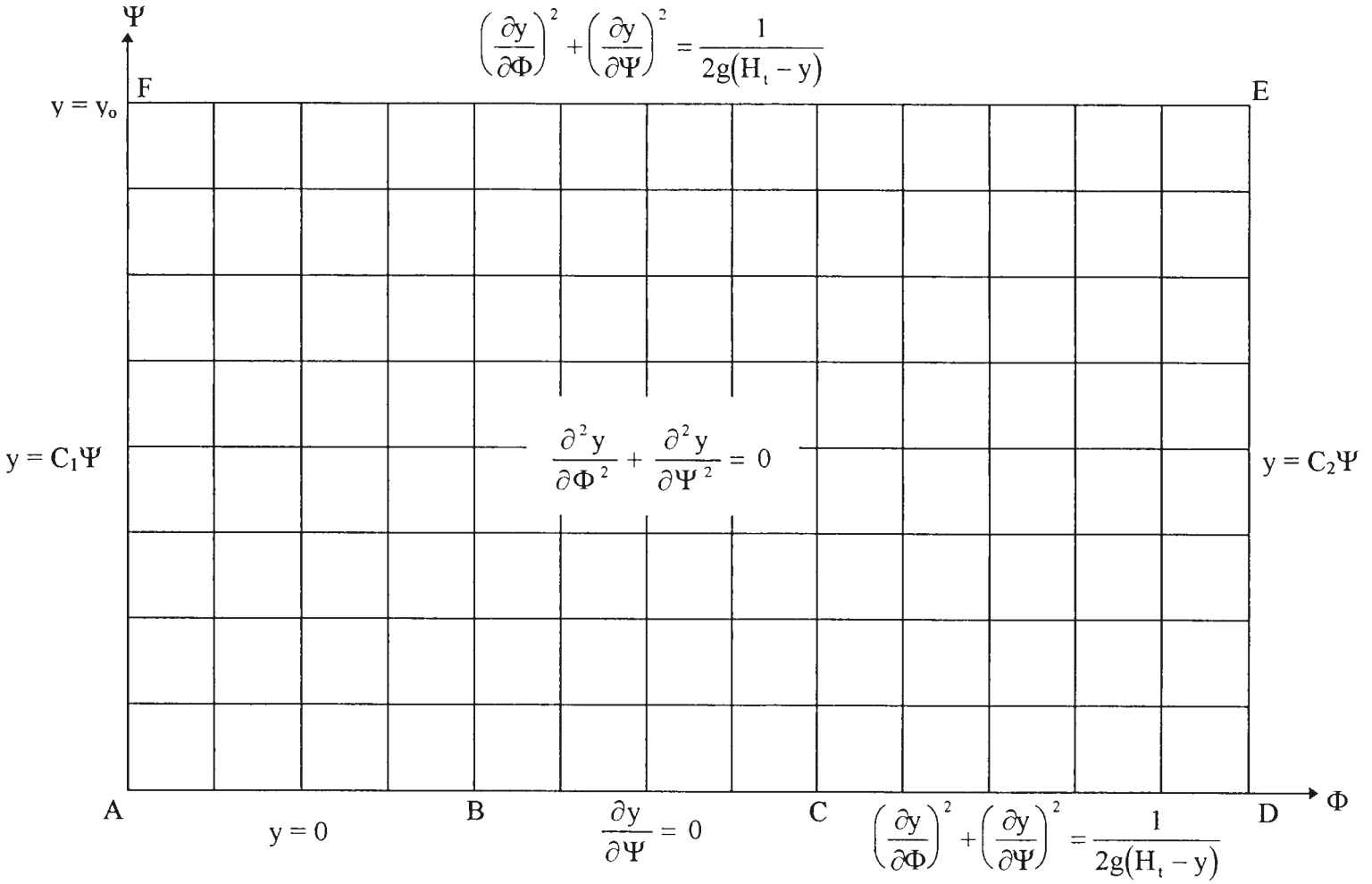

Figure 4. Mapping of physical plane into Φ-Ψ plane with governing equation and boundary conditions for inverse formulation.

Discussion of Boundary Conditions

The free surface boundary conditions, F-E and C-D, arise from the Bernoulli equation applied at any point on the free surface. The gage pressure on the free surface is zero and is not maintained in the equation. The left boundary, A-F, is assumed to have a uniform flow with no component of vertical velocity. By specifying the initial depth, y_o, at uniform flow makes y a linear function of Ψ at the upstream boundary A-F. When the elevations of the free surfaces on the nappe, both upper and lower, are calculated, the elevations of the streamlines on the right boundary, D-E, between the free surfaces are linearly interpolated. The weir face, B-C, is governed by a derivative boundary condition to force the potential lines to come into it at right angles. The number of potential drops across the weir face must be specified so the numerical scheme can calculate the height of the weir. The simplest boundary condition is for the floor of the channel, A-B, where the elevation of the streamline is zero.

Finite Differencing the Inverse Equations

There is no analytical solution to equations 37 and 38 and therefore they must be solved numerically. The finite difference approximation to the derivatives contained in equations 37 and 38 are given by the following equations:

First-order backward first derivatives:

$$\frac{\partial y}{\partial \Phi} = \frac{y_{i,j} - y_{i-1,j}}{\Delta \Phi} + O(\Delta \Phi) \tag{39}$$

$$\frac{\partial y}{\partial \Psi} = \frac{y_{i,j} - y_{i,j-1}}{\Delta \Psi} + O(\Delta \Psi) \tag{40}$$

Second-order backward first order derivatives:

$$\frac{\partial y}{\partial \Phi} = \frac{1.5y_{i,j} - 2y_{i-1,j} + 0.5y_{i-2,j}}{\Delta \Phi} + O(\Delta \Phi^2) \tag{41}$$

$$\frac{\partial y}{\partial \Psi} = \frac{1.5y_{i,j} - 2y_{i,j-1} + 0.5y_{i,j-2}}{\Delta \Psi} + O(\Delta \Psi^2) \tag{42}$$

Second-order central second derivatives:

$$\frac{\partial^2 y}{\partial \Phi^2} = \frac{y_{i-1,j} - 2y_{i,j} + y_{i+1,j}}{\Delta \Phi^2} + O(\Delta \Phi^2) \tag{43}$$

$$\frac{\partial^2 y}{\partial \Psi^2} = \frac{y_{i,j-1} - 2y_{i,j} + y_{i,j+1}}{\Delta \Psi^2} + O(\Delta \Psi^2) \tag{44}$$

The terms O( ) represent an error of order less than or equal to the term in parenthesis in the finite difference approximation and are dropped for the numerical solution. To simplify the numerical solution, the terms $\Delta\Phi$ and $\Delta\Psi$ are assigned the same value while maintaining consistency with the specified problem (i.e., $\Sigma\Delta\Psi = q$).

Numerical Attempt to Solution of Flow over a Flat Wall

Before a full solution to the problem shown in Figure 3 was attempted, the solution to the uniform flow over a flat wall was attempted. The purpose for this was to gain insight into the numerical scheme and determine if a solution is possible. The reason a flat wall was selected was because it has simple boundary conditions on the left and right boundaries and is an approximation to the flow approaching a weir.

Five different FORTRAN programs were written to attempt to solve the inverse problem of flow over a flat wall. They incorporate the free surface boundary condition, and in two of the programs allow the right boundary to be solved in the solution process. The programs prompt the user for: H_t, the total head; y_o, the known depth at the left boundary; an absolute convergence tolerance; and the maximum number of iterations to achieve a solution at the tolerance indicated.

Program FSA.FOR was the first program written. It utilized a successive over-relaxation (SOR) technique to solve for the unknowns in the interior of the domain, and the Newton method to solve for each unknown on the free surface. The interior of the domain was solved by a second-order approximation to Equation 37 and a second-order backward approximation to Equation 38 on the free surface. The program initially showed promise for convergence, but soon into the iteration process it diverged.

Program FSB.FOR was the second program developed. It was written to determine whether using first-order approximations for the derivatives on the free surface would yield a solution. This program utilized a SOR technique in the interior of the domain and the Newton method to solve a system of nonlinear equations for the depths on the free surface. This program converged even though convergence was somewhat erratic.

Program FSC.FOR utilized second-order approximations for the derivatives on the free surface. It is essentially identical to program FSB.FOR, but uses second order approximations. The results were similar to those found with program FSB.FOR.

Program FSD.FOR was written to solve a system of linear equations coupled with the nonlinear equation on the free surface. This solution solved the system while holding Φ constant and allowing Ψ to vary. The solution moved from the first Φ line away from the left boundary and proceeds to the Φ line adjacent to the right boundary. This solution was the most erratic and had difficulty converging. When convergence did occur, the governing equations were satisfied, but the results were not those desired.

The last program written was FSE.FOR. This program solved the entire system of linear equations coupled with the nonlinear equations on the free surface. This presented some computational difficulty because the system to be solved, when using the Newton method, is a square matrix with the dimensions equal to the number of streamlines minus one multiplied by the number of potential lines minus two. This program fixed the bottom, left, and right boundaries with the correct solution. It was desired that by solving the entire system of equations, that the solution would be forthcoming and produce the numbers expected for the free streamline elevations. Unfortunately, the program would not converge on the correct elevation of the free streamline, even though it did run to convergence on a solution. The governing equations were satisfied; however, the resulting elevations were not realistic.

Each of the programs with the exception of program FSA.FOR did converge to a solution. Many times the solution process would proceed nicely, then suddenly the error would increase by several orders of magnitude. The error would then show an erratic behavior and eventually converge to a solution.

Figure 5 shows the flow net for the uniform flow over a flat wall. Each horizontal line is for a particular value of Ψ equal to a constant and each vertical line is for a particular value of Φ equal to a constant. The top boundary is where the free streamline equation governs the depth. The interior points are determined by satisfying the Laplace equation.

Figure 6 shows the numerical solution for the uniform flow over a flat wall obtained by using program FSC.FOR. In order to have the numerical scheme begin iteration, the elevation of the top surface was estimated. Even though the governing equations were satisfied, the solution is not correct. The simulated free surface shows an erratic behavior that has not been experimentally observed for a uniform flow over a flat wall. The interior of the problem domain also shows difficulties which are associated with the fluctuating free surface. Again, the horizontal and vertical lines represent values of Φ and Ψ, respectively. Obviously, the numerical representation of the free surface condition is highly unstable.

Numerical Solution Difficulties

In order to understand what is happening with the numerical solution, it would be appropriate to evaluate the governing equations. The governing equation, the inverse LaPlace equation, presents no difficulty and has only one root because it is a linear equation. The free streamline equation, on the other hand, is nonlinear and may have multiple roots. It would be useful to analyze the free streamline equation to determine the

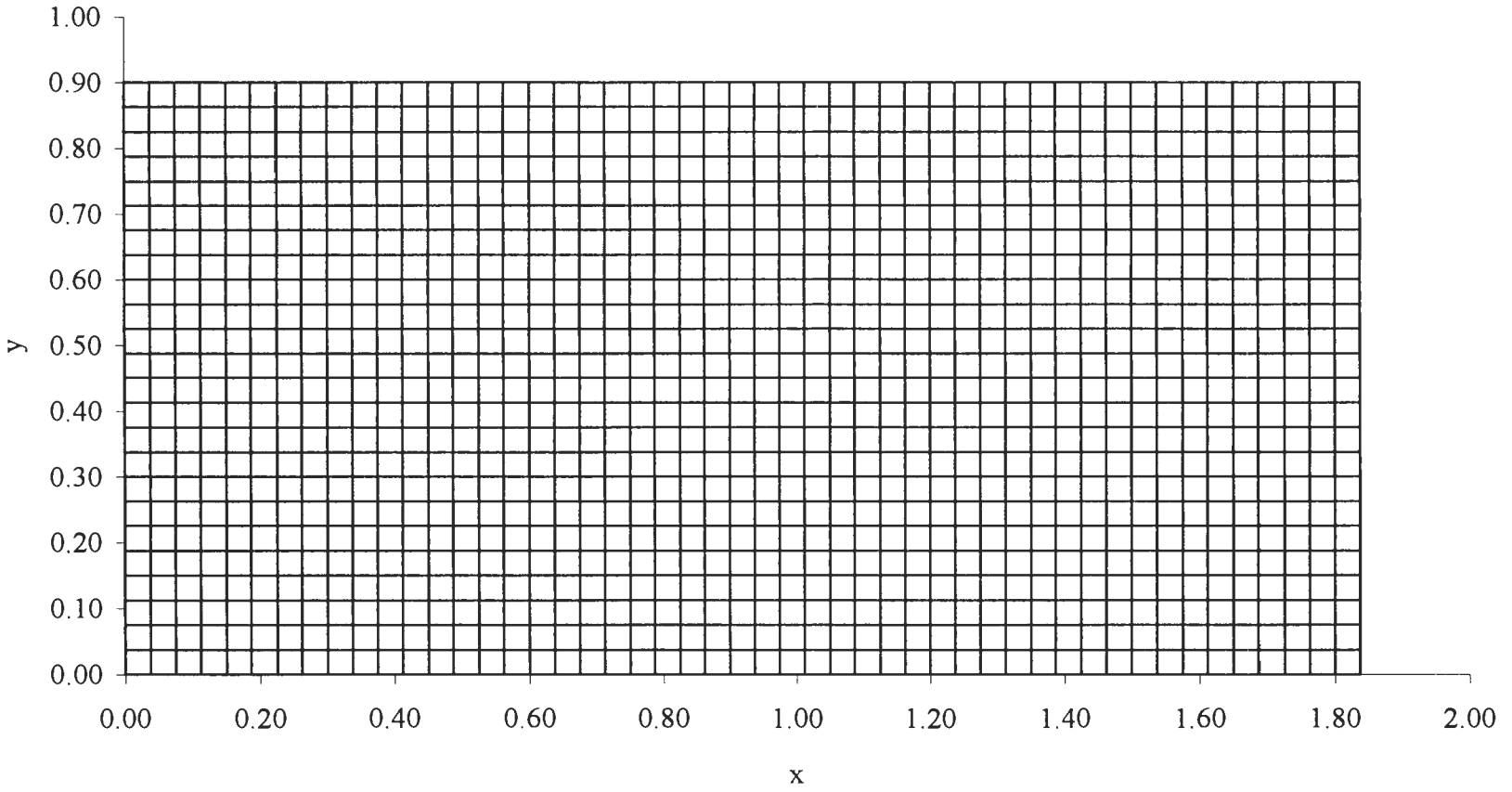

Figure 5. Correct flow net for the ideal flow of water over a flat wall.

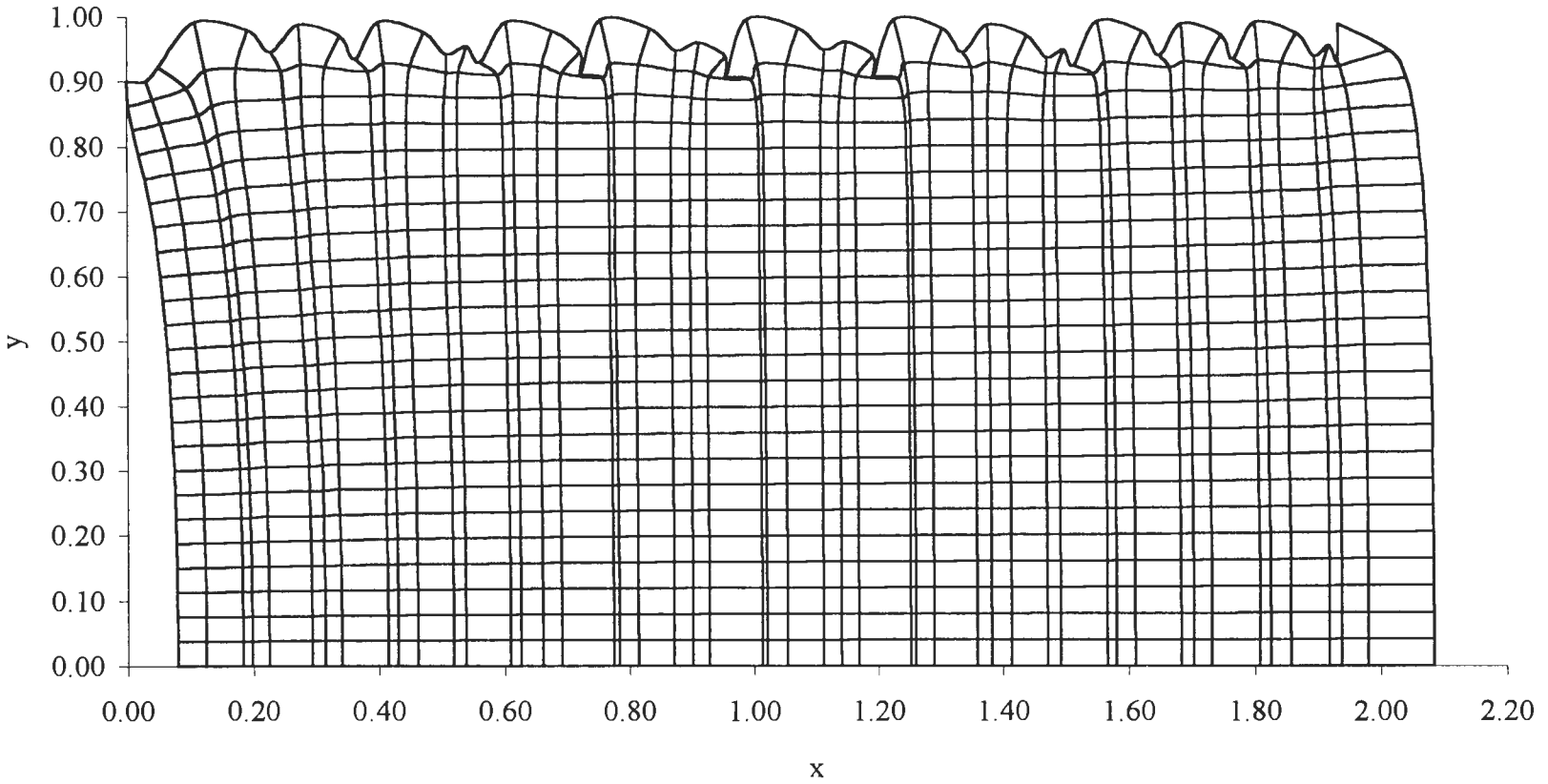

Figure 6. Numerical flow net solution for the ideal flow of water over a flat wall.

nature of the roots. The ideal situation would be if the free streamline equation has one real and positive root and two imaginary roots. If this is the case, it would be a simple matter for the Newton method to converge on the correct root.

The free streamline equation in finite difference form is:

$$\left(\frac{1.5y_{i,j} - 2y_{i,j-1} + 0.5y_{i,j-2}}{\Delta\Psi}\right)^2 + \left(\frac{1.5y_{i,j} - 2y_{i-1,j} + 0.5y_{i-2,j}}{\Delta\Phi}\right)^2 = \frac{1}{2g\left(H_t - y_{i,j}\right)} \qquad (45)$$

All y values indicate those located at the i,j point as shown by their subscript. The terms $\Delta\Psi$ and $\Delta\Phi$ are constants that are consistent to the total head H_t and the initial depth of flow, y_o. The term g is the acceleration of gravity.

To gain insight into Equation 45, assume that the following assignments have been made: $y_{i,j-1} = 0.8625$ feet, $y_{i,j-2} = 0.8250$ feet, $y_{i-1,j} = 0.9000$ feet , $y_{i-2,j} = 0.9000$ feet, $H_t =$ 1.0000 feet, $g = 32.2$ ft/s^2, $\Delta\Psi = \Delta\Phi = 0.0952$ ft^2/s. With these assignments the only unknown in the equation is $y_{i,j}$. The three roots to this equation are 0.9000 feet, 0.8776 feet, and 0.9974 feet. These numbers indicate three real positive roots that satisfy the free streamline equation on the free surface. The desired root is 0.9000 feet; however, the roots of 0.8776 feet and 0.9974 feet are only -2.5 and 10.8 percent from the desired root. With the proximity of the roots, it is impossible for the Newton method to "know" the root to which it should converge. An inappropriate root at one grid point obviously affects the results at adjacent points. This explains the erratic behavior of the free surface and the difficulty the numerical scheme faced when iterating to obtain a solution. Figure 7 shows the errors associated with the iteration process and how they vary when the free

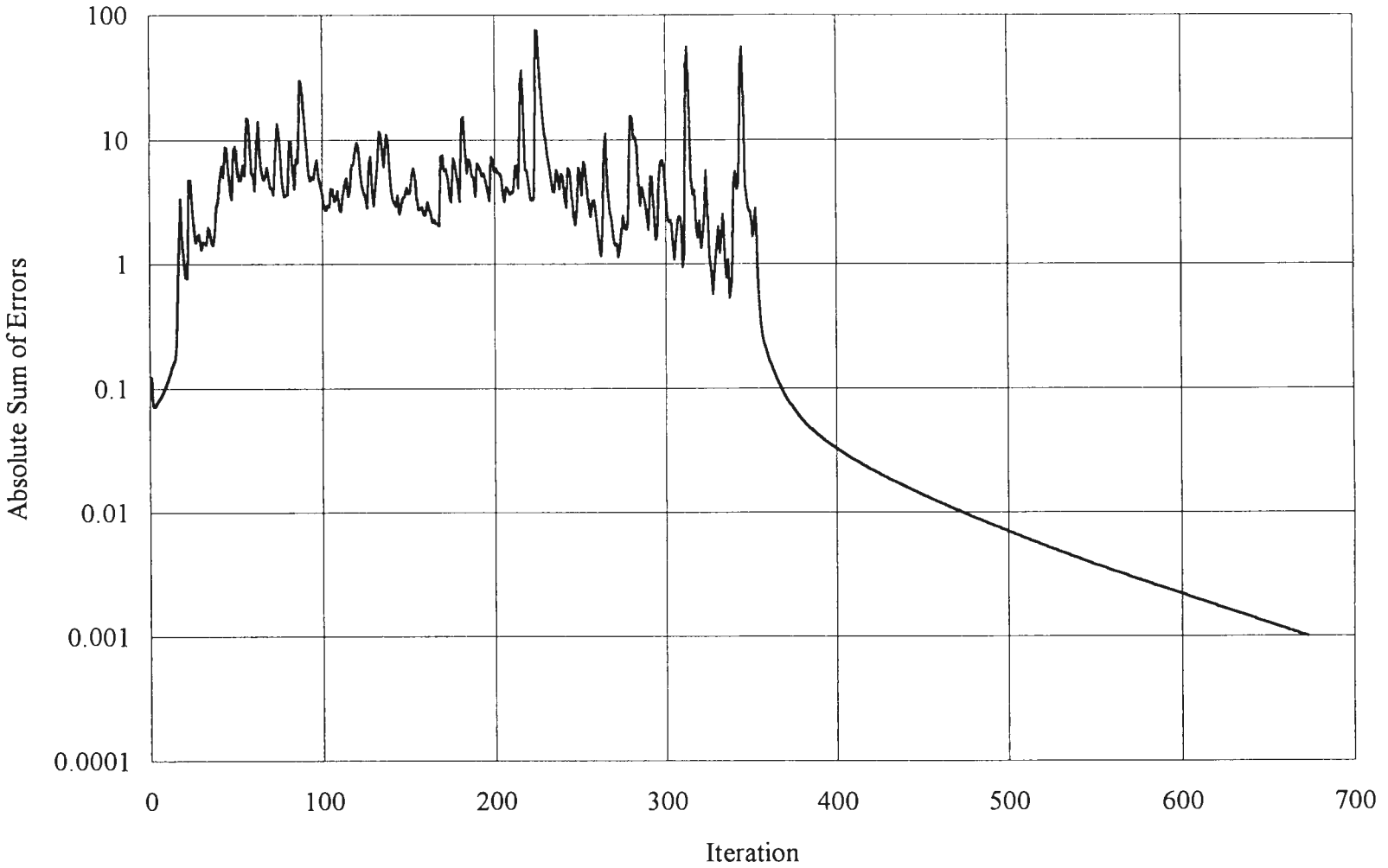

Figure 7. Absolute error vs. number of iterations for the numerical solution to the ideal flow of water flow over a flat wall. (Initialized to within 1 percent of the correct solution.)

surface is initialized to within 1 percent of the true solution. Because of the difficulty faced solving a simple flow over a flat wall, which approximates the upstream flow conditions at a weir, no attempt was made to solve the more difficult problem of flow over a weir with two free surface boundary conditions using an inverse formulation.

Summary of Inverse Formulation for Weir Flow

The results shown in this chapter indicate the difficulty one faces when solving flows with a free surface using the inverse formulation. A numerical scheme was developed and tested on probably the simplest flow condition possible, the flow over a flat wall, and failed. The difficulty arises in that the free streamline equation on the free surface has multiple real positive roots that are similar in sign and magnitude. The technique developed by Cassidy incorporates a single free surface and perhaps could be adapted to handle two free surfaces. Because of time and resource limitations, the writer will not attempt further numerical solutions but will rely on experimental means to quantify discharge coefficient scale effects for Froude models of weirs.

EXPERIMENT SETUP AND PROCEDURE

Flume Description

Testing for the research was completed at the Utah Water Research Laboratory (UWRL) at Utah State University. The primary flume utilized was 24 feet long, 3 feet wide and 2 feet deep. The flume had a metal floor with glass sides. The last 8 feet of the flume had wood sides installed for this research. The purpose for wood siding was to simplify installation of the weirs. Prior to testing, the flume was leveled using a spirit level in the horizontal plane, and then checked by maintaining a static water surface in the flume. A 16-inch remote controlled valve was used to regulate the supply of water to the flume. The flume was equipped with a point gage mounted on a roller carriage. This enabled precision point gage readings at any location in the flume. Figure 8 shows a schematic of the flume. In one series of tests a 3-foot wide by 7-foot deep tank was used to test a weir that was 2 feet high.

Water Supply

Water was supplied under gravity flow through a 48-inch pipe from First Dam, which is located at the mouth of Logan Canyon, on the Logan River. Because of its size, roughly 85 acre-feet, First Dam Reservoir acted as a constant level tank throughout the testing. This eliminated the need to use a skimming weir at the entrance of the flume. In order to keep large particles of debris from entering the laboratory, a screen was placed at the supply line entrance.

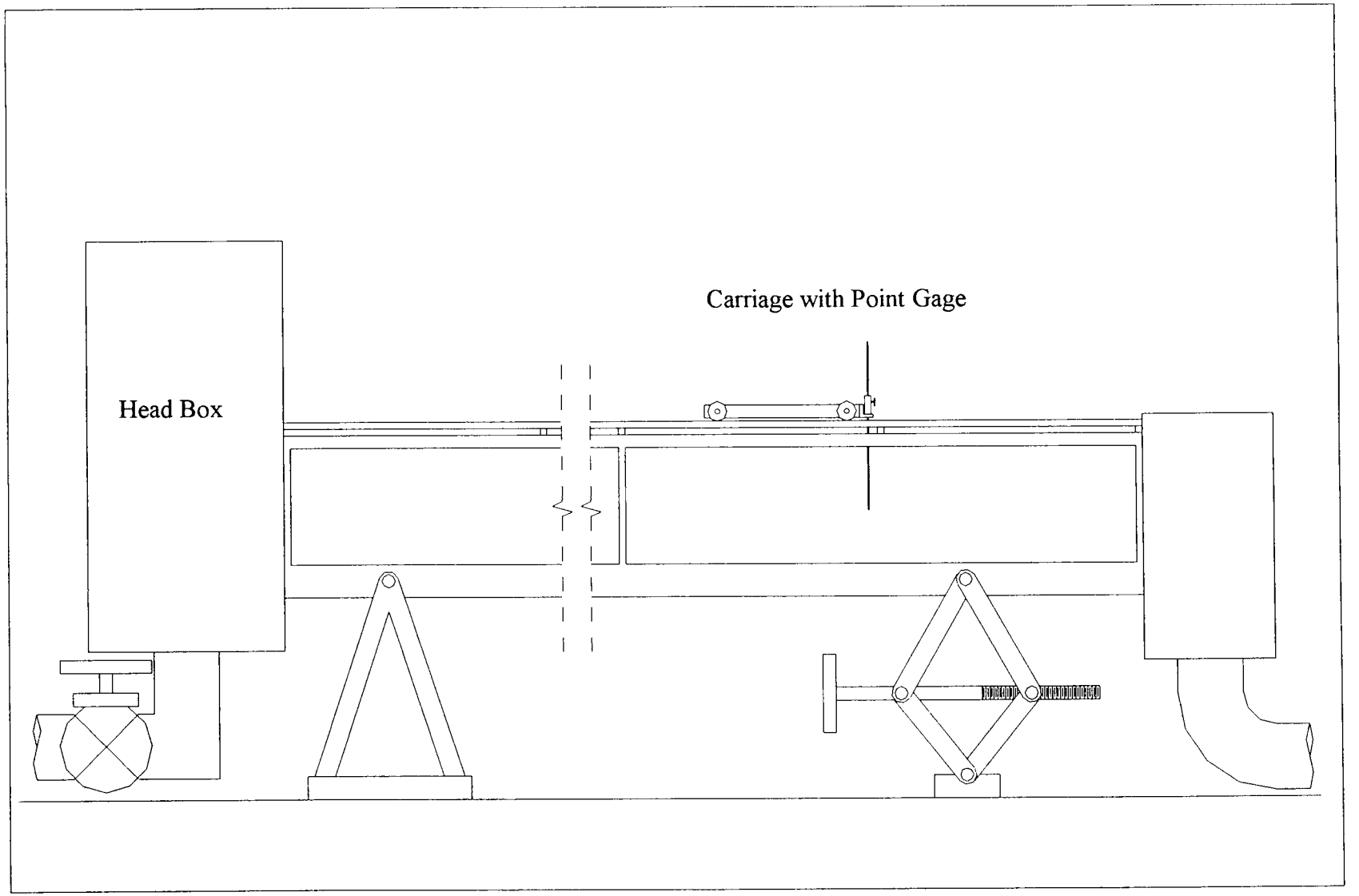

Figure 8. Schematic of the 3-foot wide by 24-foot long flume.

Flow Measurement

Most flow measurements were made using a weigh tank with a capacity of 25,000 pounds or, when the flowrate exceeded 2.5 ft^3/s, a volumetric tank with a capacity of 3,500 ft^3 was used. The weigh tanks and volumetric tanks are calibrated yearly by UWRL.

A critical issue in using the weigh tanks is the time over which the measurement is taken. By using a relatively long time, a more accurate flow measurement is possible. For the purposes of this study, weigh times of approximately 200 seconds were used. The exception to this was for larger flow rates, which filled the 25,000-pound tank in less than 200 seconds. When this was the case, two or three different flow readings were taken to verify the flow rate. The temperature was taken at the beginning of each data set to account for the specific weight of the water and ensure an accurate flow measurement when the weigh tanks were used to measure the volumetric flow rate.

Point Gage

A precision point gage was used to determine the elevation of the weir crest and obtain the water surface elevations of the approaching flow. The gage had a verneir scale marked in 0.001-foot divisions. The verneir scale was such that readings to the nearest 0.0005 foot were possible by interpolating between divisions. This was done periodically throughout the testing when the verneir scale divisions did not line up precisely to a 0.001-foot division.

To correct for roller carriage deviations, the flume was filled with enough water to cover the floor over the length of the flume and allowed to stabilize. The point gage was then moved to the locations where the water surface was to be measured during the testing. By subtracting the static water surface elevations at the measuring locations from the static water surface elevation at the weir, a correction for the carriage at each water surface measuring location results. These corrections account for slight deviations in the carriage and flume.

The location of the point gage relative to the weir for the water surface readings is a critical issue. Bos, Replogle, and Clemmens (1984) stated that the gauging station should be located sufficiently far upstream to avoid the area of water surface drawdown, yet it should be close enough for the energy loss between the gauging station and the structure to be negligible. Bos, Replogle, and Clemmens then stated that the stilling well should be located between 2 and 3 times the maximum total head over the structure upstream from the structure's leading edge. However, for this research, several scales of each weir were constructed and installed. To be consistent, it would be necessary to scale the roughness of the flume. To avoid this difficulty, several point gage readings were taken upstream from the weir, away from the drawdown region, and a straight line was regressed through the points and extended to the face of the weir being tested. The value of the regressed water surface elevation at the face of the weir was then used to calculate the piezometric head over the weir. Extending the regressed water surface elevation was the most consistent means to avoid the effects of flume roughness for different scale models. The velocity head was computed using the area of flow associated with the

piezometric head measurement and is based on the width of the weir and the sum of the piezometric head over the weir and the height of the weir.

Error Analysis

When hydraulic structures are calibrated, it is important to quantify the errors associated with the test facilities. Because it is not possible to obtain "exact" measurements, experimenters must realize that any measurement taken falls into a range where the "true" measurement is found. For example, the weigh tanks at the UWRL are calibrated to within ±10 pounds and even though the scale may indicate a weight measurement of 250 pounds, the "true" weight lies in the range between 240 to 260 pounds. Thus, the weigh tanks have a measurement uncertainty of ±10 pounds.

The following analysis, adapted from Kline and McClintock (1953), provides insight into the maximum magnitude of errors for the data collected for this study. The largest errors possible for this study are for the smallest weirs operating at the smallest heads. This is due to the ratio of the measurement uncertainty to the actual measurement being a maximum.

Because discharge coefficient errors need to be quantified, Equation 16 is solved for the discharge coefficient to give (note that Q and A are used to get V):

$$C_d = \frac{3Q}{2L\sqrt{2g}\left(h + \frac{V^2}{2g}\right)^{\frac{3}{2}}} \tag{46}$$

$$Q = \frac{\text{weight}}{\gamma \cdot \text{time}} \tag{47}$$

$$V = \frac{Q}{L(h+P)} \tag{48}$$

where V is the average velocity in the channel, γ is the specific weight of water, and all other variables are as previously defined. The variables with uncertainty are h, L, P, γ, weight (wt) of water measured, and time (t) of weight measurement. By using the data for the 2-inch high by 2-inch thick flat-topped weir, the measurements and their corresponding uncertainties (ω) are:

h	=	0.0160 ± 0.0005 feet
L	=	3.026 ± 0.0104 feet
P	=	0.171 ± 0.0005 feet
γ	=	62.42 ± 0.1 pounds/feet^3
wt	=	250 ± 10.0 pounds
t	=	282.93 ± 5 seconds

To asses the uncertainty for the discharge coefficient with the uncertainties given, Equation 46 must be differentiated with respect to each variable where uncertainty exists and then multiplied by the amount of uncertainty for that variable. These results are then squared and summed, and then the square root is taken. Finally this result is divided by the value of the discharge coefficient to determine the ratio of the error to the discharge coefficient for the conditions given. This equation is given by:

$$\frac{\left(\left(\frac{\partial C_d}{\partial h}\omega_h\right)^2+\left(\frac{\partial C_d}{\partial L}\omega_L\right)^2+\left(\frac{\partial C_d}{\partial P}\omega_P\right)^2+\left(\frac{\partial C_d}{\partial \gamma}\omega_\gamma\right)^2+\left(\frac{\partial C_d}{\partial wt}\omega_{wt}\right)^2+\left(\frac{\partial C_d}{\partial t}\omega_t\right)^2\right)^2}{C_d} \quad (49)$$

where ω with its associated variable subscript indicates the uncertainty for the variable.

In carrying out the mathematics and substituting the values given on the previous page, Equation 49 yields 0.065 or 6.5 percent error. This represents the maximum error in the discharge coefficients of this study. This error decreases with increasing head and weir size because the ratio of the uncertainty to the measurement decreases for the variables that cause the greatest influence in the errors. The average error for the data collected was 2.8 percent. Less than 10 percent of the data collected had errors exceeding 4.6 percent. Therefore, even with 6.5 percent error for the small weirs operating at small heads, the data for this study are sufficiently reliable to analyze discharge coefficient scale effects.

Weirs Tested

Two weir geometries were tested: flat-top and sharp-crested. The w/P ratio was used to define the geometry of a flat-topped weir, where w is the thickness of the weir crest (in profile) and P is the height of the weir. The ratio of w/P for the weirs tested varied from 0.0 to 2.0, with intermediate values of 0.25, 0.5, and 1.0. Figure 9 provides a general definition sketch of weir-walls. When the value of w was 0.0 (sharp-crested), a

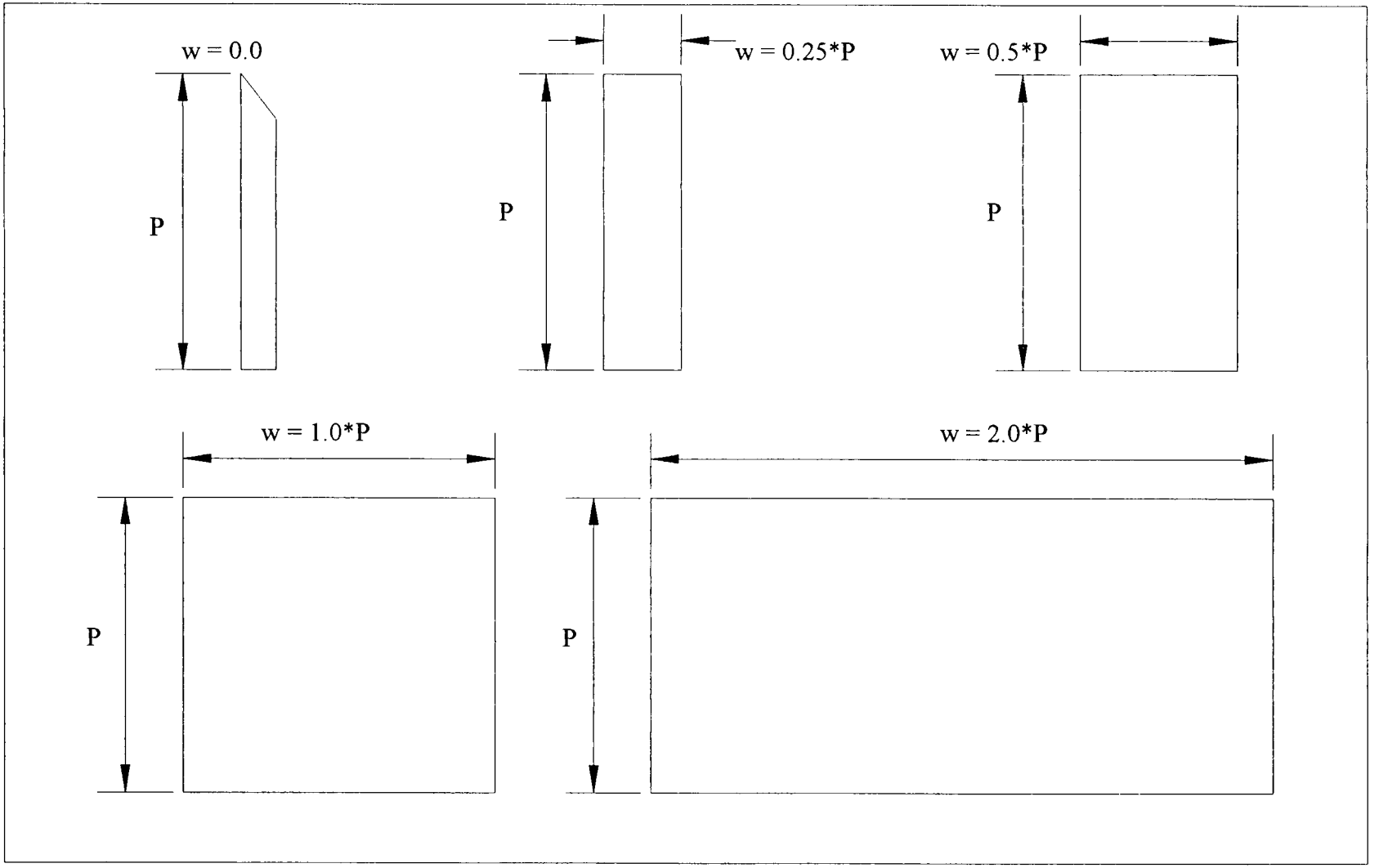

Figure 9. Weir geometries tested.

finite width weir was used, for structural stability, and tapered to a sharp edge ($w \approx 0$) at the crest. To avoid problems of warping and irregularities in the material used to construct the weirs, Plexiglas or Lexan was used for all weirs studied, with bracing in the flume as needed. Plexiglas and Lexan provide very smooth surfaces, which when scaled should not introduce weir roughness effects.

Side Wall Effects

In order to establish the existence of scale effects, one must ensure that a true model of the prototype is being tested. In this study, weirs of different scale of the same geometry in cross section were tested. It is a simple matter to construct a scale model in a two-dimensional sense. To obtain a three-dimensional model, dividers in the flume were utilized to test for side wall effects. Figure 10 shows a plan view of the 3-foot flume with dividers.

The dividers were placed in the flume upstream from the weir being tested. They were placed such that they would allow ample distance for fully developed flow to occur prior to reaching the weir. For the 2-inch high weir, dividers extending 4 feet upstream from the weir were used. This length was 32 times the maximum head over the weir. For the 3-inch high weir, the dividers extended upstream from the weir a length of 24 times the maximum head over the weir.

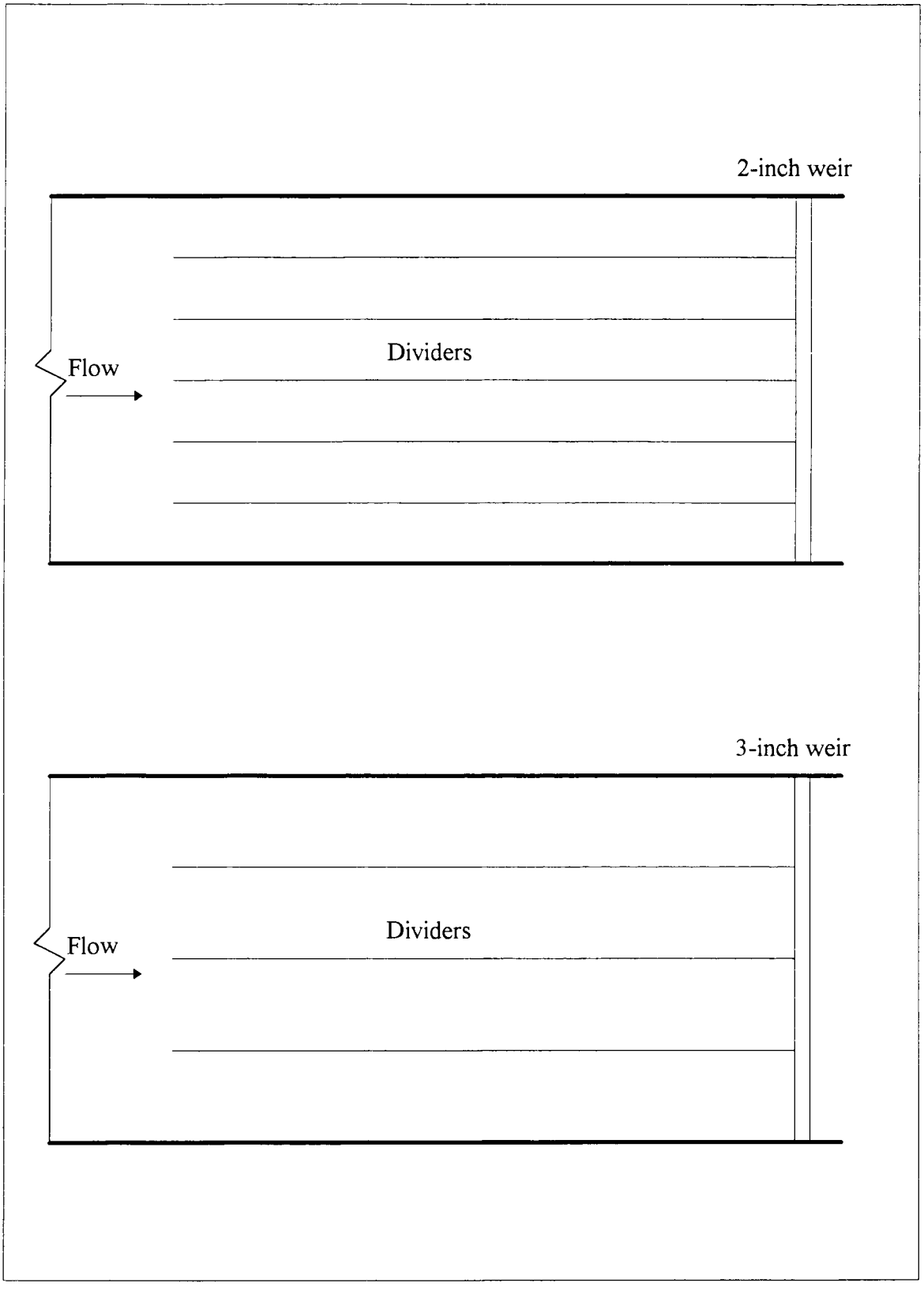

Figure 10. Flume with dividers for 2-inch and 3-inch high sharp-crested weirs.

Aeration

With the exception of one weir series, all weirs were installed at the end of the flume. This was done to provide an unrestricted air supply under the nappe so that atmospheric aeration could be maintained under the nappe at all times. For testing on weirs located midway in the flume, the writer was unable to maintain aeration under the nappe for smaller scale weirs. This created a small negative pressure under the nappe, which resulted in a discharge coefficient that was larger than that for atmospheric pressure under the nappe.

SCALE EFFECTS ANALYSIS

Regimes of Flow

Throughout the data collection phase of the research, three different flow regimes were observed for flat-topped weirs: clinging, leaping, and springing flow. Figure 11 shows each flow regime. Sharp-crested weirs had two different flow regimes: clinging and springing.

Clinging flow was observed for each weir geometry tested and was most prevalent for the smaller weirs with narrow crests. The clinging condition only occurred for small heads over the weir and was difficult to maintain for larger weirs with relatively longer crests. Because of the difficulty maintaining the clinging condition, the only data taken for clinging flow was for the weir with $w/P = 0.25$. Clinging data were taken with the weir installed midway in the flume and occurred naturally without being induced by increasing the tail water. Clinging would continue until the flow energy was large enough to cause the water to leap away from the downstream face of the weir. As the weir size increased, the maximum H_t/w value for which clinging flow occurred reduced, indicating scale effects.

As testing proceeded, it became evident that the discharge coefficient was dependent on the upstream depth and the depth of the tail water when clinging flow prevailed. Depending on the depth of the tail water, even at levels well below the crest of the weir, the discharge coefficient could assume a range of values. This is because the depth of the tail water influences the negative pressure region at the trailing edge of the

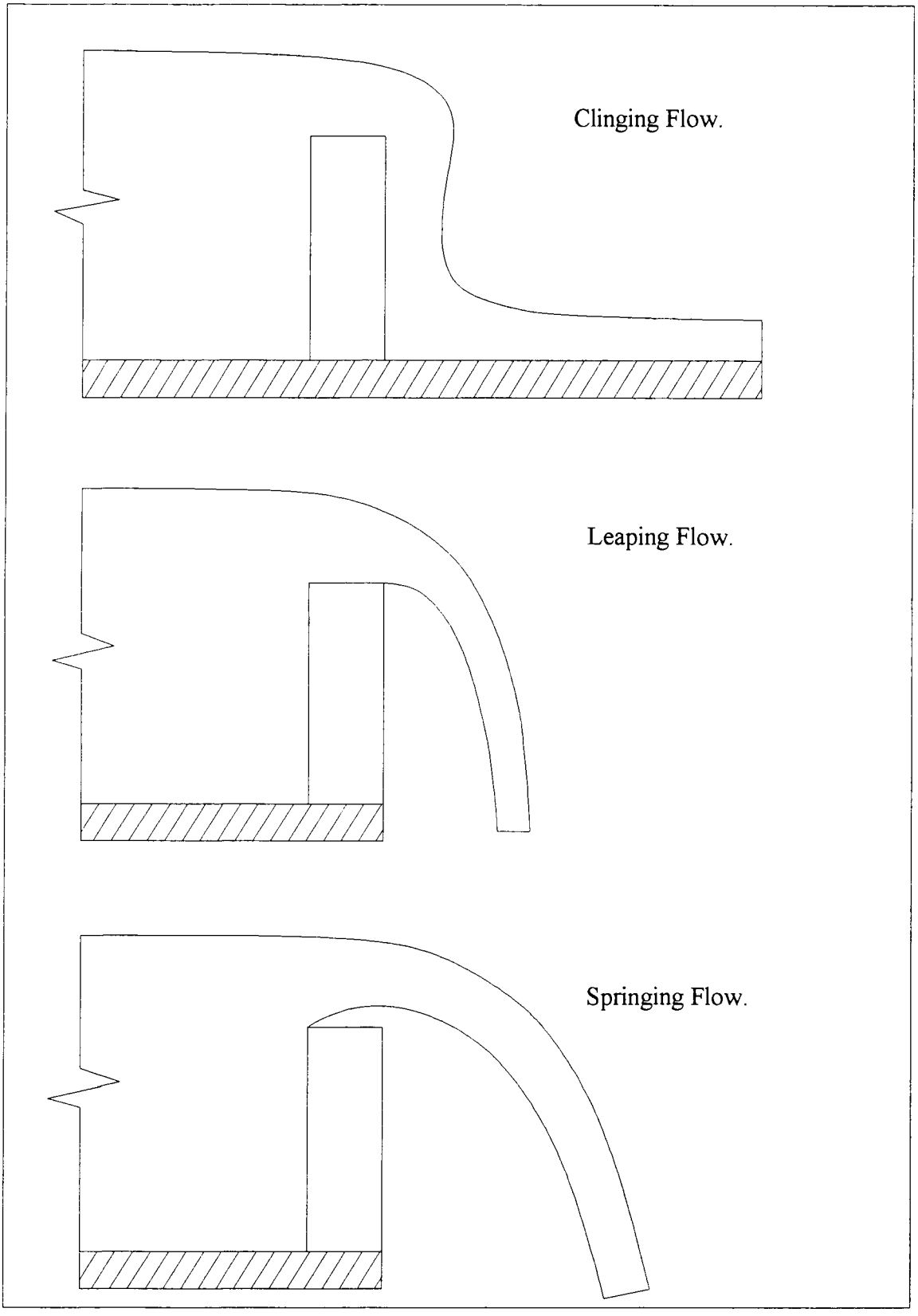

Figure 11. Flow regimes observed during data collection.

weir. By raising the tail water, the negative pressure at the trailing edge of the weir increases (approaches atmospheric) and no longer assists the flow over the weir. Because of the tail water effects, the weir location was changed to the end of the flume where a larger downstream drop prevented tail water effects. This research dealt only with unsubmerged flow conditions.

Leaping flow occurred when the flow energy was sufficient for the water to leap away from the downstream face of the weir. With the weir installed midway in the flume, leaping flow was difficult to maintain because atmospheric pressure is required under the nappe. However, with the weir installed at the end of the flume, atmospheric pressure could easily be maintained under the nappe. As with clinging, the H_t/w value for this condition differed for each weir size, reducing with increasing weir size, indicating scale effects. Leaping flow continued until H_t/w was large enough to facilitate springing from the leading edge of the weir.

Springing flow loses contact with the weir at the leading edge of the weir's crest. Thus, when springing flow occurs, the weir behaves as if it is sharp-crested. Springing required atmospheric aeration under the nappe and was also a function of H_t/w and the geometry of the weir. Because of the depth limitations of the flume, springing was only observable for weirs with $w/P = 0$, 0.25 and the 2- and 4-inch high weirs with $w/P = 0.50$. Along with clinging and leaping, scale effects were present for springing, such that larger values of H_t/w were required to initiate springing flow from the leading edge of the weir for decreasing weir sizes.

To understand the effect each flow regime has on the discharge coefficient, the flow regimes must be analyzed relative one to another at the same total head, assuming that each regime is possible. The discharge coefficient for clinging flow is larger than the discharge coefficient for leaping and springing flow due to the negative pressure region at the trailing edge of the weir, which increases the weir's capacity. Springing flow, on the other hand, causes the nappe to contract and decrease the weir's capacity. One may desire to operate a weir in one regime of flow over another; however, each regime can only occur when conditions corresponding to that regime prevail.

Effects of Side Walls

As discussed in the previous chapter, side walls were installed to examine the effects of channel width on the discharge coefficient. To accurately quantify side wall effects, a flow was established with the dividers in place (five dividers for the 2-inch high weir and four dividers for the 3-inch high weir). Flow rate and point gage readings were recorded. Then the dividers were removed without changing the flow rate, and point gage readings were recorded. The discharge coefficients for the two conditions were compared. The results indicated that the effects of the side walls were minimal, less than ± 0.5 percent average change for the 2-inch high sharp-crested weir and less than ± 0.2 percent change for the 3-inch high sharp-crested weir, showing that side wall effects were negligible. This is in agreement with Rehbock's (1929) findings, that the length of the weir has no effect on the discharge coefficient. Therefore, for all the data collected, the full width of the 3-foot wide flume was used for each weir size.

Nonerated and Aerated Comparison

Figure 12 shows the data collected for the weir with w/P = 0.25 with and without aeration. The nonaerated data were collected with the weir installed mid-way in the flume while the aerated data were collected with weir installed at the end of the flume. The midway installation allowed the weir to operate with the flow clinging to the downstream face of the weir and without any trapped air under the nappe. The end of flume installation allowed complete atmospheric aeration under the nappe without requiring vent tubes.

Figure 12 shows that the data compare reasonably well for the range $1.25 < H_t/w < 2.0$ and when $H_t/w > 4.5$. For $H_t/w = 0.25$, the difference in the discharge coefficient is approximately 30 percent with the difference decreasing until the curves merge at $H_t/w = 1.25$. When $H_t/w = 2.0$, the curves begin to deviate with a maximum difference in the discharge coefficient of 8.5 percent at $H_t/w = 2.5$. The curves merge when $H_t/w = 4.5$.

There is insufficient data to identify the cause of the difference between aerated and nonaerated discharge coefficients for $H_t/w < 1.25$; however, the cause of the difference for $2.0 < H_t/w < 4.5$ is clear. Weirs with atmospheric aeration spring, reflected by the sudden drop in the discharge coefficient while those without aeration show a gradual reduction in the discharge coefficient as friction and the downstream tailwater increase. After springing had occurred, the discharge coefficient was constant for flat-topped weirs.

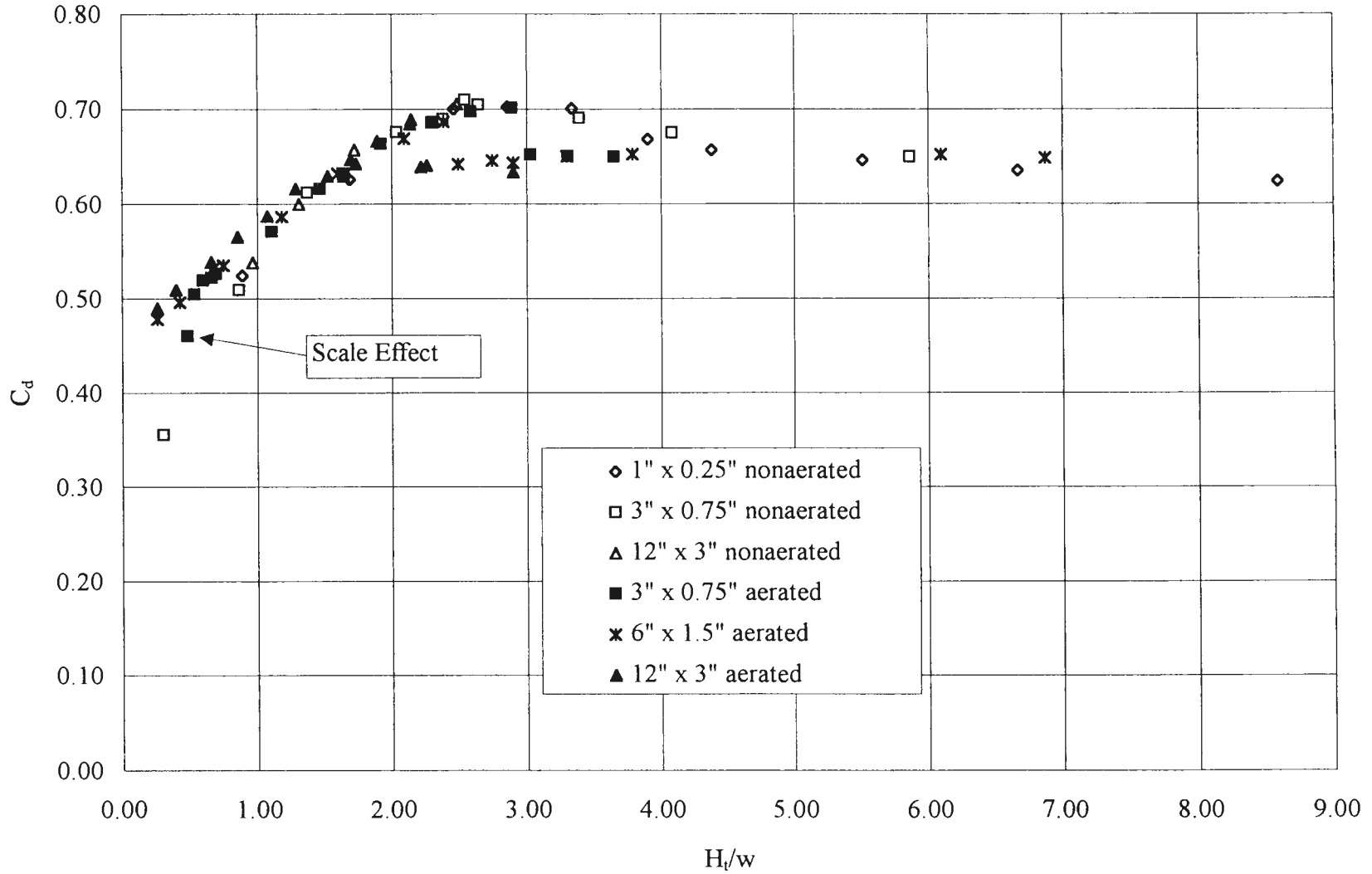

Figure 12. C_d vs. H_t/w for nonaerated (mid-flume installation) vs. aerated (end of flume installation) flows with w/P = 0.25.

Because not all weir geometries were tested without aeration, no specific conclusions for nonaerated scale effects can be made. The writer believes that scale effects will be present for the nonaerated condition for each weir geometry because the scale effects are probably related to the separation region and the boundary layer. If the weir is submerged, the discharge coefficients shown for the nonaerated condition are not valid.

Laboratory Data Presentation

Figures 13 through 17 show the discharge coefficient data for w/P equal to 2.0, 1.0, 0.5, 0.25 and 0.0, respectively. The data in each of these are for leaping flow (except where springing is noted). The discharge coefficient in Figures 13 through 16 is plotted against H_t/w, while Figure 17 (sharp-crested weir) shows the discharge coefficient plotted against H_t/P.

In the literature, researchers have used the piezometric head (h) as an important variable when displaying discharge coefficients. This presentation makes curves easier to use than the total head because total head contains an unknown velocity head. However, using h can introduce errors because it does not account for the velocity of approach. For deep approach channels with low approach velocities, the velocity head does not significantly affect the discharge, but for weirs with shallow approach channels, the approach velocity can significantly affect the discharge capacity of the control structure because momentum aids the flow of water over the weir. Thus, for the same piezometric

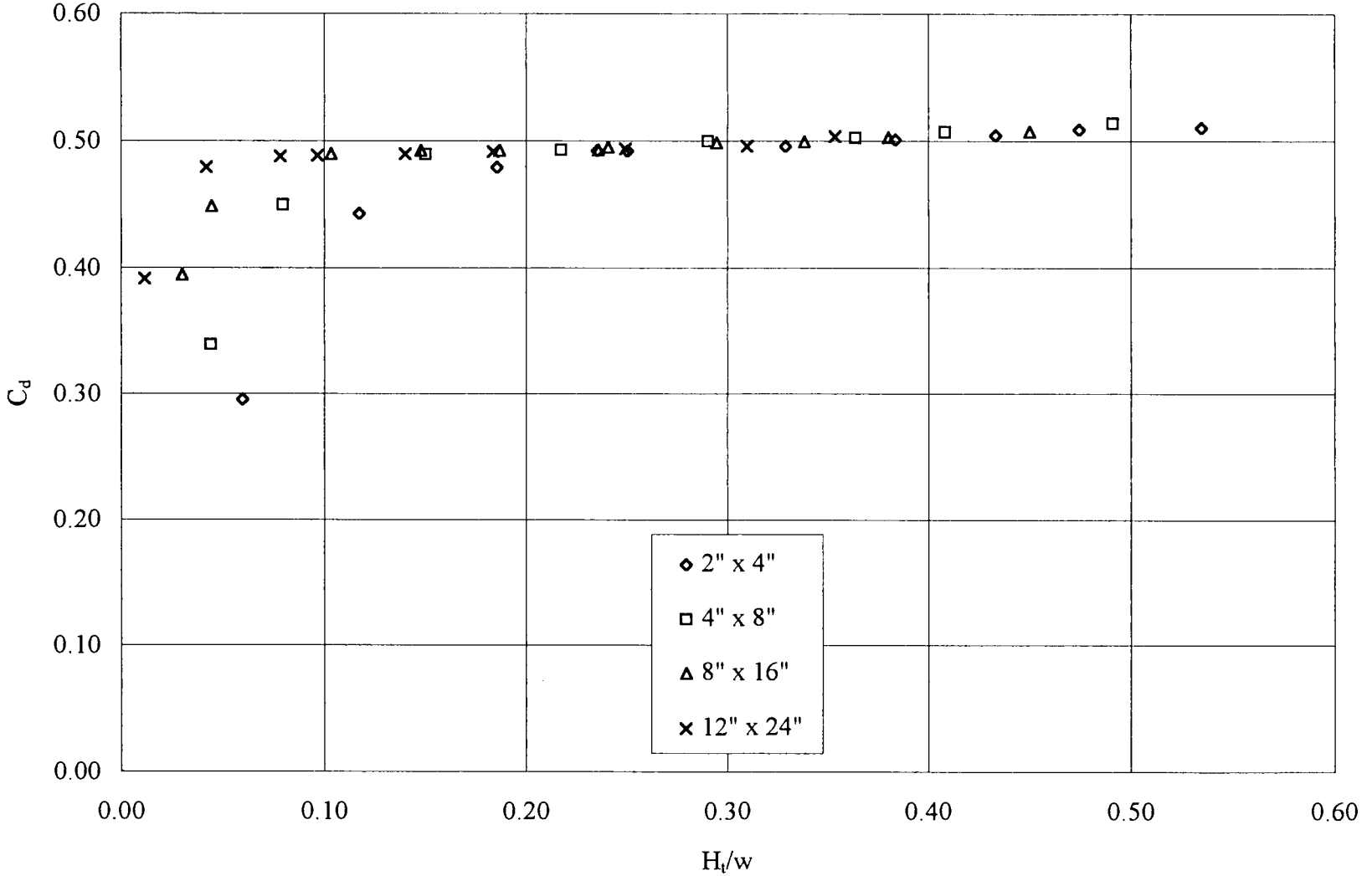

Figure 13. C_d vs. H_t/w for w/P = 2.0.

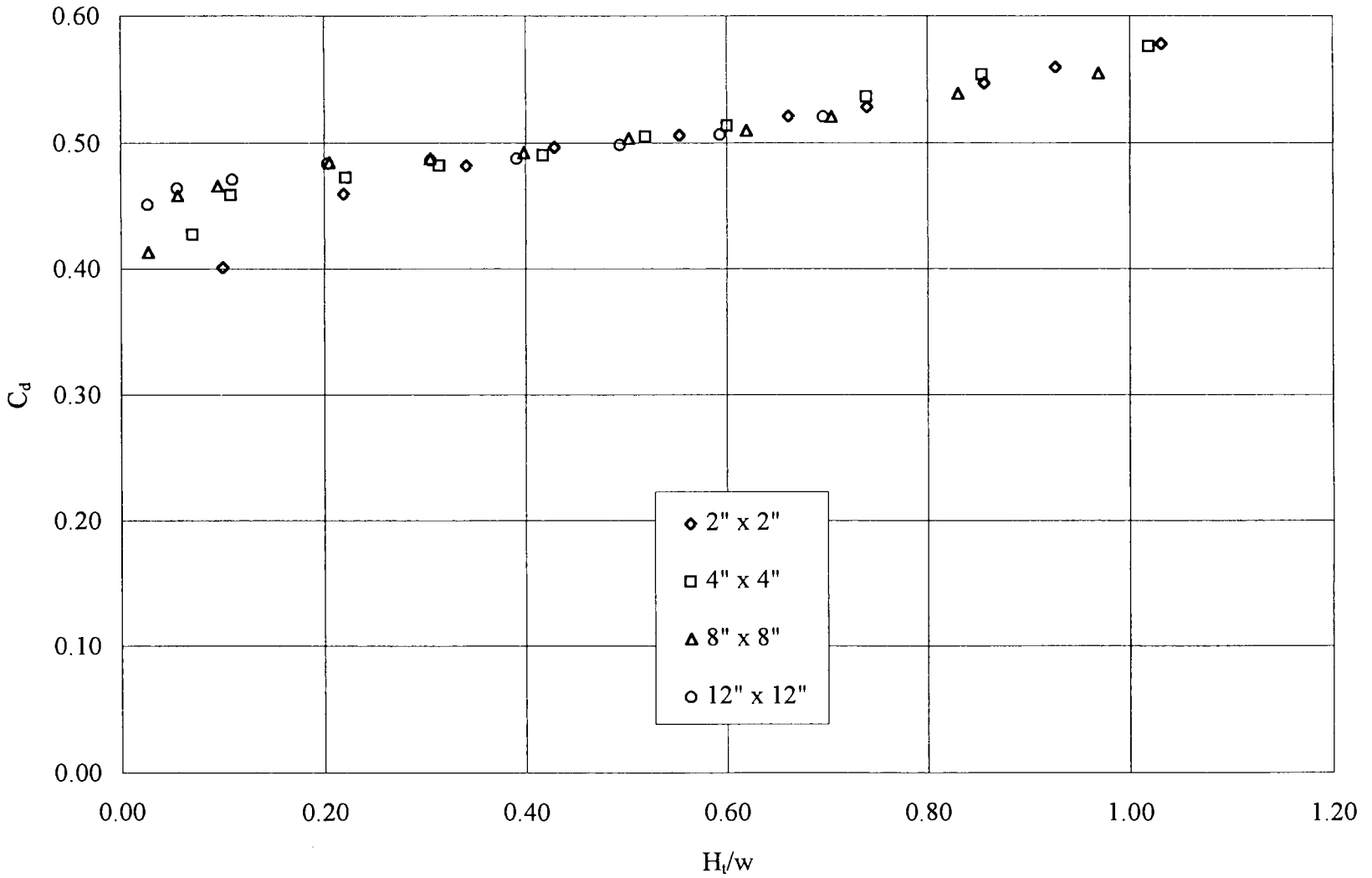

Figure 14. C_d vs. H_t/w for w/P = 1.0.

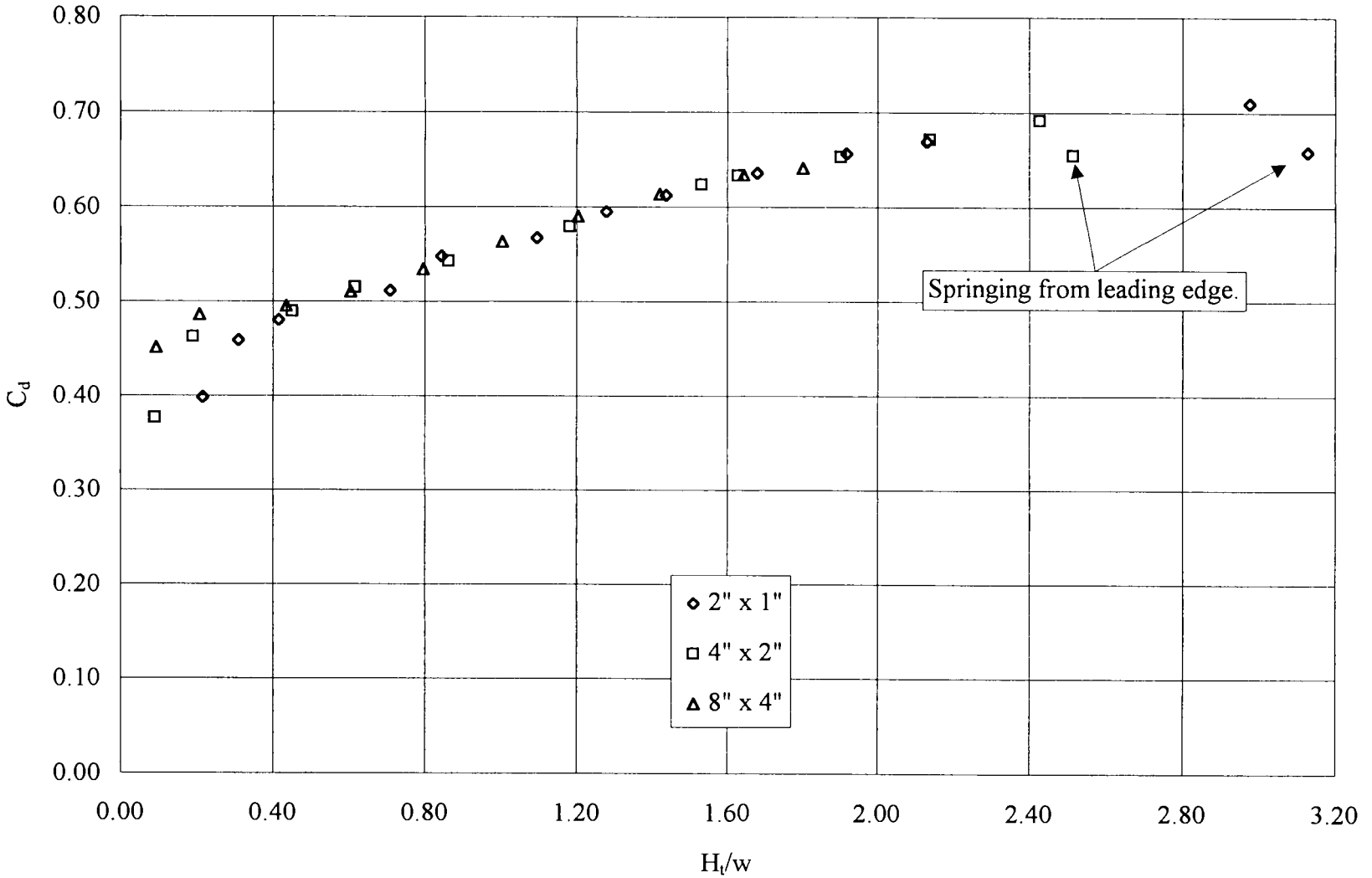

Figure 15. C_d vs. H_t/w for w/P = 0.5.

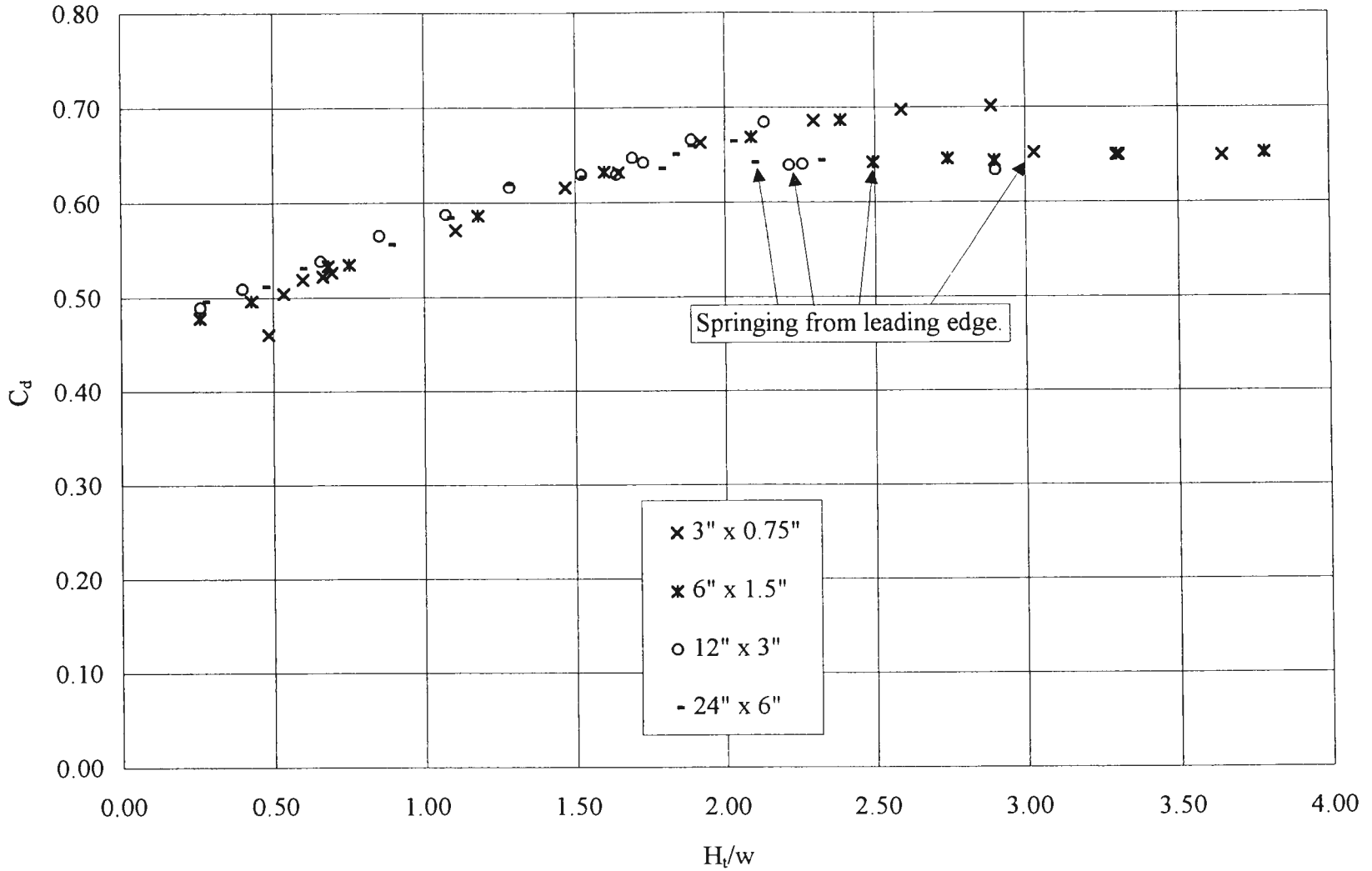

Figure 16. C_d vs. H_t/w for w/P = 0.25.

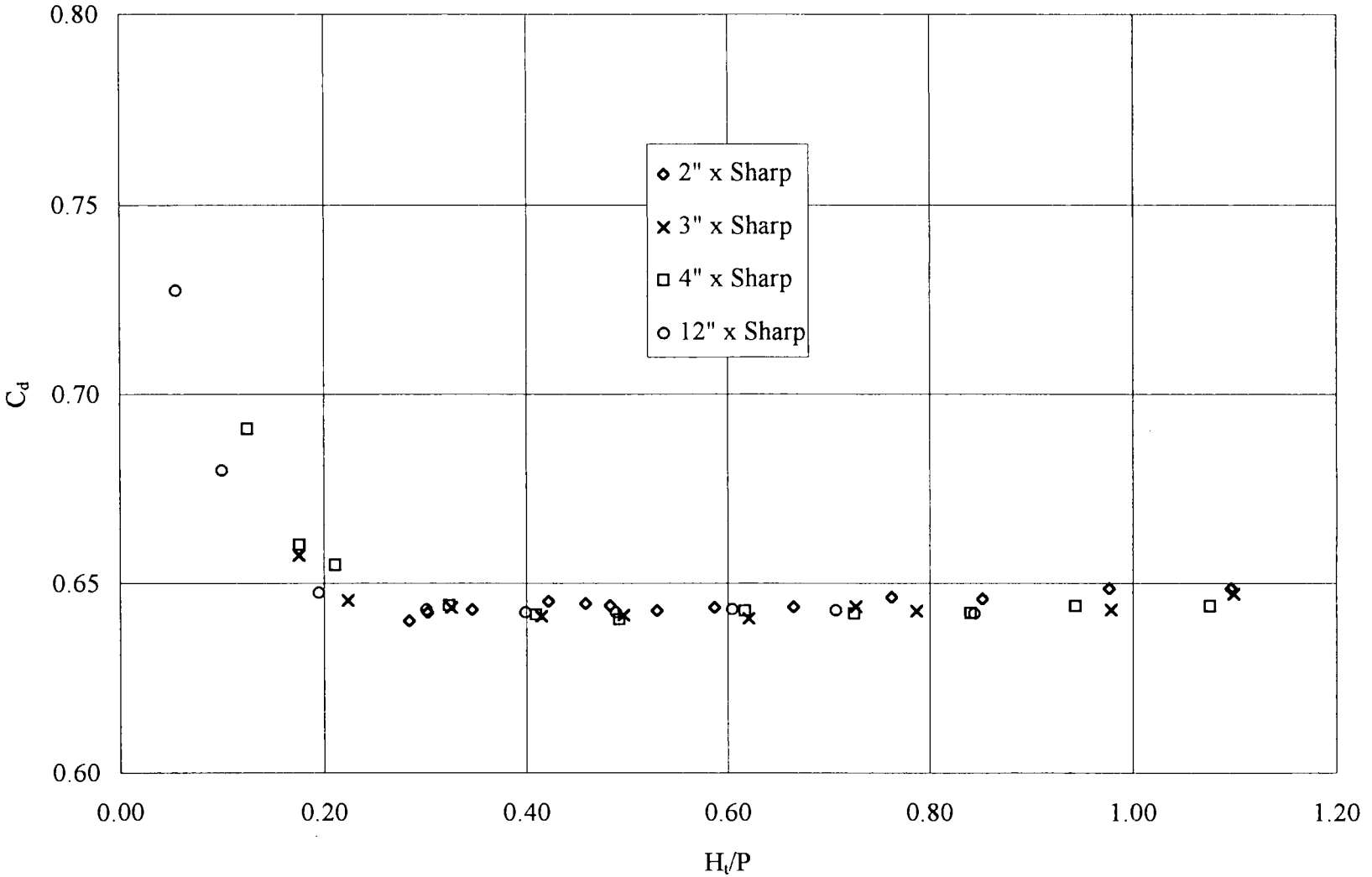

Figure 17. C_d vs. H_t/P for w/P = 0.0.

head, a weir with a shallow shallow approach channel will have a greater discharge than a weir with a deeper approach channel.

Some researchers, for example Rao and Shukla (1971), have used P as the important geometric variable and have plotted the discharge coefficient against h/P regardless of the weir geometry. The issue of h versus H_t has been resolved, but what about the use of the weir height (P) as the important geometric variable?

Govinda Rao and Muralidhar (1963) used the crest width w, as the important geometric variable and plotted the discharge coefficient against h/w. They showed that the coefficient of discharge for weirs with a flat top is only a function of h/w. This approach is more sensible than using the weir height because the flow is controlled more by the width of the weir rather than height of the weir. Another argument for using the crest width is that by using the crest width, the discharge coefficients for weirs with varying heights and crest widths fall on a single curve rather than producing a family of curves if the discharge coefficient is plotted against h/P or H_t/P. The only case where the weir height should be used as the important geometric variable is for the sharp-crested weir where w is zero causing the parameter H_t/w to be infinite.

Figure 13 shows significant discharge coefficient deviations between different weir sizes for $H_t/w < 0.2$, while for values of $H_t/w > 0.2$ the discharge coefficient does not deviate between weir sizes. Previous research on flow over prototype-sized broad-crested weirs has shown that the discharge coefficient does not decrease as dramatically for small H_t/w as is shown in Figure 13 for the tests on the small weirs; rather the discharge coefficient approaches the ordinate linearly (Govinda Rao and Muralidhar, 1963). The

decrease shown on Figure 13 is due to scale effects associated with the weir size and the low head over the weir.

Figure 14 shows discharge coefficient deviations for values of $H_t/w < 0.3$ with no deviations in the discharge coefficient for $H_t/w > 0.3$. Once again the decrease is due to scale effects associated with the weir size and the low head over the weir.

Figure 15 shows deviations for small values of H_t/w similar to Figures 13 and 14. Figure 15 also shows that for $0.4 < H_t/w < 2.4$ the discharge coefficients define a common line. However, above $H_t/w = 2.4$ the springing phenomenon causes a sudden drop in the discharge coefficient's value, which was not observed in the two previous figures. The drop is due to the flow changing from leaping to springing. The figure shows that the value of H_t/w at which springing occurs differs depending on weir size. The 4-inch by 2-inch weir requires H_t/w to be approximately 2.4, while the 2-inch by 1-inch weir requires H_t/w to be approximately 3 for springing to occur. Because of flume limitations, it was not possible to observe springing for the 8-inch by 4-inch weir.

Figure 16 shows trends similar to those in Figure 15 with scale effects being below $H_t/w = 0.51$ and above $H_t/w = 2.0$. Data for small H_t/w are limited because it becomes increasingly difficult to obtain reliable data at low values of H_t/w for decreasing values of w/P because the depth is small and the flow changes from leaping flow to clinging. For $w/P = 0.25$, the springing phenomenon was observed for each weir size tested. The figure shows that as the weir size is increased, smaller and smaller values of H_t/w are required for the flow to spring from the leading edge of the weir. Again, the deviations shown are attributed to scale effects.

One should note that the x axis for Figures 13 through 16 has a different scale for each weir geometry. Without observing this, one might assume that the scale effects for weirs with larger w/P values are more severe than for weirs with smaller w/P values. Actually, the range of H_t/w where scale effects exist increases as w/P decreases.

Figure 17 shows the discharge coefficients for the sharp-crested weirs. Initially the trend in the data was disturbing, because it shows the discharge coefficient decreasing as H_t/P is increased for $H_t/P < 0.23$. However, this trend is not new and was documented by Bazin (Horton, 1907). The reason for this can be attributed to the extent to which the nappe springs above the weir crest. The higher the springing, the less efficient the weir becomes, eventually reaching a limiting discharge coefficient. At low heads, the water does not have enough energy to spring above the weir crest and cannot cause the nappe to contract. The nappe is not contracted above the weir at low heads, so the weir is more efficient than it is at high heads with the nappe contracted.

The only scale effect observed for the sharp-crested weir was the value of H_t/P where the flow changes from clinging to springing from the crest. The data point at the smallest H_t/P value for the 2-, 3-, and 4-inch high weirs corresponds to the condition where the water first springs from the leading edge. The data for the 12-inch high weir begin at a point beyond the initial springing condition. The figure shows that the springing value of H_t/P decreases with increasing weir size. After the flow springs, there appears to be no deviation between the discharge coefficients for the weir sizes shown.

Comparison to Other Researchers' Data

Figure 18 shows data from the present study for sharp-crested weirs plotted with sharp-crested weir data from other researchers (see Literature Review pages 6-11 for formulas). The discharge coefficients from the other researchers were converted to make a direct comparison with the data of this study. The data, in general, have the same trend although there is some deviation at smaller values of h/P. Rehbock's data are lower than the other data sets. The reason for this is that he added 0.0011 meters (0.00361 feet) to the piezometric head measurement, which reduces the discharge coefficient. He was apparently trying to linearize the discharge coefficient. The data show an average deviation of 0.67 percent, excluding Rehbock's data. The only significant deviations between the data sets are for $H_t/P < 0.2$.

Figure 19 shows data from this study plotted with data obtained by using other researchers' discharge coefficients. The data from the other researchers were converted to make a direct comparison with the data of this study.

Swamee (1988) claimed that his equation fit the data and equations of Govinda Rao and Muralidhar (1963) nearly perfectly, making smooth transitions throughout the data. However, Figure 19 shows that his equation does not agree with the Govinda Rao and Muralidhar equations. Swamee's equation was compared to all the data of this study that was free from scale effects and did not compare very well. This is due to the fact that the weir height, which was included in Swamee's equation, mathematically influences the discharge coefficient.

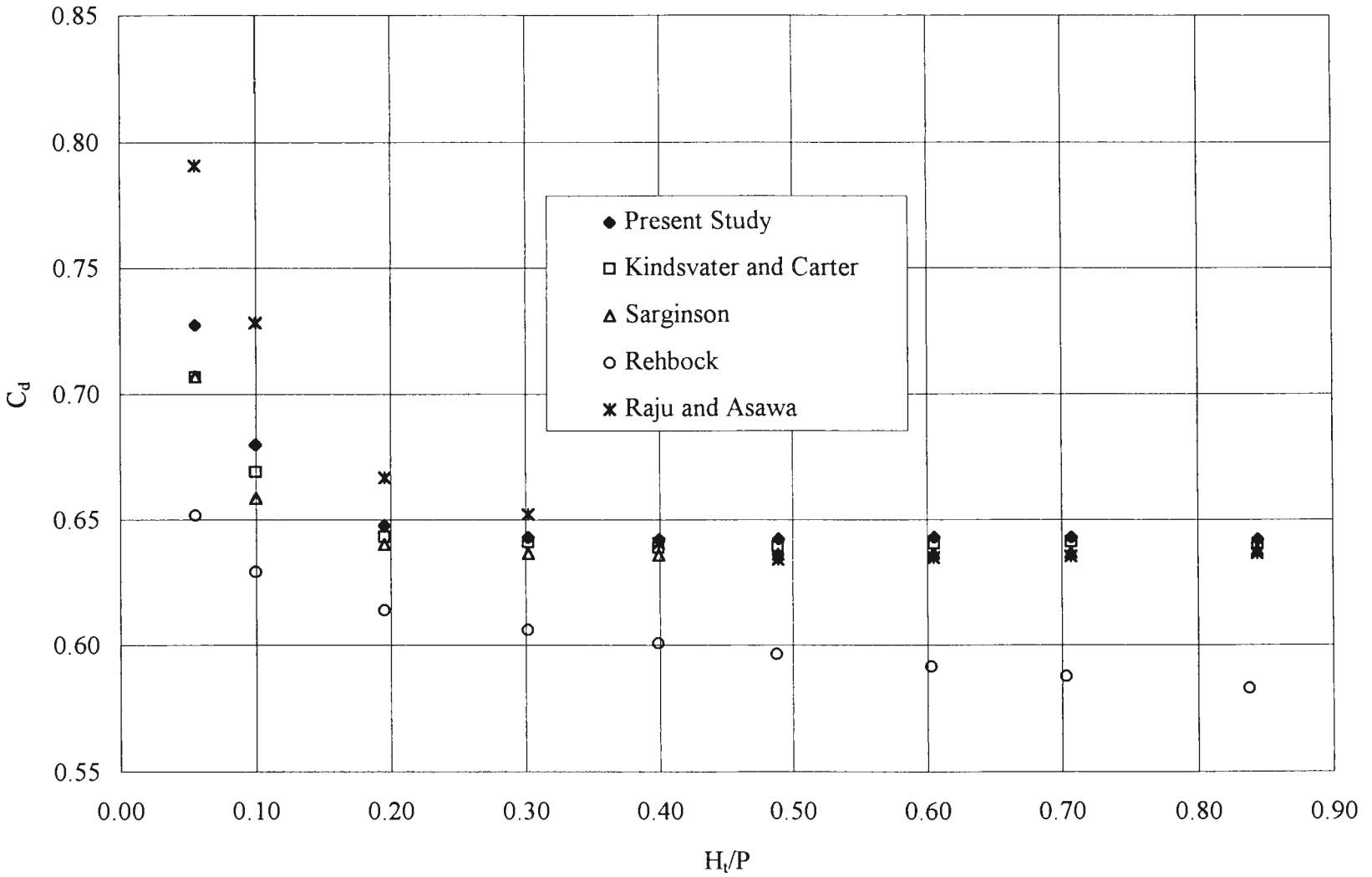

Figure 18. Comparison of discharge coefficients from other researchers for sharp-crested weirs.

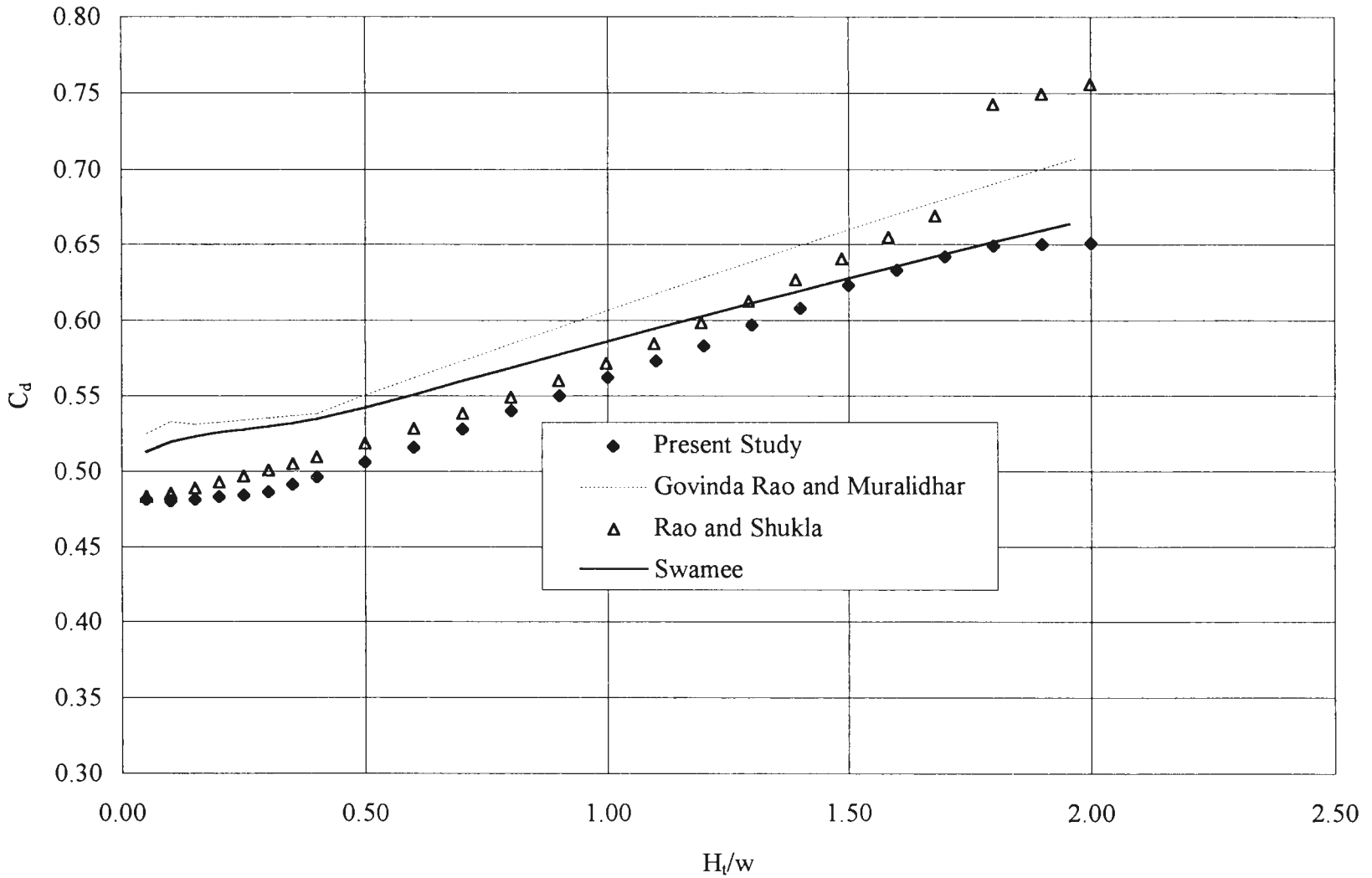

Figure 19. Comparison of discharge coefficients from other researchers for flat-topped weirs.

Govinda Rao and Muralidhar (1963) presented equations that fit their data with a maximum error of 3 percent. When compared to Bazin's data (Horton, 1907), Govinda Rao and Muralidhar's data were approximately 7 percent higher throughout the entire range of h/w tested.

Rao and Shukla (1971) also studied weirs with a flat crest. Data points obtained by using their equations are shown on Figure 19 because their equations do not plot as functions with H_t/w as the abscissa.

The data from this research showed a difference between Govinda Rao and Muralidhar's (1963) discharge equations, which was less than 8 percent throughout the range shown. (Recall that Govinda Rao and Muralidhar's data were 7 percent higher than Bazin's.) The difference may be partly attributed to the fact that Govinda Rao and Muralidhar used a V-notch weir to measure the discharge, which was not as accurate as the weigh tank and volumetric tank used in this study. Differences could also be caused by test conditions not being similar or that their weirs were not sufficiently aerated. The data of Rao and Shukla (1971) fit the data of the present study very well at smaller values of H_t/w and show scatter that is less than 5 percent for $H_t/w < 1.6$. Their data diverges for $H_t/w > 1.6$ because their equation assumes a different flow regime. On average, the data of the present study compare reasonably well with that of other researchers, showing less than 5.5 percent average error compared to the averages of the other researchers' discharge coefficient. The deviations shown in Figure 19 are of minor concern because the scale effects analysis of this study does not include the data from other researchers.

Clinging Flow Scale Effects

The scale effects associated with clinging are such that as the weir size was increased, the value of H_t/w for which clinging would no longer occur decreased. In order for clinging to occur, the water must take an abrupt turn at the trailing edge of the weir's crest. As the weir's size is increased, the velocity of the water tangent to the weir's crest is larger in magnitude than for the smaller weirs at the same H_t/w and is able to overcome gravity and surface tension forces (which assist clinging) and leap away from the downstream face of the weir. This explains why the clinging value of H_t/w decreases with increasing weir size.

The clinging condition was difficult to maintain and was very unstable as H_t/w increased for larger weir sizes and would probably only occur at very small heads for prototype structures. Consequently, there will be no specific scale effects analysis for clinging flows. However, one must realize that errors in the discharge coefficient can result if a model is tested with clinging flow for an H_t/w value for which clinging flow is not possible in the prototype.

Leaping Flow Scale Effects Analysis for Flat-Topped Weirs

The discharge coefficient scale effects associated with leaping flow will be investigated in depth because this regime of flow is expected to occur most often for prototype structures with flat tops. Leaping flow discharge coefficient scale effects were present for $H_t/w < 0.5$.

As previously discussed, scale effects are deviations between the model and prototype. For this research, the 24-inch high weir with a crest width of 6 inches served as the prototype because Figure 16 shows no scale effects for this weir. Another reason this weir is sufficient to use as a prototype is that the data for smaller weirs where no scale effects were present plotted on its discharge coefficient curve, indicating that size scale effects are no longer present.

For all weirs smaller than 24 inches high, Figures 13 through 16 show definite discharge coefficient scale effects for each model size and w/P ratio, except where no data were taken (12- and 6-inch high weirs with w/P = 0.25 operating at small heads). In each figure there is an H_t/w value corresponding to weir each size, above which, scale effects are no longer present.

It has been established that it is impossible to maintain complete dynamic similarity from the prototype to the model. Because of this, hydraulic modelers try to build models large enough so that surface tension and viscosity effects are minimal. However, for small H_t/w values, the effects of not maintaining dynamic similarity are evident even for models that seem large enough to avoid scale effects. What is the cause of the scale effects? It is reasonable to assume the scale effects are related to either surface tension effects (Weber Number) or viscous effects (Reynolds Number) because dynamic similarity was not achieved simply by using Froude similitude alone and because pressure and elastic effects have little influence on weir flow.

The Weber Number based on total energy head and average velocity above the leading edge of the weir is given by:

$$We = \sqrt{\frac{\rho V^2 H_t}{\sigma}} \tag{58}$$

where ρ is the density of the water, V is the average velocity of the flow above the leading edge of the weir, H_t is the total head over the weir, and σ is the surface tension of the water. Analysis of the data failed to show any consistent trends with Weber Number. This confirms the conclusion of Hall, Maxwell, and Weggel (1969).

Recall that surface tension forces are predominant only when very small radii of curvature exist at an interface. Even with the smallest weirs tested, the radii of curvature for the upper and lower nappe profiles were not excessively small (between 0.5 and 1.0 inches). The only time excessively small radii of curvature existed in this study was when water flowed over the weir in such a manner that there was a continuous water bead across the crest, with small radii of curvature defining its boundaries, from the leading to trailing edge of the weir. For this case the entire weir crest was not wetted and the effects of surface tension were obvious. Throughout this study this condition was avoided because it is of little practical value.

The Reynolds Number based on the total energy head and average velocity above the leading edge of the weir is given by:

$$Re = \frac{\rho V H_t}{\mu} \tag{60}$$

where μ is the dynamic viscosity and all other variables are as previously defined. It became evident that the Reynolds Number did define the H_t/w value below which leaping

scale effects exist for each weir size. Even more important was that the Reynolds Number was constant at the limiting H_t/w value for all weir sizes with a constant w/P value.

As with pipe flow, lower Reynolds Numbers are associated with larger friction. Because the coefficients of discharge show a dramatic reduction for smaller heads and velocities, this is a plausible explanation. Another possible explanation is that the boundary layer and separation region at the leading edge do not scale geometrically with the weir. Therefore, for the smaller weirs, the size of the separation region and boundary layer may be proportionally larger than at the same H_t/w value for the larger weirs. Keutner (1934) and Moss (1972) showed that the length and maximum height of the corner separation were 0.77h and 0.15h, respectively.

Figures 20 through 23 show the trends of the discharge coefficient and the approximate locations where scale effects cease for each weir size at each w/P ratio. The dashed lines at smaller values of H_t/w for Figures 20 through 23 represent equations fit through the discharge coefficient data and are given to provide more definition to region of leaping scale effects. With the exception of weirs with the w/P ratio equal to 0.5 and 0.25, which show springing scale effects for larger H_t/w values, leaping scale effects cease where the dashed line for each weir size merges with the other data points.

The process used to obtain the Reynolds Number where scale effects ceased for leaping flow was iterative, requiring a Reynolds Number to be assumed for each w/P ratio and then checked with the discharge coefficient curves (Figures 20 through 23) to identify whether or not the assumed Reynolds Number corresponded to the value of H_t/w where

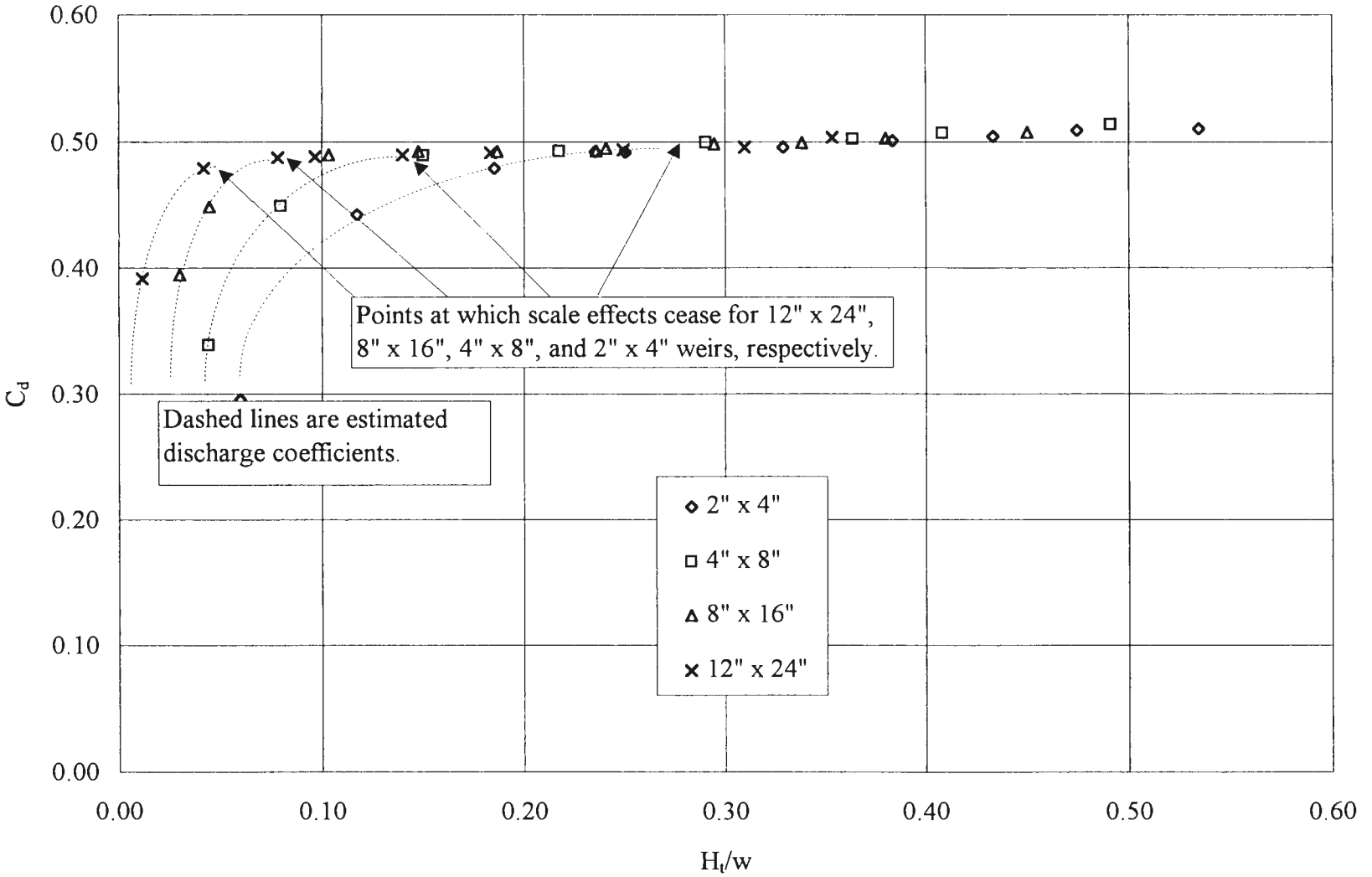

Figure 20. C_d vs. H_t/w for w/P = 2.0 showing scale effects and discharge coefficient trends.

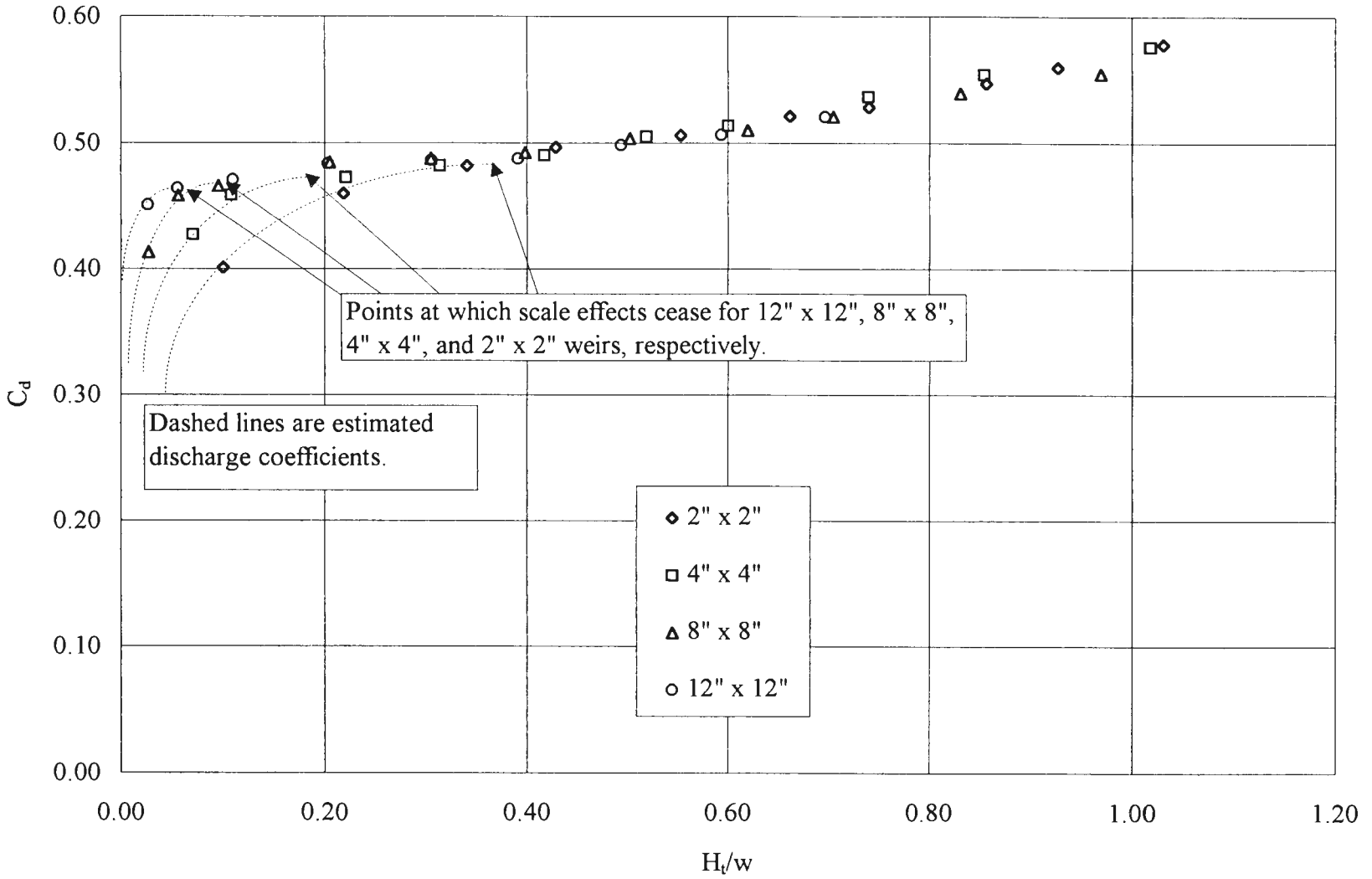

Figure 21. C_d vs. H_t/w for $w/P = 1.0$ showing scale effects and discharge coefficient trends.

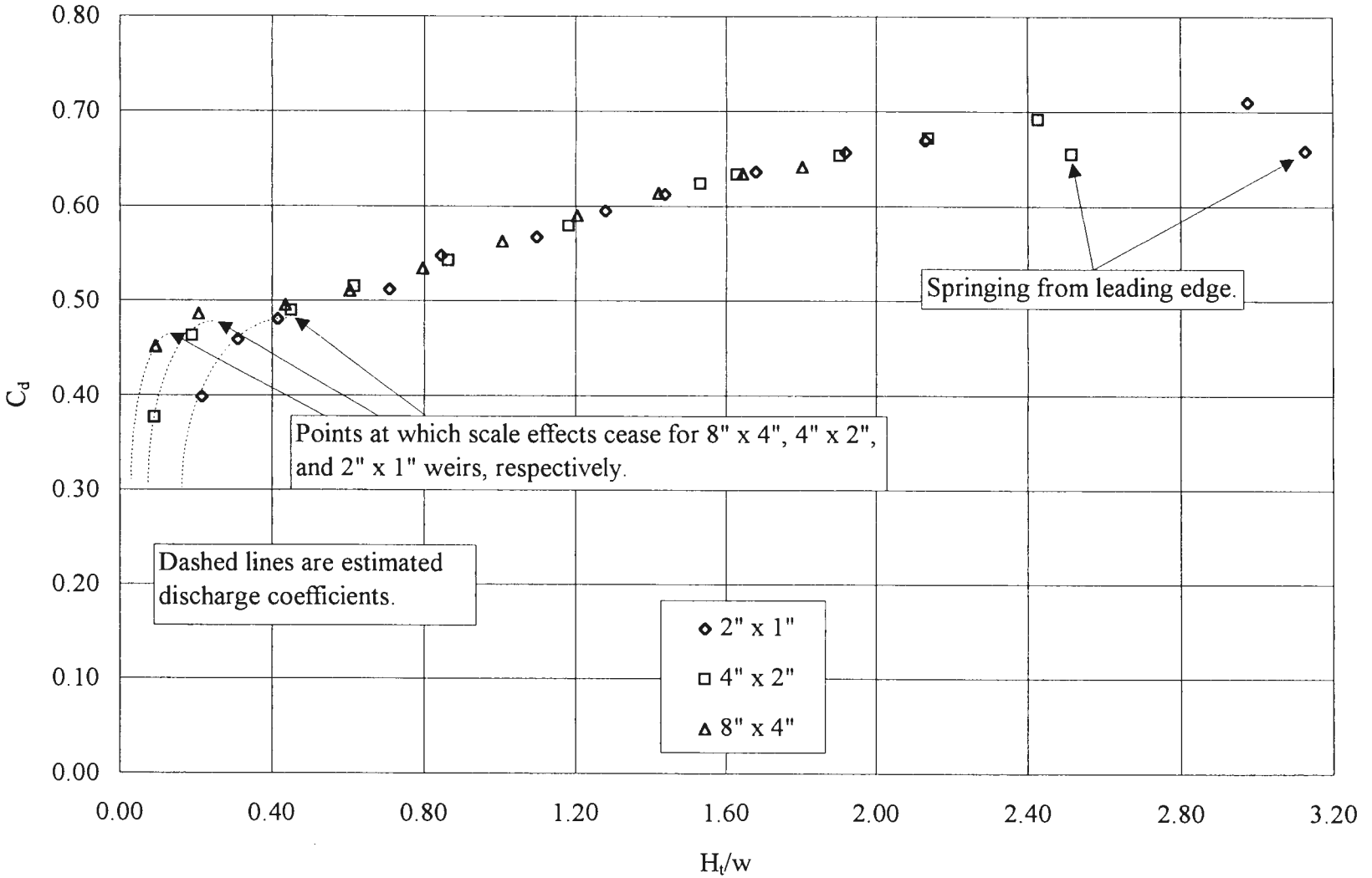

Figure 22. C_d vs. H_t/w for w/P = 0.5 showing scale effects and discharge coefficient trends.

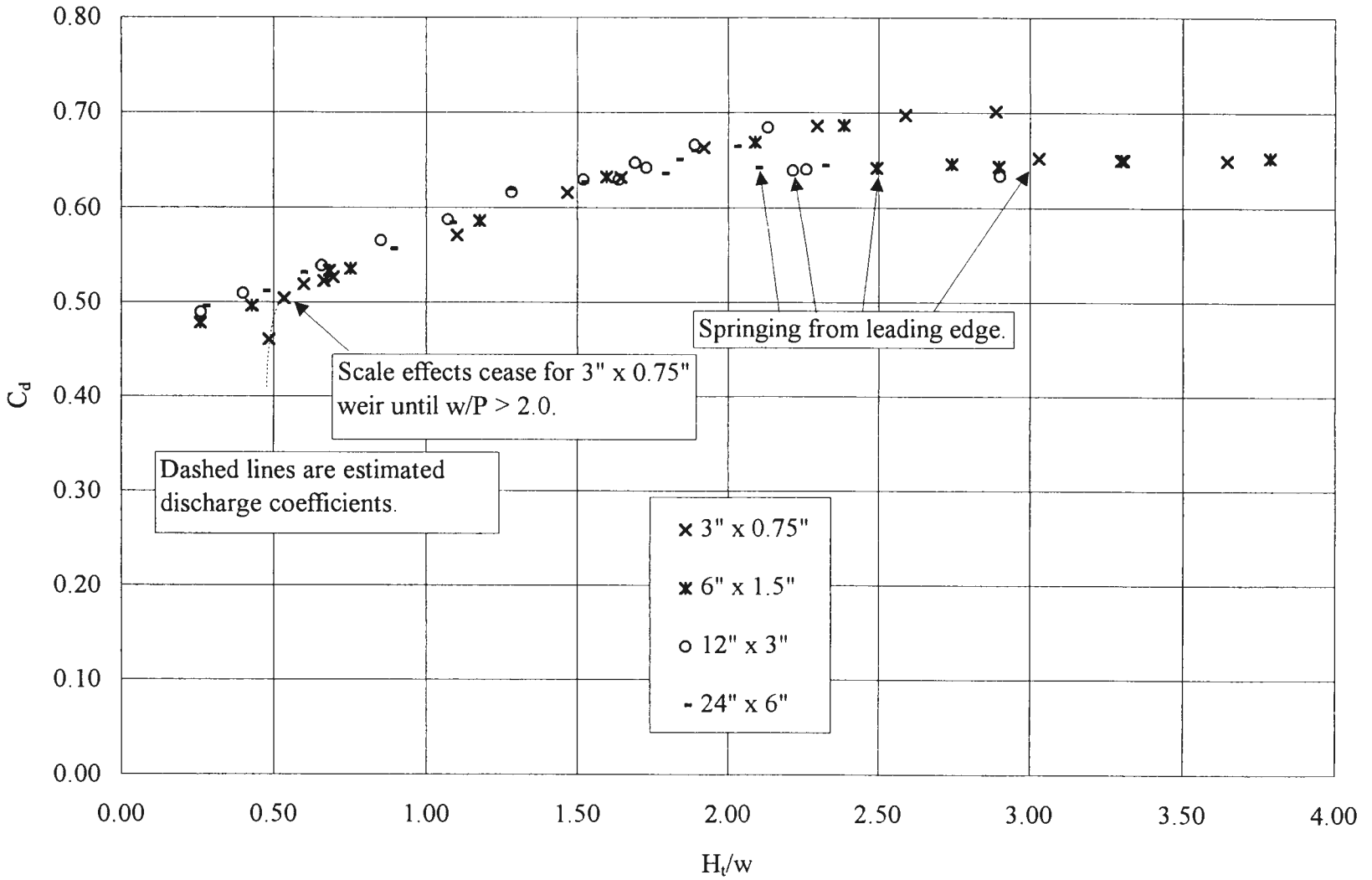

Figure 23. C_d vs. H_t/w for w/P = 0.25 showing scale effects and discharge coefficient trends.

leaping scale effects ceased. The results of the iteration process are shown as arrows on Figures 20 through 23 indicate the location on the discharge coefficient curve where scale effects cease for each weir size. The Reynolds Number associated with each point indicated by the arrows in these figures is constant for each weir size but varies with w/P.

To expedite the iteration process, second-order polynomials were fit through the experimental data for the Reynolds Number using H_t/w as the independent variable. With equations, it was easy to evaluate many different Reynolds Numbers until the correct one that fits all model data for each w/P ratio was found. This procedure was used for each flat-topped weir and the results for w/P equal to 2.0, 1.0 and 0.5 are shown in Figures 24 through 26. No figure for w/P = 0.25 is shown because only the 3-inch by 0.75-inch weir shows scale effects in the H_t/w range shown. Figures 24 through 26 show the results of the iteration process with the Reynolds Number plotted against H_t/w, and Table 1 summarizes the results of the iteration process for flat-topped weirs.

It is apparent that the ratio of w/P rather than the value of w or P independently influences the presence of scale effects. If w is held constant, 4 inches for example, the total head required to overcome scale effects is 1.09, 0.75, and 0.51 inches for w/P ratios of 2, 1, and 0.5, respectively (see Table 1). If P is held constant at 4 inches, the total head required to overcome scale effects is 1.12, 0.75, and 0.48 inches for w/P ratios of 2, 1, and 0.5, respectively. However, when the two are combined as w/P, the total head required to overcome scale effects is essentially constant for each w/P ratio. Therefore, the w/P ratio is the important geometric parameter and the Reynolds Number is the important dynamic parameter to use when identifying the presence of scale effects.

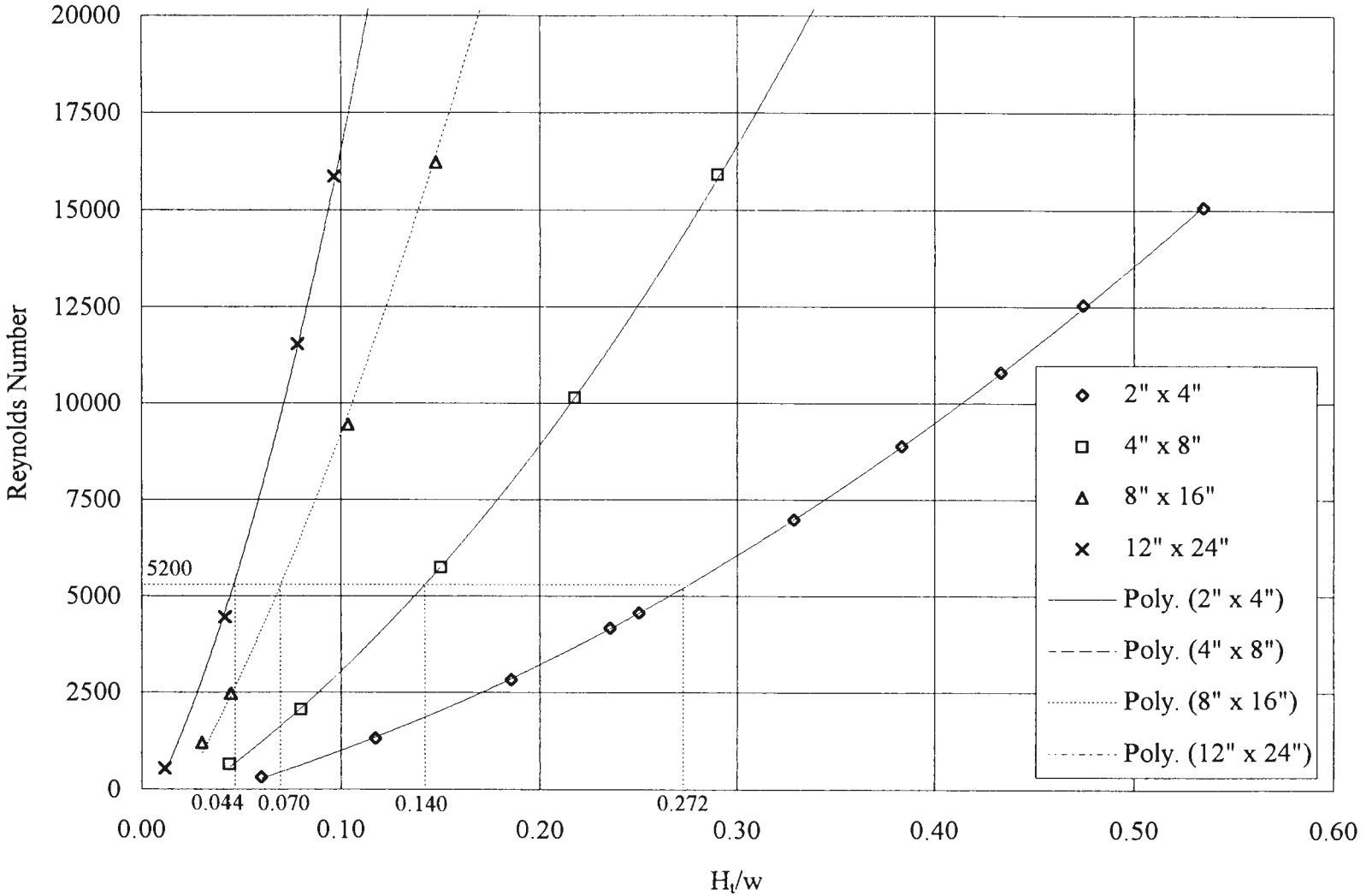

Figure 24. Reynolds Number vs. H_t/w for w/P = 2.0.

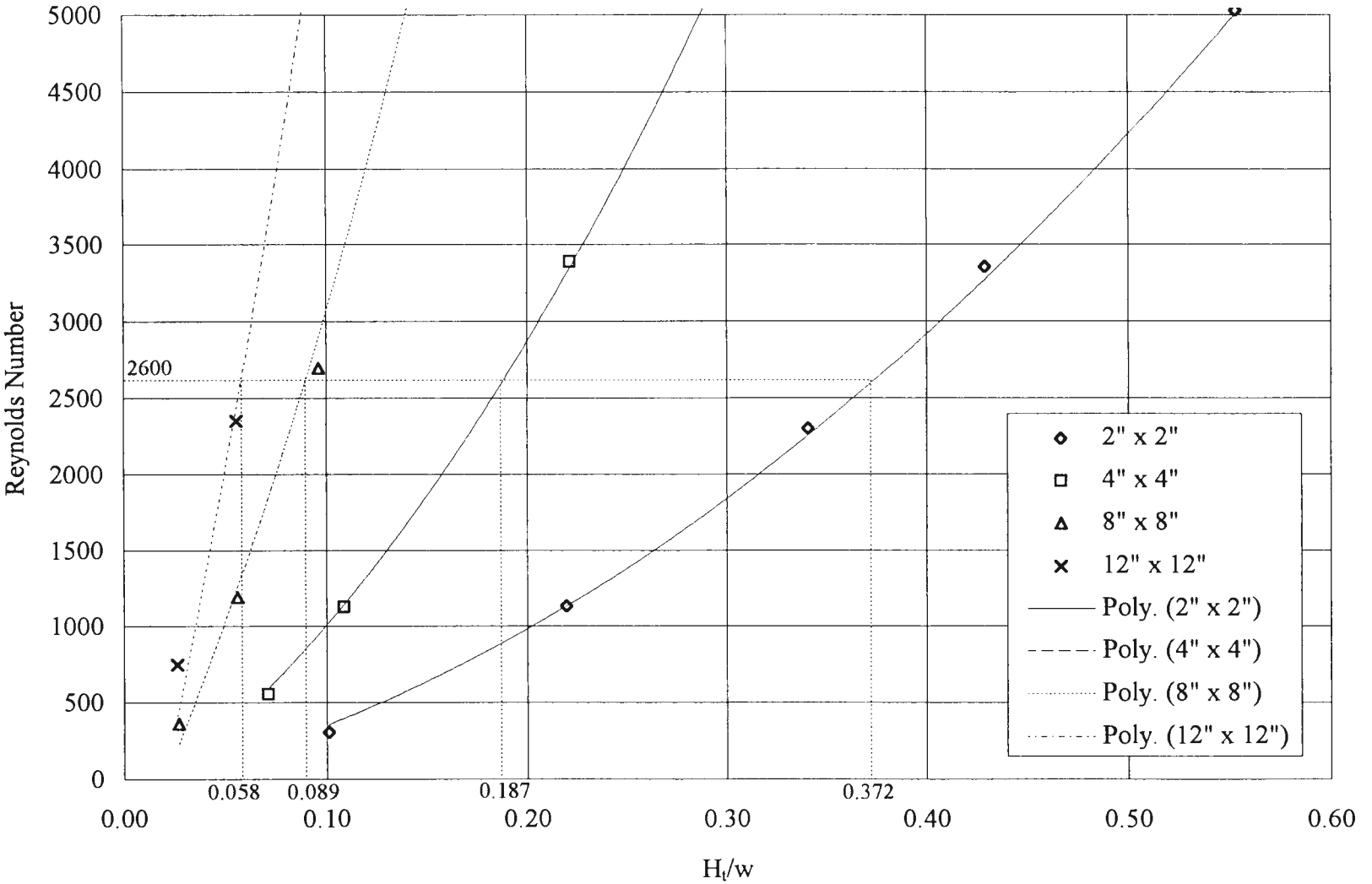

Figure 25. Reynolds Number vs. H_t/w for w/P = 1.0.

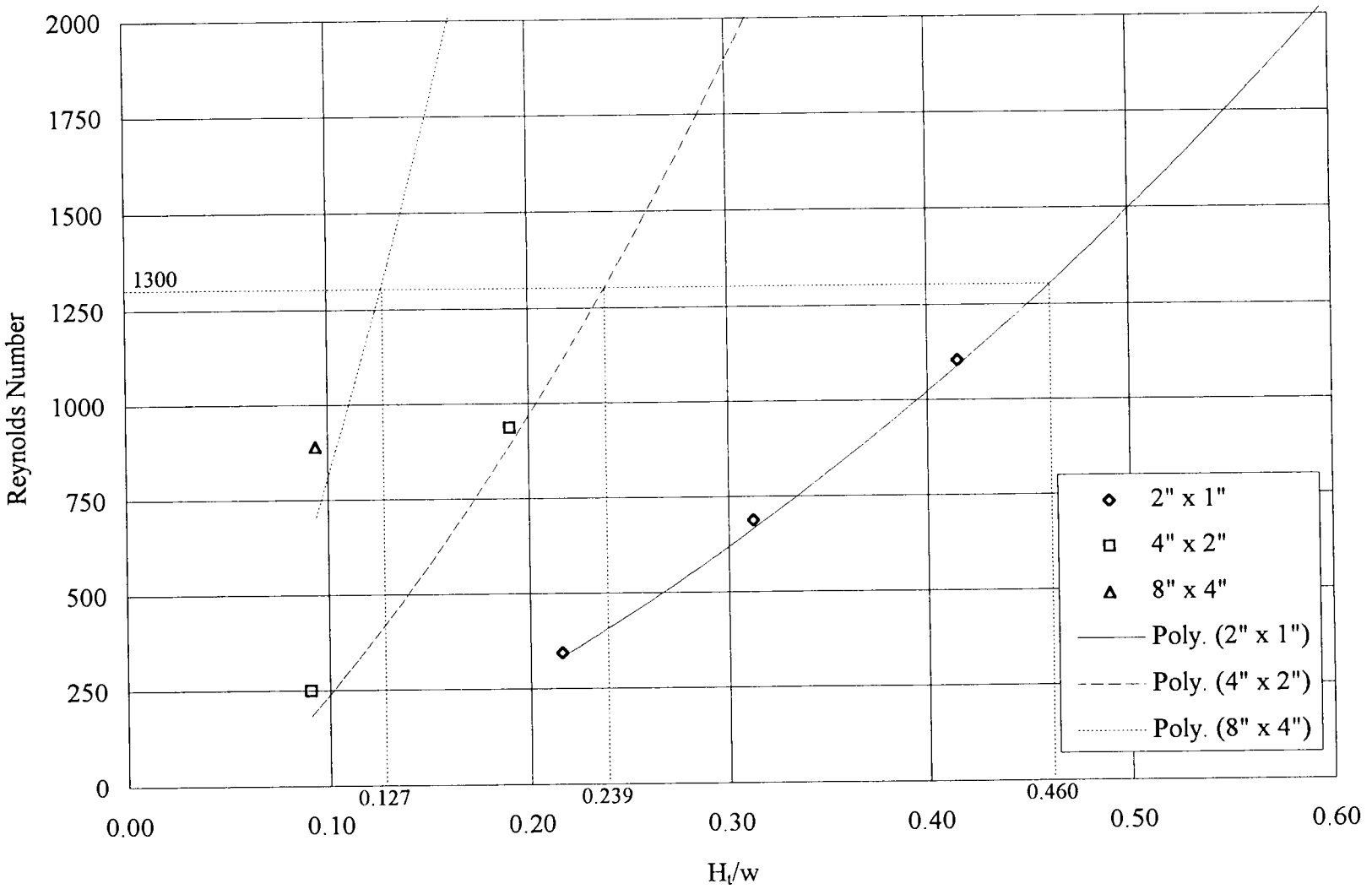

Figure 26. Reynolds Number vs. H_t/w for w/P = 0.5.

The previous analysis also strengthens the argument that leaping flow scale effects are strongly associated with viscous (Reynolds Number) effects because, for any w/P ratio, the total head required to overcome scale effects was essentially constant for each scale of that geometry tested. Thus, the ratio of the height of the separation region or the height of the boundary layer to the total energy should be essentially constant for each w/P ratio. For w/P = 0.25, there was only one point available to calculate the Reynolds Number. This point was on the curve for the 3-inch by 0.75-inch weir and occurs at $H_t/w = 0.511$ and corresponds to a Reynolds Number of 650 and a total head of 0.38 inches. Note that for w/P = 0.25, the H_t/w values marked with an asterisk are smaller than any

Table 1. Summary of iteration results for conditions at which leaping scale effects cease for flat-topped weirs

w/P	Weir Size (P x w, inches)	Reynolds Number	H_t/w	H_t (inches)	Average H_t (inches)
2	12 x 24	5200	0.044	1.06	
	8 x 16	5200	0.070	1.12	
	4 x 8	5200	0.140	1.12	
	2 x 4	5200	0.272	1.09	1.10
1	12 x 12	2600	0.058	0.70	
	8 x 8	2600	0.089	0.71	
	4 x 4	2600	0.187	0.75	
	2 x 2	2600	0.372	0.74	0.73
0.5	12 x 6	1300	0.080*	0.48*	
	8 x 4	1300	0.127	0.51	
	4 x 2	1300	0.239	0.48	
	2 x 1	1300	0.460	0.46	0.48
0.25	24 x 6	650	0.064*	0.38*	
	12 x 3	650	0.128*	0.38*	
	6 x 1.5	650	0.253*	0.38*	
	3 x 0.75	650	0.511	0.38	0.38

* value calculated using average value of H_t from other weir's with the same w/P value.

shown on Figure 23, indicating that the data shown on Figure 23 does not extend into the range of expected scale effects.

Springing Flow Scale Effects Analysis for Flat-Topped Weirs

Figures 22 and 23 show the discharge coefficients for weirs with w/P = 0.25 and 0.5, respectively, and also show the sudden reduction in the discharge coefficient after springing occurred. The sudden drop represents a difference between leaping and springing discharge coefficients, which is approximately 8.5 percent. The drop is caused by a contraction of the nappe above the weir, which is a consequence of springing. Contracting the nappe causes the piezometric head to increase for a constant flow rate, which reduces the discharge coefficient.

The scale effects associated with springing may seem minor relative to leaping flow scale effects; however, modelers should be aware of the H_t/w value where springing is initiated for the prototype to properly correct model discharge coefficient curves.

Figure 27 shows H_t/w plotted against weir crest width for weirs with w/P = 0.5 and 0.25. Because of flume limitations, these were the only data collected. From Figure 27 it is apparent that springing is related to the length of the crest width and the w/P ratio. From the limited data shown, the incipient springing point curve for each weir geometry, when plotted together, produces a family of curves. Thus it can be concluded that springing is related to the crest width and w/P is reasonable when one considers the flow over a weir with a constant height and variable crest width. For example, a head of 2 inches will spring from a 12-inch high sharp-crested weir but will not spring from the

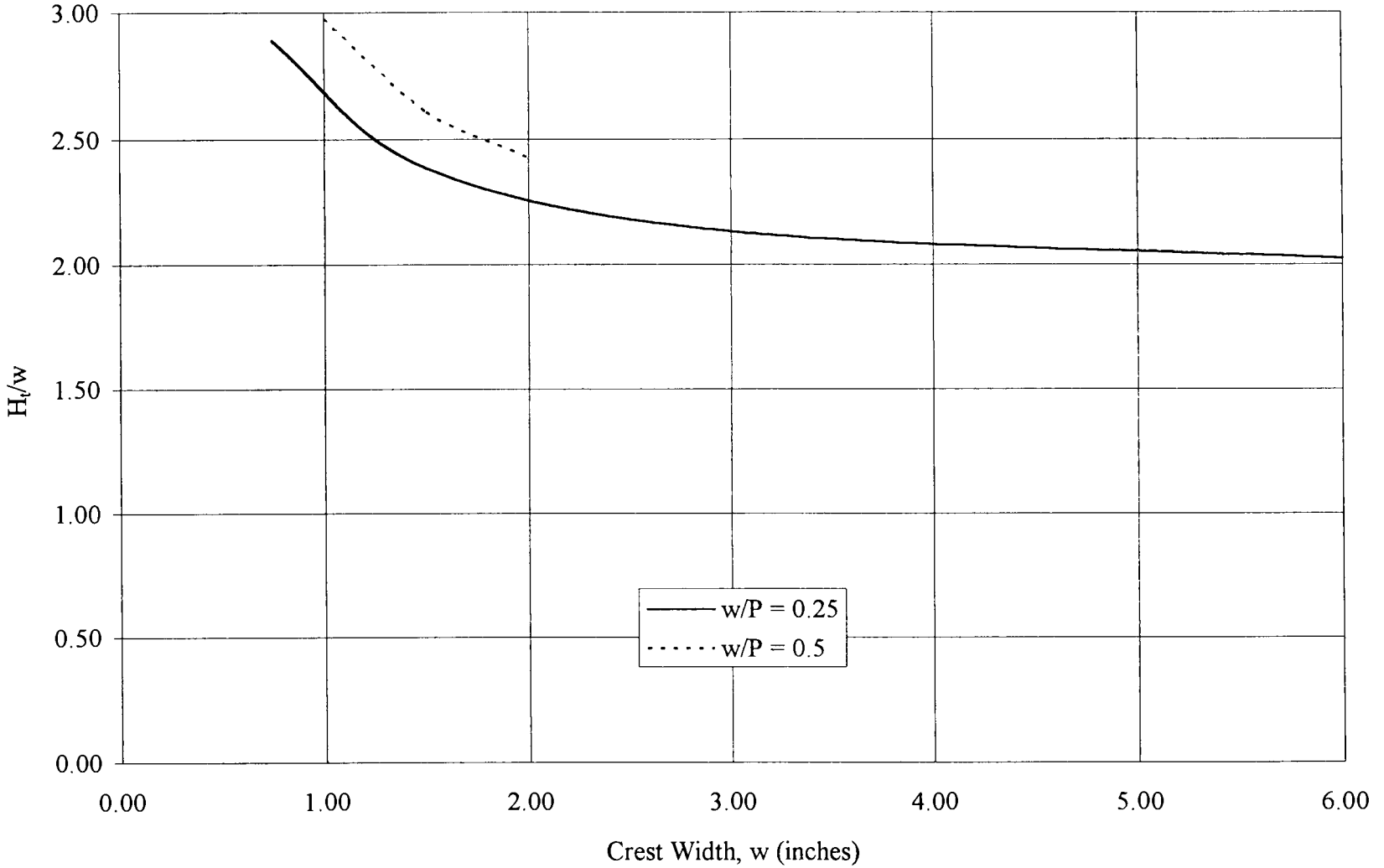

Figure 27. H_t/w vs. crest width at incipient springing flow for flat-topped weirs.

leading edge of the crest for a 12-inch by 6-inch wide flat-topped weir simply because the nappe reattaches to the crest of the weir.

The writer suggests that the data for w/P = 0.25 be used to correct for springing scale effects for flat-topped weirs. The data indicate that the springing value of H_t/w approaches 2 for increasing crest widths. This value should be used for the incipient springing point for prototype structures. For example, if one tests a model flat-topped weir for H_t/w values exceeding 2 and the flow fails to spring from the crest, the discharge coefficients for H_t/w values exceeding 2 should be set equal to the discharge coefficient at $H_t/w = 2$.

Another method for correcting springing data, if possible, is to operate the model at the springing condition and extend the discharge coefficient associated with springing horizontally back such that it intersects the discharge coefficient curve. The H_t/w value corresponding to the intersection represents the prototype H_t/w value for which springing should be expected.

Springing Flow Scale Effects Analysis for Sharp-Crested Weirs

Figure 28 shows the trend of the discharge coefficient for each sharp-crested weir size. The figure shows arrows indicating the first data point for each weir size where the flow first springs from the crest. (No data were taken for clinging sharp-crested weir flows because sharp-crested weirs are designed to facilitate springing.) To maintain consistency, a limiting Reynolds Number was also obtained for sharp-crested weirs by using the first data point (the point where springing from the crest initiates) for the 4-, 3-,

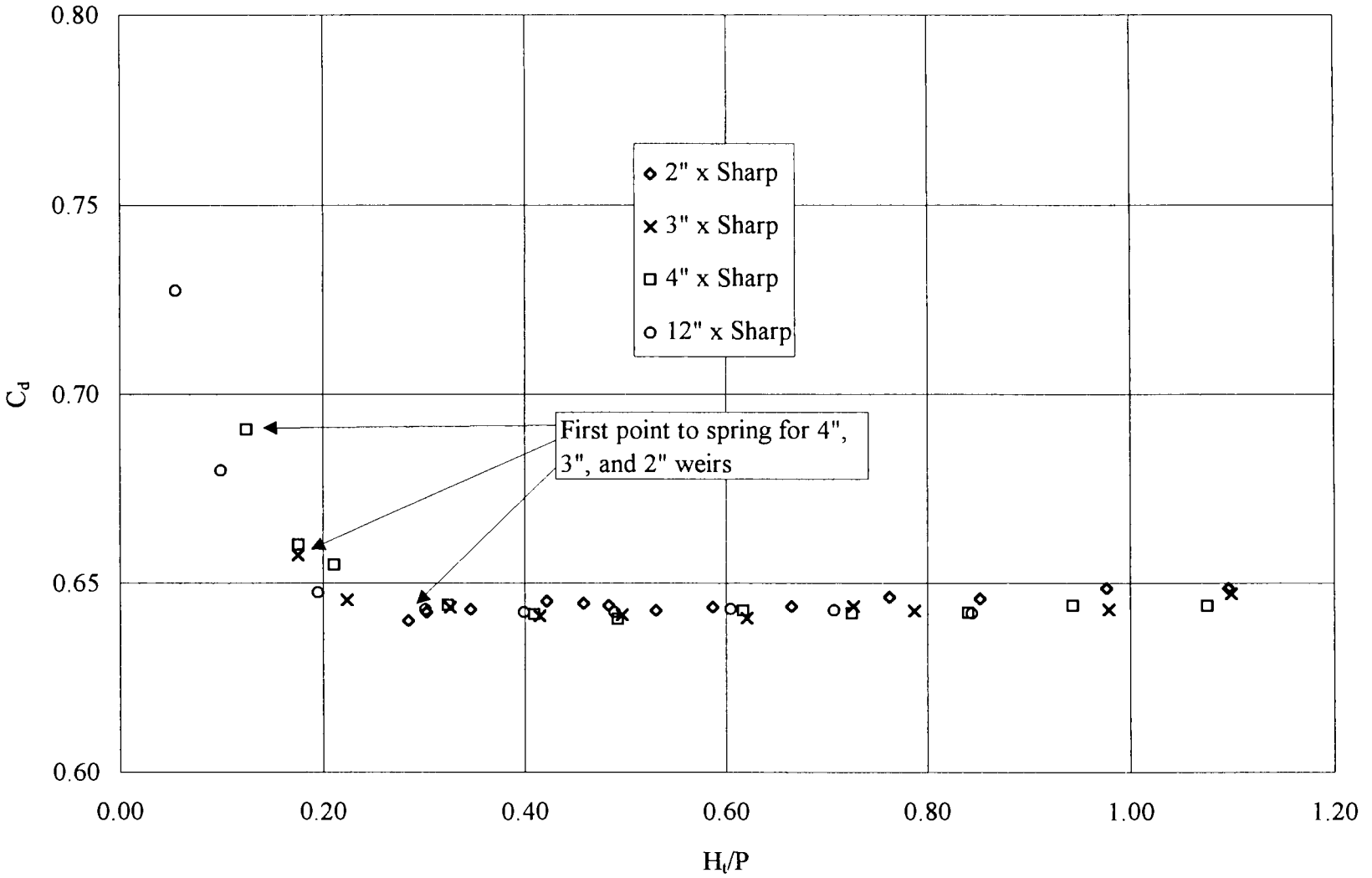

Figure 28. C_d vs. H_t/P for w/P = 0.0 showing scale effects and discharge coefficient trends.

and 2-inch high weirs. This point corresponds to a conservative Reynolds Number of 3000 for each weir size and an average depth of 0.53 inches. No discharge coefficient for the 12-inch sharp-crested weir is given for the initial springing point; however, the H_t/P value for which springing should first occur is 0.044 based on the average H_t value at springing flow from the other weirs. Table 2 summarizes the analysis of sharp-crested weirs.

If one uses the procedure of Raju and Asawa (1977), all of the data for the 2, 3, and 4-inch high sharp-crested weirs must be corrected for scale effects. Their method also requires the discharge coefficients of the 12-inch high sharp-crested weir be corrected for H_t/P values less than 0.4. Clearly the data of the smaller weirs are not in error to the extent that they must be corrected. It appears that the method of Raju and Asawa is questionable.

Table 2. Summary of iteration results for conditions when springing initiates for sharp-crested weirs

w/P	Weir Size (P x w, inches)	Reynolds Number	H_t/P	H_t (inches)	Average H_t (inches)
0	12 x 0	3000	0.044*	0.53*	
	8 x 0	3000	0.125	0.50	
	4 x 0	3000	0.176	0.53	
	2 x 0	3000	0.284	0.57	0.53

* value calculated using average H_t value from other weir sizes.

Model Size Selection and Operation

Figure 29 shows the limiting Reynolds Number plotted against w/P. This figure shows the regions where leaping scale effects are present for w/P ratios between 0 and 2. Hydraulic modelers should find particular interest in this figure because it can be used to identify scale effects for w/P ratios not exceeding 2.

It is possible to build a model that is 1/2 inch high by 1/4 inch thick that has w/P equal to 0.50 and meets the Reynolds Number criteria for larger heads (discharge coefficients would be suspect at smaller heads because the Reynolds Number criteria cannot be met for smaller heads and flows). For practical purposes this model size is much too small when compared to the weirs tested in the development of the curve shown in Figure 29. The basic testing for this study was completed on weirs with a height of at least 2 inches to obtain the data used to develop Figure 29. However, the writer also tested a 1-inch high by 0.25-inch thick weir, but the results showed such excessive scale effects that testing on that size was discontinued.

If it is necessary to operate a model in the region of leaping scale effects shown in Figure 29, the modeler must scale his results to obtain the prototype discharge coefficient. For example, suppose the Reynolds Number for a 4-inch high by 8-inch wide weir with a quarter-rounded trailing edge is 3000 (this weir is different than those of this study). Figure 29 shows that the Reynolds Number must be at least 5200 for w/P equal to 2 for scale effects to cease. The process to scale the model results for Reynolds Numbers less than 5200 to the prototype would be to multiply the discharge coefficient found for

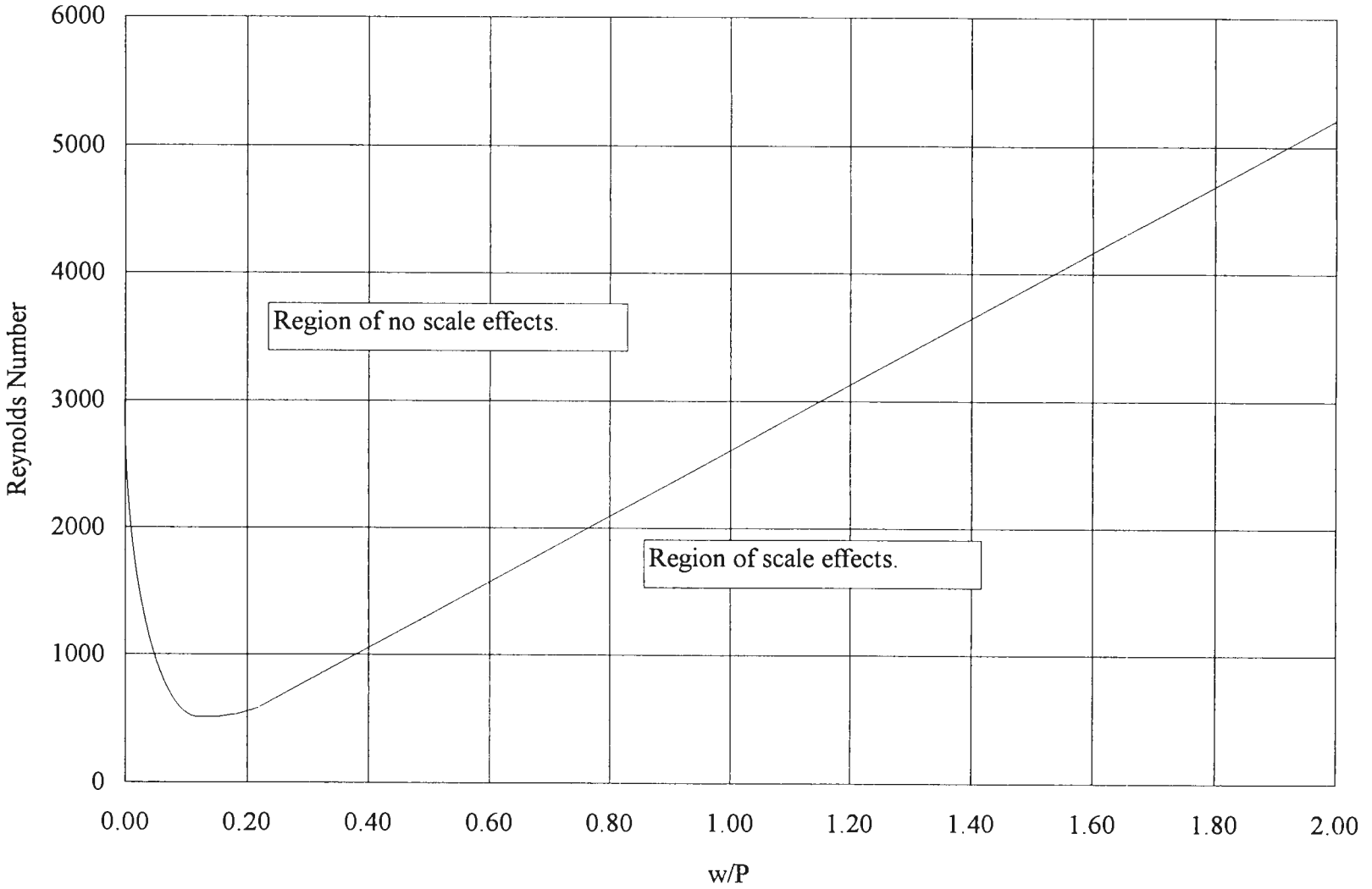

Figure 29. Reynolds Number vs. w/P showing the region where scale effects are present.

the weir by the ratio of the discharge coefficient with no scale effects and the discharge coefficient with scale effects for the given w/P ratio using Figures 20 through 23, for example, if the discharge coefficient found for $H_t/w = 0.5$ is 0.45 (which is higher than that of a square-edged weir but still smaller than the prototype value). This number may be corrected by multiplying it by the ratio of 0.48/0.35 to obtain the prototype discharge coefficient. The numbers 0.48 (no scale effects on 12-inch by 24-inch discharge coefficient curve) and 0.35 (scale effects on 4-inch by 8-inch discharge coefficient curve) are the discharge coefficients from Figure 20 for a weir wall with $w/P = 2.0$ and $H_t/w = 0.50$, respectively.

Not only is it useful to know when leaping scale effects affect the discharge coefficient, it is also useful to know beforehand the minimum value of H_t/w or H_t/P that one can test with a given weir size without scale effects. Figures 30 and 31 provide this information. The figures can be used in two ways. First, if one knows what size his model will be, he can determine the minimum value of H_t/w or H_t/P that he can achieve with his model without having scale effects. Second, if one knows the minimum H_t/w or H_t/P for which he desires data, he can determine the minimum size his model weir must be constructed to avoid scale effects.

Model Sizing Example

Suppose a model study is to be conducted for a flat-topped weir that is 4 feet high and has a crest thickness of 6 feet. Suppose further, that the researcher is required to obtain discharge coefficients that are free from scale effects for $0.15 < H_t/w < 1.5$. The

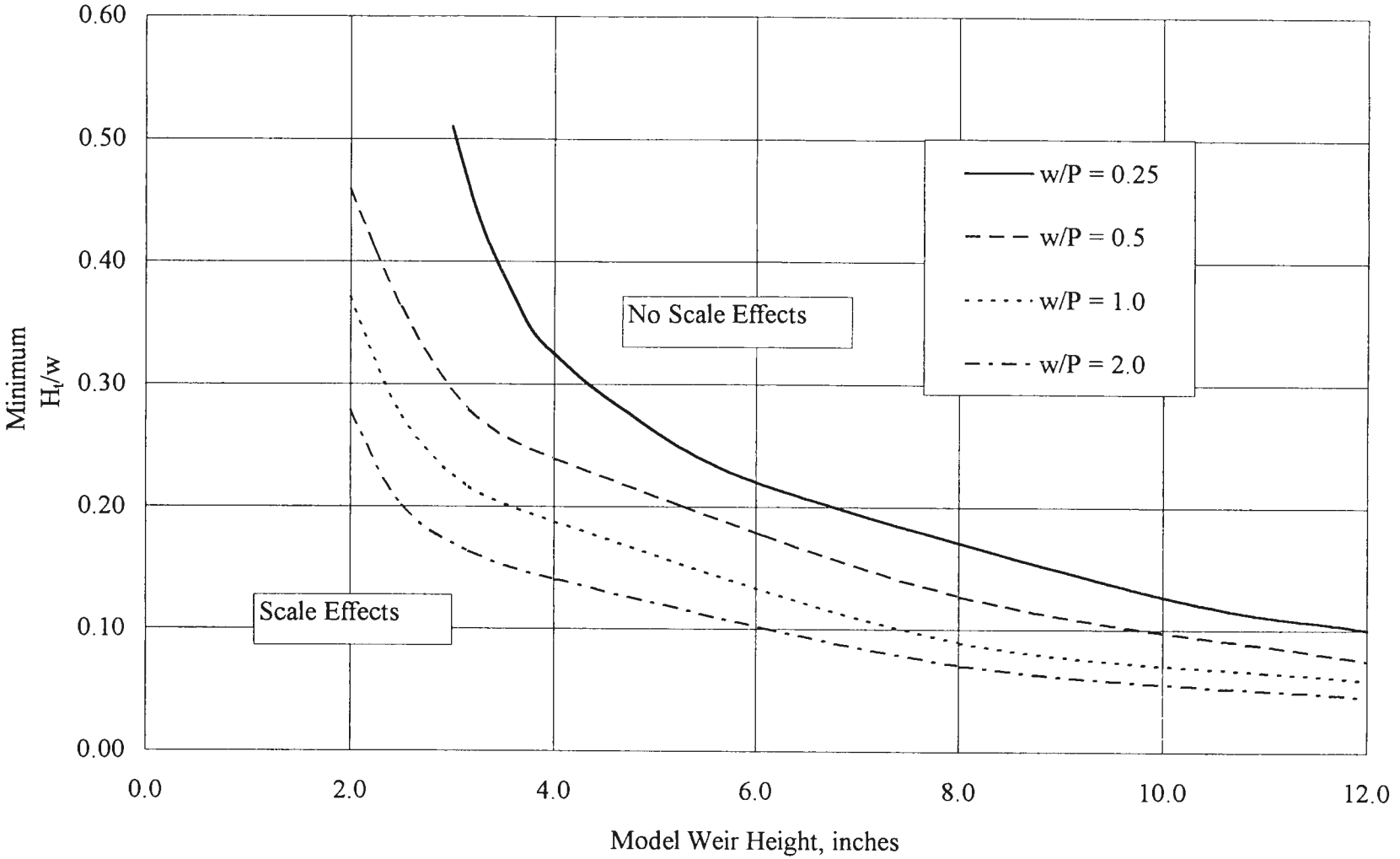

Figure 30. Minimum H_t/w vs. model weir height needed to determine the limiting size (smallest) of flat-topped weirs to avoid leaping flow scale effects.

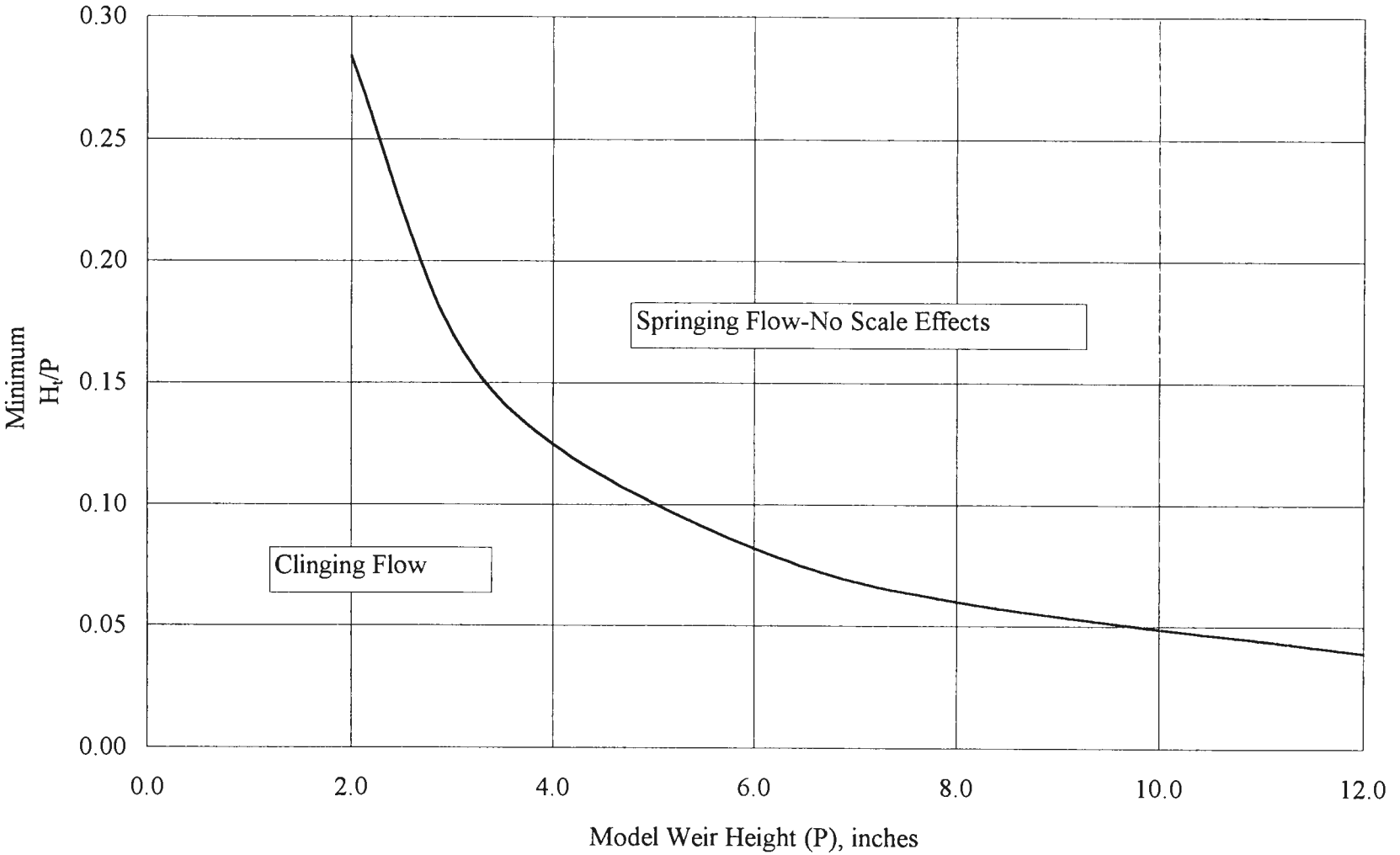

Figure 31. Minimum H_t/P vs. model weir height needed to determine the limiting size (smallest) of sharp-crested weirs to enable springing.

objective of the researcher is to size the model appropriately to avoid scale effects. The w/P ratio for this example is 1.5.

To obtain the appropriate model size, find the minimum H_t/w value for which data are to be obtained on the ordinate, which for this example is 0.15. The next step is to traverse horizontally until intersection is made with the curve where w/P = 1.5 and then project vertically down to the abscissa to size the model. Note that there is no curve for w/P = 1.5 so an approximation of its location must be made. Approximating the curve for w/P = 1.5 yields a model size that is approximately 4.5 inches high. Figure 31 is used in a similar manner for sharp-crested weirs.

General Discharge Coefficient Curves

To complete the analysis, the discharge coefficient data are presented as a continuous curve with an error of ±5 percent for flat-topped weirs. Figure 32 shows the discharge coefficients plotted against H_t/w for all flat-topped weirs analyzed. The data on this curve correspond to conditions where there are no scale effects; i.e., it represents the prototype discharge coefficient. This curve also shows three regions of constant or linear-varying discharge coefficients. The first is for $H_t/w \leq 0.3$ where the discharge coefficient is relatively constant, the second is for $0.3 \leq H_t/w \leq 1.8$ where the discharge coefficient changes linearly, and the third is for $H_t/w \geq 1.8$ where the discharge coefficient is constant.

If $H_t/w \geq 2.0$, springing flow for prototype weir-walls should be anticipated (see Figures 21 and 22). One must use the value of $H_t/w = 2.0$ with caution. For example, if a prototype weir is 1 inch high and has a crest width of 4 feet, one cannot expect springing

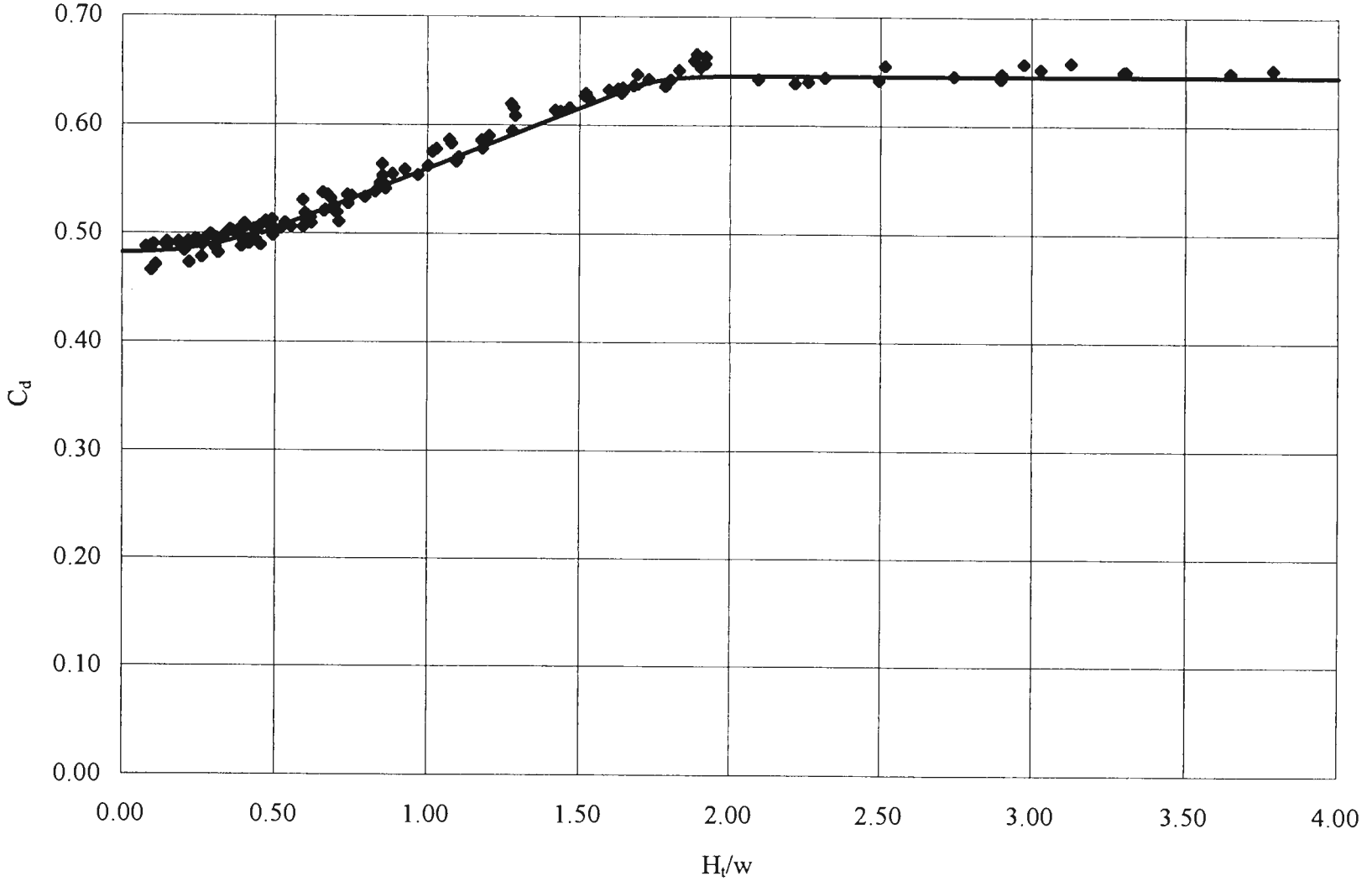

Figure 32. Discharge coefficient vs. H_t/w for all flat-topped weirs excluding points with scale effects.

to occur because springing is not possible (springing forces are small compared to gravity forces) for this weir configuration even though it is possible to have $H_t/w > 2.0$. Hopefully, a weir-wall such as this would not be designed because the depth over the structure would be hundreds of times its height. For practical purposes, weirs should not be designed with heights less than 1/3 times the maximum depth of flow expected over the weir. No equation for the discharge curve will be given because equations are too often misused. Readers are invited to develop their own equation(s) if necessary.

Figure 33 gives the discharge coefficient curve that can be used for prototype sharp-crested weirs. Note that the curve begins at an H_t/P value that is greater than zero. If values for the discharge coefficient are needed below the range shown, one should model a weir that is sufficiently high so that the ratio of 0.53 inches (average total head to facilitate springing) to P is within the range of desired data.

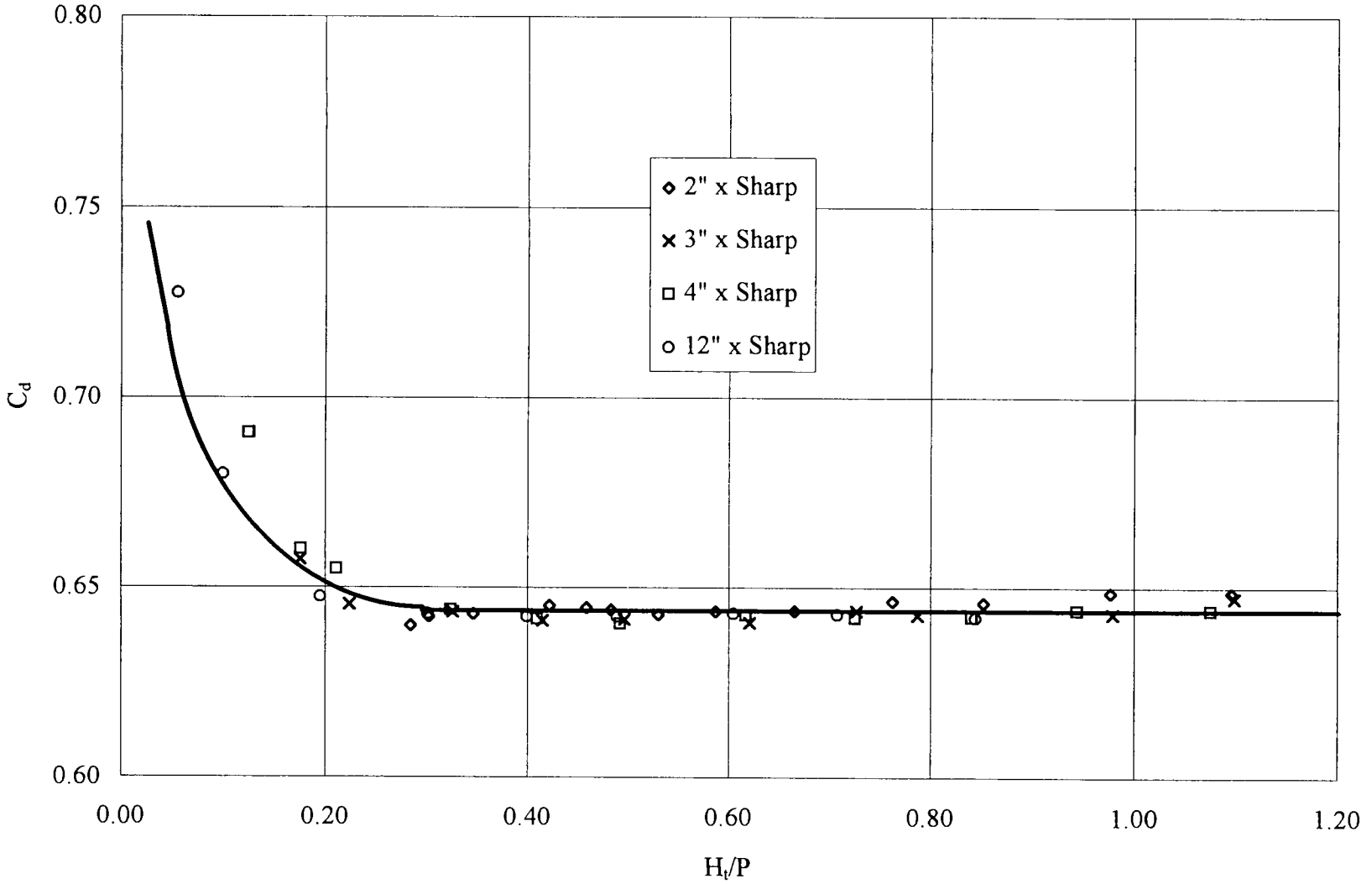

Figure 33. C_d vs. H_t/P for sharp-crested weirs.

SUMMARY AND CONCLUSIONS

Discharge coefficient scale effects for weir-walls (a weir with a flat top that is rectangular in side profile) were studied. Scale effects in models are present because complete dynamic similarity is not met when testing models using Froude scaling. The most significant factor contributing to scale effects in Froude Modeling of weirs appeared to be viscosity. To maintain similarity for all important forces acting (i.e., viscous), a fluid with properties that would enable prototype-model force ratios to be equal is needed. For example, a fluid that is less viscous than water would be needed to maintain Reynolds similarity.

The writer observed differences in the character of the flow for large and small weirs and noted that the flow appeared more "sluggish," or viscous, for smaller models at any H_t/w value (H_t = total head = $h+V^2/2g$, V = velocity of approach at piezometric head measuring location, w = crest thickness parallel to the flow). Thus, factors related to viscosity, such as the size of the separation region, height of the boundary layer, and friction, appeared to contribute to scale effects. Surface tension scale effects were examined and dismissed because surface tension forces are only important when small radii of curvature exist at fluid interfaces. Testing for this study was completed with radii of nappe curvature in excess of 1/2 inch.

Weir-walls (hereafter referred to simply as weirs) are weirs with height, P, and a flat-top with crest thickness, w, parallel to the flow with square leading and trailing edges. They are used primarily as hydraulic control structures but may also be used for flow

measurement. Much effort in past research has been directed at determining weir discharge coefficients for various weir configurations, but the treatment of scale effects pertaining to the discharge coefficient is quite limited in the literature. Scale effects caused discharge coefficient errors exceeding 40 percent for weirs of this study.

To quantify discharge coefficient scale effects, a significant amount of laboratory data was collected at the Utah Water Research Laboratory. Two geometries were tested, sharp-crested and flat-topped. The flat-topped geometries tested included w/P ratios of 0.25, 0.5, 1.0, and 2.0. For each geometry, several scale models were tested and compared with one another to identify scale effects. Table 3 shows the weir geometry and the sizes of each weir tested.

Three different flow regimes were observed for flat-topped weirs: clinging (the flow clinged to the downstream face of the weir), leaping (the flow leaped away from the downstream face of the weir), and springing (the flow would spring from the leading edge of the weir, losing contact with the weir). Sharp-crested weirs had only two flow regimes: clinging and springing. As the flow was increased, flat-topped weirs transitioned from clinging to leaping to springing flow while sharp-crested weirs simply transitioned

Table 3. Weir geometry and sizes of that geometry tested

Geometry	Sizes Tested (P x w, inches)
w/P = 0	2 x 0, 3 x 0, 12 x 0
w/P = 0.25	1 x 0.25, 3 x 0.75, 6 x 1.5, 12 x 3, 24 x 6
w/P = 0.5	2 x 1, 4 x 2, 8 x 4
w/P = 1.0	2 x 2, 4 x 4, 8 x 8, 12 x 12
w/P = 2.0	2 x 4, 4 x 8, 8 x 16, 12 x 24

from clinging to springing flow without leaping. With the exception of clinging flow, all data were taken with atmospheric aeration under the nappe.

Clinging Flow Scale Effects

The scale effects associated with clinging flow for the flat-topped weirs were such that as the weir size increased, the H_t/w value for which clinging would no longer occur decreased (i.e., scale effects decreased with increasing weir size). This phenomenon was observed and no data were taken because clinging only occurred for small very small heads (usually less than 1/4 inch depending on weir geometry). As the w/P ratio increased, the value of H_t/w for which clinging occurred also decreased because of increasing velocities tangent to the weir's crest.

Leaping Flow Scale Effects

Transition from clinging flow to leaping flow occurred when the flow energy was large enough for the flow to detach from the downstream face of the weir. Leaping flow is most likely to occur for prototype weirs with a flat-top; hence most of the data were collected for this condition.

Scale effects for leaping flow were such that the discharge coefficient for smaller weirs of the same geometry was significantly less (at times exceeding 40 percent) than for larger weirs at the same H_t/w value in the range of scale effects. Leaping scale effects existed for H_t/w values that were less than 0.52.

The most important finding for leaping flow scale effects was that the Reynolds Number ($Re = \rho V H_t/\mu$, V is the average velocity of water over the weir) for which scale effects ceased was constant for each geometry tested and was independent of model scale (see Table 4 for summary results). This limiting Reynolds Number increased linearly with increasing w/P ratios. Because the Reynolds Number was constant for each weir size of a given geometry, viscous effects appeared to be the most significant contributor to discharge coefficient scale effects.

Related to the Reynolds Number was the value of H_t for which scale effects ceased. This value was essentially constant for each w/P ratio, regardless of model scale. The total head at which leaping scale effects stopped was larger for flat-topped weirs with larger w/P ratios than for narrower weirs with smaller w/P ratios at the limiting Reynolds Number.

Several design curves (see Figures 29, 30, and 31) were developed to help hydraulic modelers select the model size necessary to avoid discharge coefficient scale effects. Size selection requires selecting the minimum H_t/w value at which one desires reliable model data. If one must operate in the region of scale effects, a procedure to correct for scale effects discrepancies was given.

Springing Flow Scale Effects

When the flow had sufficient energy, it would spring from the leading edge of the weir. Both the flat-topped and the sharp-crested weirs had springing scale effects.

Springing for flat-topped weirs was a function of the thickness of the weir's crest and the H_t/w value. Because of flume limitations, springing was only observed for weirs with $w/P \leq 0.5$. The springing value of H_t/w was larger for smaller weirs than it was for larger weirs. However, after springing had occurred, there were no discharge coefficient scale effects. Weirs with increasing w/P ratios required larger H_t/w values to spring than weirs with smaller w/P ratios, indicating that springing is related to both the weir's crest thickness and total head. Two curves were presented to indicate the springing value of H_t/w for a given crest thickness (see Figure 27).

The most significant scale effect finding for springing flow in sharp-crested weirs was the value of H_t for which springing from the crest initiated. Weirs with 2-, 3-, 4-, and 8-inch heights all required approximately 0.53 inches of total head to spring. A limiting Reynolds Number was also associated with springing flow scale effects to maintain consistency with the flat-topped weir analysis. Table 4 summarizes the results of the scale effects findings for each weir geometry tested.

Table 4. Summary of scale effects testing for leaping flow

Geometry	Total Head to Overcome Leaping S.E. (inches)	Reynolds Number Necessary To Overcome Leaping S.E.
w/P = 0	0.53	3000
w/P = 0.25	0.38	650
w/P = 0.5	0.48	1300
w/P = 1.0	0.73	2600
w/P = 2.0	1.1	5200

H_t/w vs. H_t/P

The data of this research clearly showed that the crest thickness is a more important variable than the weir's height for discharge prediction. By superimposing the discharge coefficients for each flat-topped weir geometry, a family of curves results if H_t/P is used as the ordinate axis. When H_t/w is used as the ordinate axis, the discharge coefficient data for all flat-topped weirs plotted as a single curve. In each comparison the discharge coefficient data without scale effects were plotted.

Another important point is that by using H_t, one accounts for the velocity of approach, which can have a dramatic effect on the discharge for shallow approach channels where the velocity head is significant. By including the velocity of approach, the height of the weir is accounted for because the velocity head calculation incorporates its height. Also, the same piezometric head over weirs with different heights results in different total head values. If the piezometric head is the same, the shorter weir will have a greater total head value than will the taller weir because the area of the approaching flow is smaller. It is imperative to use total head ($H_t = h + V^2/2g$) if one uses the design curves of this research.

Design Curves

Design curves for sharp-crested and flat-topped weirs were developed that can be used to predict the discharge capacity of prototype weir walls with w/P values up to 2. The curve may also be used to predict springing. For prototype weirs, those with heights

greater than 24 inches, springing flow is expected for H_t/w values exceeding 2.0. When springing occurs, the weir functions as a sharp-crested weir and has a constant discharge coefficient that is equal to that of a sharp-crested weir. By using the design curve, one can size a weir to operate with a specified discharge coefficient range. For example, narrow weirs will approach a sharp-crested weir and operate with the highest discharge coefficients. Another application could be to design the weir to operate with a low discharge coefficient (very wide crest thickness) to provide dampening of high incoming flows.

Inverse Formulation for Weir Flow

The inverse formulation was used to provide a simpler method than existing methods to numerically solve free-surface discharge problems. The inverse formulation (role reversal of the independent and dependent variables) for weir flow appeared to be theoretically sound but failed numerically. The reason for its failure was attributed to the free surface or free streamline boundary condition. This boundary condition was a cubic equation with positive real roots that were almost equal in magnitude. The Newton Method was utilized to solve the necessary equations, and although convergence to a solution was possible, the correct solution was not obtained. The Newton method is designed to converge to a root and cannot distinguish between roots. Until a "smart" nonlinear equation solver or a different free surface boundary condition is developed, there appears to be little hope for solving weir flows using the inverse formulation. Past numerical techniques have been successful for solving free-surface discharge problems and

those interested in successful numerical solutions for such problems should review the literature.

Future Research

This research provides insight into scale effects for flat-topped and sharp-crested weirs. The following are recommended for future research:

1) The influence of the boundary layer along the crest of the weir and its interaction with the separation region.

2) Scale effects associated with weirs of different geometries. For example, are there scale effects for round-crested weirs, embankments, ogee crest spillways, etc.? Determine if the research of this study applies only to flat-topped weirs or could it be applied to embankments.

3) Because the numerical model using the inverse formulation failed, is it possible to develop a reasonable free streamline boundary condition that would be free from numerical difficulties?

By researching these areas, especially for weirs of different shapes, it is possible to shed further light into the influence of scale effects for free surface spillway and open channel models.

LITERATURE CITED

Bos, M.G., J.A. Replogle, and A.J. Clemmens. 1984. Flow measuring flumes for open channel systems. John Wiley & Sons, New York. 321 p.

Cassidy, J.J. 1965. Irrotational flow over spillways of finite depth. A.S.C.E. Journal of the Engineering Mechanics Division 101(12):155-173.

Flammer, G.H., R.W. Jeppson, and H.F. Keedy. 1986. Fundamental principles and applications of fluid mechanics. Utah State University, Logan, Utah. 376 p.

Govinda Rao, N.S., and D. Muralidhar. 1963. Discharge characteristics of weirs of finite-crest width. La Houille Blanche 5:537-545.

Hall, W., C. Maxwell, and J.R. Weggell. 1969. Surface tension in Froude models. A.S.C.E. Journal of the Hydraulics Division 95(2):677-701.

Horton, R.E. 1907. Weir experiments, coefficients, and formulas. U.S. Geological Survey, Water Supply and Irrigation Paper No. 200. 1052 p.

Jeppson, R.W. 1968. Seepage through dams in complex potential plane. A.S.C.E. Journal of Irrigation and Drainage 94(3):23-29.

Johnson, J.W. 1943. Models of upper narrows dam spillway. A.S.C.E. Proceedings 69(1):171-175.

Keutner, C. 1934. Stromungsvorgange an breitkronigen wehrkopern und an einlaufbauwerken. Bauingenieur, 15(37/38): 366-377; 15(39/40): 389-392 (in German).

Kindsvater, C.E., and Rolland W. Carter. 1957. Discharge characteristics of rectangular thin-plate weirs. A.S.C.E. Journal of the Hydraulics Division 83(6):772-822.

Kirkpatrick, K.W. 1955. Discharge coefficients for spillways at TVA dams. A.S.C.E. Transactions 120:190-210.

Kline, S.J., and F.A. McClintock. 1953. Describing uncertainties in single-sample experiments. Mechanical Engineering 1:3-8.

Lamb, H. 1945. Hydrodynamics. Sixth edition. Dover Publications, New York. 738 p.

Markland, E. 1965. Calculation of flow at a free overfall by relaxation method. Institute of Civil Engineers Proceedings 31:71-78.

Matthew, G.D. 1963. On the influence of curvature, surface tension and viscosity on flow over round-crested weirs. Institute of Civil Engineers Proceedings 25:511-524.

Moss, W.D. 1972. Flow separation at the upstream edge of a square-edged broad-crested weir. Journal of Fluid Mechanics 52(2):307-320.

Raju, K.G.R., and G.L. Asawa. 1977. Viscosity and surface tension effects on weir flow. A.S.C.E. Journal of the Hydraulics Division 103(10):1227-1231.

Rao, S.S., and M.J. Shukla. 1971. Characteristics of flow over weirs of finite crest width. A.S.C.E. Journal of the Hydraulics Division 97(11):1807-1816.

Rehbock, T. 1929. Hydraulic laboratory practice, p. 194. In Ralph Freeman (Ed.). Fluid flow measurement. American Society of Mechanical Engineers, New York.

Roberson, J.A., and C.T. Crowe. 1993. Engineering fluid mechanics. Houghton Mifflin Company, Boston, Massachusetts. 785 p.

Rouse, H. 1946. Elementary mechanics of fluids. John Wiley and Sons, Inc., New York. 376 p.

Sarginson, E.J. 1972. The influence of surface tension on weir flow. Journal of Hydraulic Research 10(4):431-446.

Shimoryama, Y. 1935. Memoirs of college engineering. Institute of Civil Engineers 7:185-207.

Singer, J. 1964. Square-edged broad-crested weir as a flow measurement device. Water and Water Engineering 28(820):229-235.

Sreetharan, M. 1988. Discharge characteristics of rectangular profiled weirs. Proceedings of the National Conference of Hydraulic Engineering, May 14,1988, New York. p. 969-978

Swamee, P.K. 1988. Generalized rectangular weir equations. A.S.C.E. Journal of Hydraulic Engineering 114(8):945-949.

Vanden-Broeck, J.M., and J.B. Keller. 1987. Weir flows. A.S.C.E. Journal of Fluid Mechanics 176:283-293.

VITA

Michael Clyde Johnson

Doctor of Philosophy

Dissertation: Discharge Coefficient Scale Effects Analysis for Weirs.

Major Field: Fluid Mechanics and Hydraulics.
Minor Fields: Groundwater and Hydrology.

Biographical Information:

Personal Data: Born at Payson Utah, June 29, 1967, son of Clyde Willis and Susan Wignall Johnson; married Shawna Parkinson August 10, 1991; one child-Danielle.

Education: Attended elementary school in Spanish Fork, Utah; graduated from Spanish Fork High School in 1985; received the Bachelor of Science degree, in Civil Engineering, from Utah State University in 1992, received the Master of Science Degree, in Civil Engineering, from Utah State University in 1994; completed the requirements for the Doctor of Philosophy Degree specializing in Fluid Mechanics and Hydraulics at Utah State University in 1996.

Professional Experience: Research Assistant, Utah Water Research Laboratory, 1992 to present; Engineer, Hall Engineering, Spanish Fork, Utah, 1990-1991; Irrigation Contractor, Halco Irrigation, Spanish Fork, Utah, 1989-1991; Irrigation Sales and Design, Harward Irrigation, Spanish Fork Utah, 1984-1989.